One Dimensional Modeling of an Annular Combustor

A Thesis Submitted

In Partial Fulfillment of the Requirements

for the Degree of

Master of Technology

by

Ramanand Singh

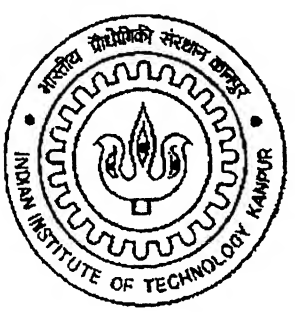

to the

DEPARTMENT OF MECHANICAL ENGINEERING

INDIAN INSTITUTE OF TECHNOLOGY KANNPUR

July, 2002

Certificate

This is to certify that the work contained in the thesis entitled ***'One Dimensional Modeling of an Annular Combustor'*** has been carried out by **Mr. Ramanand Singh** under our supervision and that this work has not been submitted elsewhere for the award of a degree.

(Dr. B. P. Pundir)
Professor,
Department of Mechanical Engineering,
Indian Institute of Technology,
Kanpur 208016. India
July, 2002

(Dr. Keshav Kant)
Professor,
Department of Mechanical Engineering,
Indian Institute of Technology,
Kanpur 208016. India
July, 2002

This thesis is dedicated to my parents and brothers
for their enduring love, support
and inspiration.

Acknowledgements

I take this opportunity to express my profound sense of gratitude to Dr. Keshav Kant (Prof. Dept. of ME) and Dr. B.P.Pundir (Prof. Dept. of ME), my thesis supervisors, for their excellent guidance, and invaluable suggestions during the period of this thesis work. They supported and encouraged me during the work while giving me complete freedom in pursuing my work. In spite of this freedom, my thesis owes enormously to their inspiring influence. It was a great pleasure to work under them as a lot of care with personal touch was available throughout.

I would like to express my gratitude to Dr. K.G. Narayana -Chief Advisor DRDO, Mr. V. Sundararajan -Director GTRE, and Mr. T.K. Sampathkumaran -Additional Director GTRE, for their being instrumental in my completing this thesis work under the given frame of time. I am indebted to Dr. Venkatraman Shankar -Group Director (CFD&ABC) GTRE, for endlessly supporting and encouraging me throughout the work and providing all necessary help to complete the work undertaken by me. I am greatly thankful to Mr. N. Muthuveerappan and Mr. G. Sivaramakrishna whose association and invaluable help gave me an opportunity to understand and think in the right direction regarding the complex phenomena involved in the combustor. My sincere thanks are also due to Dr. Haran, Dr. Kishore, Dr. Aradhya and Mr. Murthy for their active help and affectionate support while pursuing this work at GTRE. I also like to express my sincere thanks to Dr. G.N. Mathur -Dirctor DMSRDE and Dr. R.K. Singh -Joint Director DMSRDE, for their help.

I shall be failing in my duties if don't express my thankfulness to Dr. E. Rathakrishnan, Dr. Manohar Prasad and Dr. Gautam Biswas for their help and rememberable association during my stay at IIT Kanpur.

I am very thankful to Mr. Ashok Pise, Mr. Vipin Yadav, Mr. D.S. Murthy, and Mr. H.K. Paliwal for their encouragement which boosted my morale in academics during my M.Tech. at IIT Kanpur. My thanks are also due to Mr. Susheel Misra of the HT Lab who was always helpful.

I express my appreciation and thanks to my friend- Nikhil, Akhilesh, Ramesh, Abhay, Rajeev, Satish, Girdhari, Durgesh, Pravin, Manoj, Prashant and others, who apart from making my stay at Kanpur pleasant and memorable, also helped me in my work from time to time. I am also thankful to my friend Uday whose immense support helped me in completing my work in time.

Last but not the least I would like to express my gratefulness to all those who directly or indirectly helped me through successful completion of my work.

Date: July 25, 2002. (Ramanand Singh)

Contents

List of Figures

List of Tables

Nomenclature

Symbol	Description
A	Area, m^2
A_{bl}	Area occupied by boundary-layer displacement thickness, m^2
A_h	Hole area, m^2
A_{th}	Cross-sectional area occupied by a specified mass flow at diffuser station, m^2
A_w	Wetted wall area per unit length, m
A^*	Critical area, for which Mach number equals 1.0, m^2
AR	Area Ratio A_2/ A_1
C	Entrainment constant
C_1	Rate of heat transfer by convection from the hot gases (for the cooling film) to the flame-tube wall, W/m^2
C_2	Rate of heat transfer by convection from the wall to the annulus air, W/m^2
C_A	Inner wall area per unit length, m
C_B	Outer wall area per unit length, m
C_d	Discharge coefficient
C_d^1	Corrected discharge coefficient
c_p	Specific heat, kJ/kg K
C_p	Pressure-recovery coefficient
C_{pi}	Ideal pressure-recovery coefficient
C_{pm}	Ideal pressure-recovery coefficient in the presence of mixing
D_{an}^1	Hydraulic diameter of annulus, m
D_{ft}	Wall-to-wall width of flame tube, m
D_{ft}^1	Hydraulic diameter of flame tube (=$2D_{ft}$), m
D_{ref}	Combustor reference diameter, m
d_h	Effective axial length of hole, m

d_j	Effective initial jet diameter, m
$1-E$	Diffuser blockage
$1-E_{bl}$	Diffuser boundary-layer blockage
F_{12}	View factor of receiving surface 2 form radiating object 1
F	Fanning friction factor
f	Fuel-air ratio
h	Enthalpy, kJ
H	Boundary-layer shape factor
H_1	Shape factor at diffuser inlet
H_{sep}	Shape factor at which separation occurs
H/C	Fuel hydrogen-carbon ratio
$H_{eff,p}$	Effective fuel lower calorific value, kJ/kg
h_P	Fuel lower calorific value, kJ/kg
K_d	Number of dynamic heads lost in flow from diffuser outlet to dome
ΔK	Net rate of heat transfer by conduction into unit area of the flame-tube wall from adjacent wall elements, W/m^2
k	Gas thermal conductivity, W/m K
k_w	Thermal conductivity of wall material, W/m K
L	Length, m
l_b	Mean beam path length, m
M	Mach number
M_w	Molecular weight of coolant, kg/mole
M_j	Axial component of jet momentum flux
$\dot{m}$, m	Mass flow rate, kg/s
$\dot{m}_h$	Mass flow rate through hole, kg/s
N	Number of stream tubes in diffuser analysis
N_u	Nusselt number
P	Total pressure, N/m^2
ΔP_{hot}	Loss of total pressure due to combustion, N/m^2
Pr	Prandtl number

p	Static pressure, N/m^2
p_G	Partial pressure of reradiating gas, N/m^2
$\bar{q}$	Dynamic head $\rho\bar{u}_m^2/2$, N/m^2s
$\dot{q}$	Rate of heat addition due to fuel burning, kJ/s
$\dot{q}_w$	Heat transfer rate from the flame-tube wall to the annulus air, kJ/s
R	Gas constant, kJ/kg K
R_1	Rate of heat transfer by radiation from the hot gases to the flame-tube wall, W/m^2
R_2	Rate of heat transfer by radiation from the wall to the casing, W/m^2
R_3	Net rate of heat transfer by radiation from the flame-tube wall to all parts of the opposite wall, W/m^2
Δr	Diffuser inlet width, for annulus diffusers, m
r	Radius, m
Re	Reynolds number
Re_{cf}	Reynolds number of cooling film, based on slot height
Re_{ft}	Reynolds number of gas in flame tube, based on flame-tube hydraulic diameter
s	Distance along jet center-line, m
s'	Distance along jet center-line from virtual origin, m
T	Static temperature, K
T_o	Stagnation temperature, K
T_{ad}	Adiabatic-wall temperature, K
T_b	Base temperature for enthalpy, K
T_c	Casing temperature, K
T_{cf}	Temperature of cooling air, K
T_{ft}	Static temperature of hot gases, K
T_w	Wall temperature, K
TA	Total cross-sectional area of stream tubes, m^2
t_w	Wall thickness, m
U	Main-stream velocity, m/s

U_{ft}	Bulk velocity of gas in flame tube, m/s
$\overline{U}_{cf}$	Mean initial velocity of cooling film, m/s
u	velocity, m/s
$\overline{u}_a$	Area-average velocity, m/s
$\overline{u}_m$	Mass-averaged velocity, m/s
X	Non-dimensional distance downstream of cooling slot
X_o	Parameter in film-cooling correlation
x	Mole fraction
x	Downstream distance, m
x	Distance downstream of cooling slot, m
Δx_{ft}	Thickness of slab of hot gas, m
Δx_w	Axial length of strip of wall, m
Y	Non-dimensional distance across diffuser
y	Distance across diffuser of flame tube measured from the wall, m
Y_{cf}	Height of film-cooling slot, m
ζ	Streamline slope, radians
α_{ft}	Flame absorptivity
α_w	Wall absorptivity
β	Profile parameter
γ	Ratio of specific heats
δ	Boundary-layer displacement thickness, m
ε_{ft}	Flame emissivity
η	Transverse jet coordinate, m
$\eta_{½}$	Value of η at which non-dimensional velocity profile parameter equals 0.5, m
η^*	Value of η at the assumed jet boundary, m
θ	Boundary-layer momentum thickness, m
Λ	Luminosity factor
λ_{diff}	Diffuser total-pressure-loss coefficient
μ	Dynamic viscosity, Nm/s

ν	Kinematics viscosity, m^2/s
φ	Initial jet angle, radians
ξ_m	Diffuser effectiveness in the presence of mixing
ξ_{12}	Diffuser effectiveness between station 1 and 2
ρ	Density, kg/m^3
σ	Stefan-Boltzmann constant, $W/m^2 K^4$
τ	Film-cooling effectiveness
Γ	Transmittance

Abstract

The present trend is to use high Mach number aircrafts. This necessitates the design and development of an aircraft gas turbine engine which could fulfill this requirement. Annular combustors have been found to be more suitable in high speed aircraft engines. There are many ways of simulating a combustor. Among these, **one-dimensional** simulation can play an important role. It gives an idea about the performance parameters of a combustor when there is a change in geometry and inlet conditions. One-dimensional analysis may be less accurate compared to 2D or 3D analysis, but the time taken and cost associated is considerably less.

The present work is an attempt to simulate and analyze the fluid flow, combustion and heat transfer processes taking place in a high performance annular combustor to predict various performance parameters. Some important parameters are diffuser effectiveness, pressure recovery coefficient; combustor total pressure loss, mass flow split, mass flow distribution among various components; and the temperature distribution on the flame tube wall. In the diffuser part of the combustor, primarily 'stream tube method' has been used for the simulation of pre-diffuser and 'mixing equation method' for the mixing zone of annulus region. The air flow analysis has been carried out by solving a combination of continuity, momentum, energy, and state equations. Heat transfer analysis is performed by solving the equations for heat balance to obtain the liner wall temperature distribution, film cooling effectiveness, etc.

The simulation results, obtained from the computer program developed, are compared with the experimental data and 3D analysis for the same inlet conditions and are found to be in good agreement. The output data are presented in tabular and graphical forms for better understanding of the effects of change in various parameters of combustor on its performance. It is expected that the present modeling of an annular combustor and the resulting computer program would be an useful tool for the design of high performance annular combustors.

CHAPTER 1

GENERAL BACKGROUND

1.1 INTRODUCTION

In modern research, computer simulation of processes and systems has become a powerful tool in that it saves time and is also economical when compared with experimental study. A proposed theory can be analyzed quickly using a computer and the cost of setting up an experimental apparatus can be postponed until optimization is achieved. However, it may be noted that simulation is only a step prior to experimentation and results obtained from simulation studies must be validated with experimental results to establish the reliability. Once validated, this tool can provide deep insight into the performance characteristics of the system.

The aim of the work described in this thesis has been to develop a computer simulation model for the analysis of fluid flow, combustion, and heat transfer in an annular combustor with diffusers of making use of currently available analytical methods and correlations. The resulting program, used in conjunction with experimental data, will prove to be a useful tool for the design of high performance annular combustors.

In a gas turbine combustor, the processes involved are extremely complex. Until the last decade, the design of a combustor relied heavily on previous experience and know-how. As a result of this, in combustor design extensive testing of the prototype is considered necessary. Selecting the best design from such testing is a task of considerable magnitude. Because of these difficulties, analysis by means of computer simulation has become quite popular in recent years. Further, computer simulation offers the following advantages:

- It serves as a tool for better understanding of the parameters involved and their effect on combustor performance.
- It systemizes knowledge obtained through expensive engine testing.
- It reduces considerably the time-consuming tests by narrowing down the parameters that must be studied.
- It helps in optimizing the engine design for particular application, reducing cost and time.

1.2 COMBUSTOR

The function of the combustion chamber or combustor, Figure 1.1, is to accept the air from the compressor and to deliver it to the turbine at the required temperature, ideally with no loss of pressure. For the common open-cycle gas turbine, this implies the internal combustion of fuel and thus the problem of fuel preparation, mixing and burning. The fuel is commonly gaseous or liquid. Gaseous or liquid fuels are almost invariably hydrocarbons, the former usually being natural gas, mostly methane, with some small

proportion of heavier compounds such as propane and butane and some CO_2 and nitrogen, while the latter may range from highly refined gasoline through kerosene and

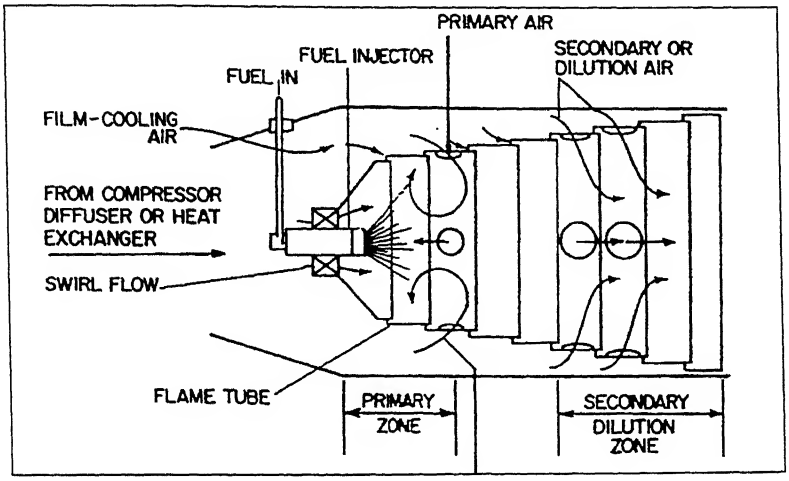

Figure 1.1 General form of combustion chamber

light diesel oil to heavy residual oils. It may be said that the combustion problem itself is seldom difficult, as all the fuels used for gas turbines are used in combustion apparatus of one type or another and have been used for many years. The difficulty arises in getting the combustion with low pressure loss in a size of combustor compatible with the high power to weight ratio or high output potentialities of the rotating elements.

1.3 REQUIREMENT FOR A GAS TURBINE COMBUSTOR

Requirements for a gas turbine combustion system include:

i) Release of the fuel chemical energy in the smallest space (length and diameter) possible
ii) Minimum pressure drop over the operating spectrum
iii) Stable and efficient operation over a wide range of fuel-air ratios, altitudes, flight speeds, and/or powers levels
iv) Reliability equal to or greater than the overall life of the engine
v) Relight capability at altitudes for aircraft engines
vi) Uniform temperature distribution at the inlet to the turbine stator (nozzles).

However, many of these desirable properties are in competition. For example, both complete combustion and low pressure loss are contrary to small size. Hence, the design of a combustor is a compromise.

1.4 TERMINOLOGY

Certain conventional terminology is traditionally used in discussing gas turbine combustors. Refer to Figure 1.2 which is a cross-section of a generic diffusion flame combustor.

The outer container of the combustor is called a **casing.** Proceeding in the flow direction, air exits the compressor and enters the **diffuser**. A portion of the air is captured

for the primary zone by the **snout**. The hemispherical upstream end of the combustor portion is called the **dome**. The **fuel atomizer**, surrounded by a **swirler**, is situated in the center of the dome. Air captured by the snout enters the primary zone through the swirler.

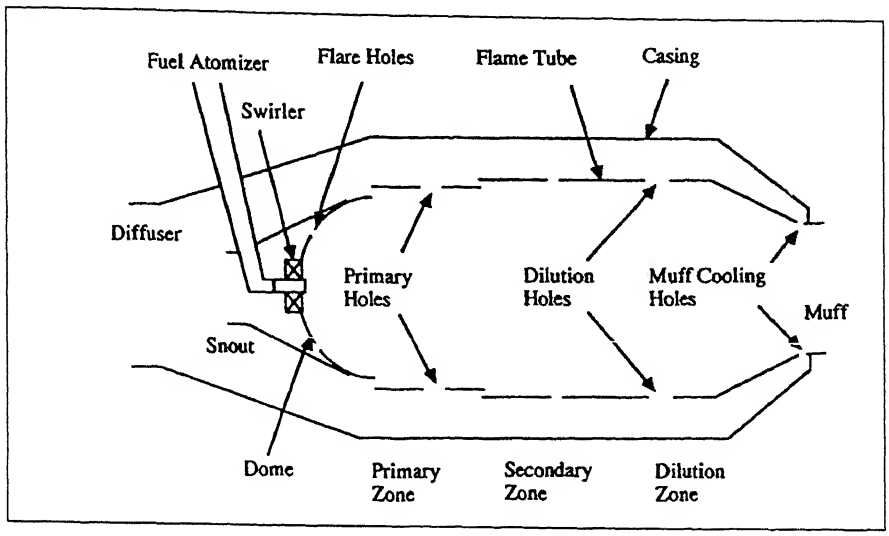

Figure 1.2 Typical combustor cross-section.

The body of the combustor is called the **flame tube**. Several rows of holes and slots penetrate the flame tube to admit air to the combustion process. Generally, there are some holes in the dome to cool its interior surface, typically called **flare holes**. Further downstream, **primary** holes admit air, a portion of which flows upstream into the primary zone, and the remainder flows downstream into the secondary (or intermediate) zone. At the downstream end of the flame tube, sometimes called the **muff**, a row of small **muff cooling holes** admit the last of the air mainly to cool the roots of the first stage turbine blades. At appropriate points along the flame tube, slots and louvers admit film-cooling air to control the temperature of the inner surface of the flame tube. The combustion volume is divided into three zones: **primary**, **secondary**, and **tertiary** (usually called dilution zone).

If all the fuel and all the air passing through a gas turbine engine were mixed together, the resulting mixture would contain insufficient fuel to support combustion. More precisely, it would have a fuel/air ratio lower than the lean flammability limit.

Therefore, the primary function of a gas turbine combustor is to get a mixture which can sustain continuous combustion, and to maintain or stabilize this combustion over a wide range of operating conditions. This is achieved by controlled mixing of fuel and air. The function of primary zone is to initiate and stabilize combustion. Appropriate amount of fuel and air are admitted to this region to produce a near stoichiometric mixture, which is most favorable for both combustion and its stabilization. The aerodynamics of the primary zone must be arranged so as to recirculate hot combustion products continuously upstream to provide a continuous ignition source for fresh incoming mixture. Mechanical devices used to achieve this function are called flame holders. In a diffusion- flame combustor the primary zone must additionally serve as

region for fuel atomization and evaporation prior to combustion. The gases exiting the primary zone are partial combustion products at high-temperature.

Additional air must be added to the primary zone effluent gases to more completely oxidize the fuel. This is accomplished in the secondary zone. If additional air were not added to the combustion, efficiency would be extremely low due to escape of incompletely oxidized species.

The temperature of the gases leaving the secondary zone is still too high for the materials of the turbine section to withstand. Therefore, additional air is added in the tertiary or the dilution zone to reduce the gas temperature.

1.5 TYPICAL COMBUSTOR ARRANGEMENTS

There are different methods to arrange combustors on a gas turbine. Designs fall into three categories: Tubular, Annular, and Tubo-annular.

1.5.1 Tubular (or Can type) Combustors

Tubular combustors have approximately cylindrical flame tubes and casings (see Figure 1.3). Each flame tube is totally enclosed by its own casing, and the entire assembly is replicated in a multiple-combustor engine.

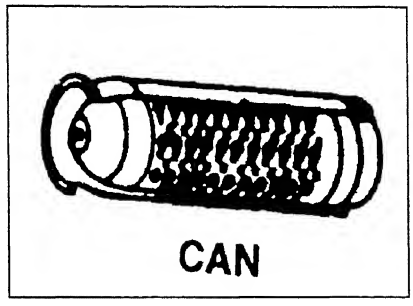

Figure 1.3 Tubular or can type combustor

'Can type' is a popular term for describing these combustors. Industrial and early aircraft applications predominantly employ tubular combustors. Older aircraft applications, particularly shaft power engines, commonly used this combustor configuration. Newer aircraft applications seldom incorporate tubular combustors because they do not provide the maximum combustion volume for a given annular space. Multiple igniters and/or interconnection tubes are required. However, within the individual combustor units, aerodynamic and combustion problems are minimized by tubular designs.

1.5.2 Annular Combustors

Annular combustors, as shown in the Figure 1.3, have a single annular flame tube and a concentric annular casing. This arrangement offers maximum utilization of available volume and is thus, widely used in modern aircraft applications. Problems related to non-uniform circumferential combustion (i.e. the propagation of combustion around the entire

circumference of the combustor from a small number of igniters) are minimal, but the aerodynamic performance and structural integrity are generally lower than the tubular designs. Achieving a uniform distribution of fuel around the annular space using a fixed number of fuel injectors is difficult. Maldistribution of fuel can result in non-uniform combustor outlet temperatures.

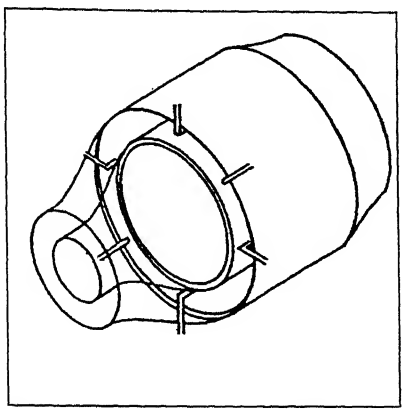

Figure 1.4 Annular combustor configuration.

Annular combustors are used mainly in aircraft type gas turbines where frontal area is important. This type of combustor is usually a straight-through flow type. The combustor outside radius is the same as the compressor casing, thus producing the streamline design. The annular combustor mentioned earlier requires less cooling air than the tubo-annular combustor, and so it is growing in importance for high temperature applications.

1.5.3 Tubo-annular Combustors

Tubo-annular combustors are hybrids of the previous two types. They have a number of cylindrical flame tubes contained in an annular casing (see Figure 1.5). Such combustors are also called "cannular" combustors.

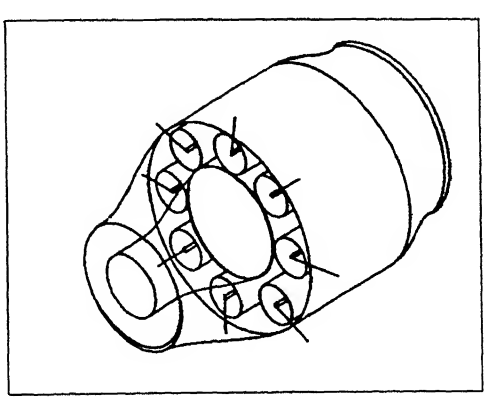

Figure 1.5 Tubo-annular or cannular combustor

1.6 MAIN COMBUSTOR COMPONENTS AND THEIR FUNCTIONS

The turbine engine main combustor system consists of three principal elements:

a) The inlet diffuser
b) The dome, and snout (or cowl)
c) The liner

In addition, important subcomponents are- the fuel injector, the igniter, the combustor case, and primary air swirler. The term "combustion zone" is used to designate that portion of the main combustor within the dome and liner in which the burning of fuel takes place. These elements are illustrated below in Figure 1.6.

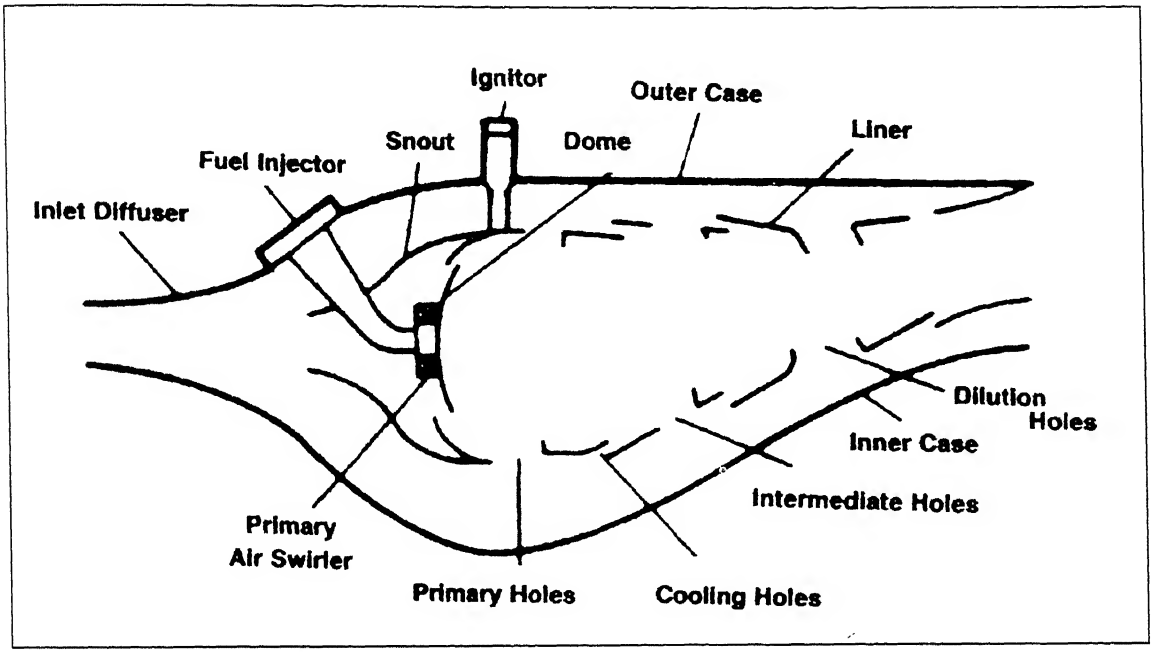

Figure 1.6 Main combustor components

The purpose of inlet diffuser is to reduce the velocity of the air exiting the compressor and deliver it to the combustion zone as a stable, uniform flow while recovering as much of the dynamic pressure as possible. The inlet diffuser represents a design and performance compromise relative to required compactness, low pressure loss, and good flow uniformity. Early inlet diffuser designs were of the smooth curved wall or contoured wall type. Because of the wide variations in the characteristics of the flow field exiting the compressor, however, the curved wall diffuser can not always provide uniform, non separated flow at all operating conditions. This can become a critical problem in the short length diffusers required in many current systems. Consequently, a trend toward a dump or combination curved wall and dump diffuser designs is emerging. Although this design results in somewhat higher total pressure losses, it provides a known and constant point of flow separation at the dump plane which prevents stalled operation at all diffuser entrance conditions. The snout divides the incoming air into two streams- primary air and the other air flows (intermediate, dilution, and cooling air). The snout

streamlines the combustor dome and permits a larger diffuser divergence angle and reduced overall diffuser length.

The combustor dome is designed to produce an area of high turbulence and flow shear in the vicinity of the fuel nozzle to finally atomize the fuel spray and promote rapid fuel-air mixing. There are two basic types of combustor domes- bluff body and swirl stabilized. The bluff-body domes were used in early main combustors, but swirl-stabilized domes are used in the most modern combustors.

The combustion process is contained by the liner. The liner also allows introduction of intermediate and dilution air flow and the liner's cooling air flow. The liner must be designed to support forces resulting from pressure drop and must have high thermal resistance capable of continuous and cyclic high temperature operation. This requires use of high strength, high temperature oxidation-resistant materials and cooling air.

Fuel injectors can be classified into four basic types according to the injection method utilized: pressure atomizing, air blast, vaporizing, and premix/prevaporising. Spark igniters are used to ignite the cold flowing fuel-air mixture in main burners.

1.7 AIRFLOW DISTRIBUTION AND COOLING AIR

The air flow distribution in, around, and through the main combustor resulting in the four basic air flow regions is illustrated in Figure 1.7. Effective control of this air distribution is vital to the attainment of complete combustion, stable operation, correct burner exit temperature profile, and acceptable liner temperatures for long life.

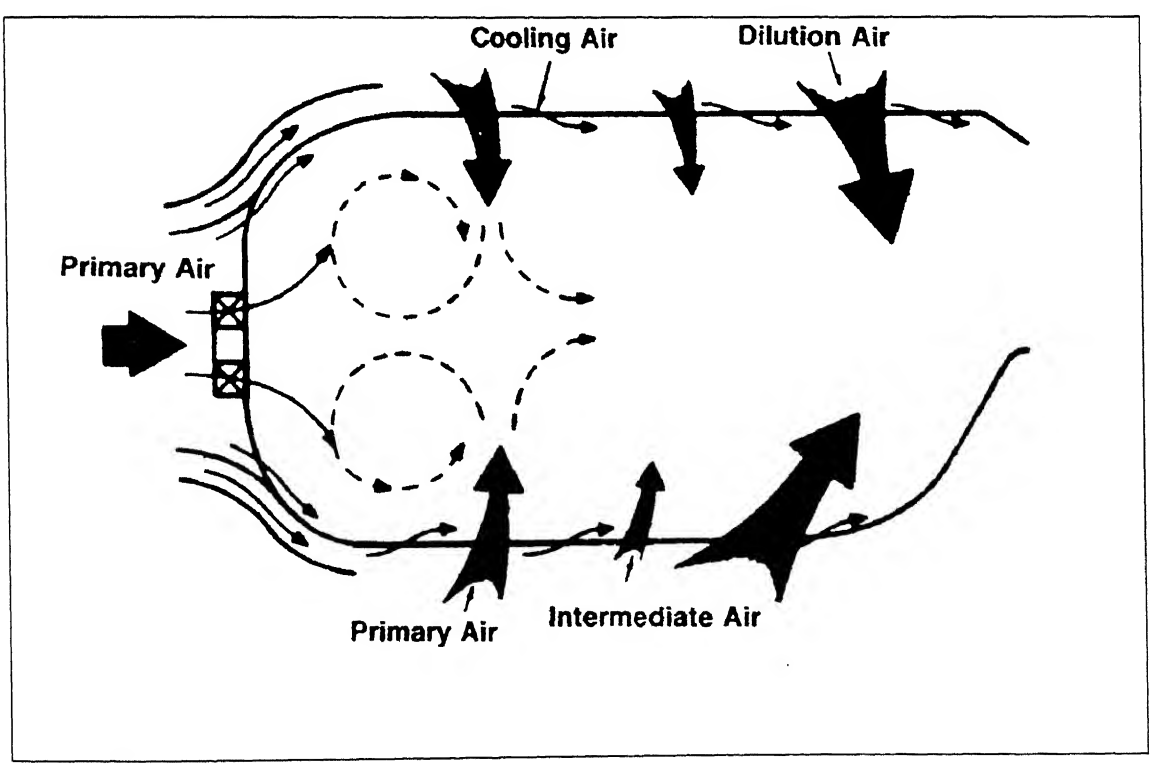

Figure 1.7 Main combustor air flow distribution.

Primary air is the combustion air introduced through the dome or head plate of the combustor and through the first row of liner air holes. The air mixes with the incoming fuel producing locally nearly stoichiometric mixture necessary for optimum flame stabilization and operation. To complete the reaction process and control the high levels of CO, H or H_2 and unburned fuel in the primary zone, intermediate air is introduced through a second row of liner holes. The reduced temperature and excess oxygen cause CO and H_2 concentrations to decrease. In contemporary systems, the dilution air is introduced at the rear of the burner to reduce the high temperature of the combustion gases. The dilution air is used to carefully tailor exit temperature radial and circumferential profiles to ensure acceptable turbine durability and performance. This requires minimum temperature at the turbine root (where stresses are highest) and at the turbine tip (to protect seal materials).

1.8 COMBUSTOR PRESSURE LOSS CONSIDERATIONS

The overall combustion system pressure loss can be broken down into several components, as described below.

1.8.1 Diffuser losses

There are four components of diffuser loss-

(i) ΔP_{Pd}, Pre-diffuser loss affected by inlet Mach number, inlet velocity profile and pre-diffuser geometry (area ratio, length and curvature).

(ii) ΔP_{cowl}, Small diffusion loss into cowl or snout

(iii) ΔP_{op}, and

(iv) ΔP_{ip}, Dumping pressure losses into the outer and inner passages, affected by Pre-diffuser exit Mach number, passage areas and cowl losses.

An overall diffuser loss (ΔP_{diff}) can be defined as the mass flow weighted average of ΔP_{cowl}, ΔP_{op} and ΔP_{ip} added to the pre-diffuser loss.

1.8.2 Combustor losses

There are also four components of combustor pressure loss-

(i) ΔP_{dome}, Pressure drop from the cowl to the combustion chamber.

(ii) ΔP_{ol}, and

(iii) ΔP_{il}, Pressure drop from the outer and inner liner passages, respectively, to the combustion zone.

(iv) $\Delta P_{\Delta T}$, Heat addition, or Rayleigh pressure loss. This loss is a function of Mach number within the combustion chamber and temperature rise. Heat addition pressure losses are generally very low compared to diffuser and liner pressure drops.

An overall pressure drop (ΔP_{liner}) can be defined as the mass flow weighted average of ΔP_{dome}, ΔP_{il}, and ΔP_{ol} added to the heat addition loss.

It is desirable to minimize diffuser loss since this is a parasitic loss. On the other hand, liner loss is used to promote uniform air distribution and provide high swirler and dilution air velocities for uniform and intense mixing within the combustor.

1.9 LINER COOLING TECHNIQUES

Cooling air must be used to protect the burner liner and dome from the high radiative and convective heat loads produced within the burner. This air is normally introduced through the liner so that a protective blanket or film of air is formed between the combustion gases and the liner wall.

The effectiveness of cooling technique is quantified by the cooling effectiveness (ε), defined by

$$\varepsilon = \frac{T_g - T_m}{T_g - T_c}$$

where Tg, Tm, and Tc are the mainstream gas, average metal, and cooling air temperatures, respectively.

As future combustor exit temperature requirement increases, the percent of combustor air available for cooling decreases requiring increased cooling effectiveness.

1.10 PREVIOUS EFFORTS

A number of attempts have previously been made to calculate the air flow and heat transfer in gas turbine combustors. Graves [1] and Grobman [2] analyzed the pressure loss and air-flow distribution in tubular combustors with uniformly tapered (or constant cross-section) flame tubes. This work included the effects of momentum transfer between the gas streams in annulus and flame tube, annulus wall friction, heat release, hole discharge coefficients, and compressibility. Flow in diffuser was not considered, and instantaneous mixing between cold-air jets and the gas in the flame tube was assumed. No heat-transfer analysis was undertaken. The results of these calculations exhibited many of the effects observable in practical combustors.

Samuel [3] used the same general approach as Grobman, with instantaneous mixing between cold-air jets and the main gas stream. A simple diffuser analysis was included, and both tubular and annular geometries could be treated. In the case of annular combustors, a calculation followed the three parallel streams in the inner and outer annuli and through the flame tube, and iterated on the initial mass-flow split between these streams until boundary conditions at the end of the combustor were satisfied. A similar approach is used in the present work. The output of Samuel's program was used as input for the heat transfer program.

The most comprehensive heat-transfer analysis of aircraft-type combustors that has been published to date is that of Lefebvre and Herbert [4]. This involved the solution of a heat-balance equation for each element of the wall, taking into account radiation from flame to wall and wall to casing, and forced convection on the inside and outside of the wall. Net heat transfer in the longitudinal direction was assumed to be negligible compared with radial heat transfer. Reasonable agreement with limited experiment was obtained.

Another heat-transfer analysis was carried out by Tipler [5] whose work dealt with an industrial combustor and included the effects of radiation transfer in a longitudinal direction.

Another heat-transfer analysis was carried out by Tipler [5] whose work dealt with an industrial combustor and included the effects of radiation transfer in a longitudinal direction.

Sovran and Klomp [6] provided a way of generalizing straight-walled two-dimensional and annular diffuser performance. An almost identical approach was used by Reneau et al. [7], who extended the work to cover different inlet boundary- layer thicknesses; this aspect was particularly important for gas-turbine combustor diffusers. For the first time, therefore, there existed a set of maps which enabled the performance of straight-walled diffusers to be predicted with fair certainty for any length and area ratio and inlet boundary-layer thickness, at least within the range of interest.

In the field of heat transfer, Spalding [8] correlated the results of 9 experiments to produce a new correlation for film-cooling heat transfer. Schirmer and Quigg [9] produced the most useful work yet published on the effect of pressure on radiation from luminous flames.

The works mentioned above, and others, provide useful new tools for combustor analysis, and open the way for removing some limitations that have previously limited the utility and validity of such analyses.

1.11 SCOPE OF THE PRESENT WORK

Present thesis work is devoted to carry out an overall analysis of an aircraft annular combustor operating under different conditions. For this purpose, an attempt has been made to develop a computer program for one-dimensional analysis. The computer program is intended to achieve the following objectives-

- To analyze the air mass flow and pressure distribution in a combustor whose geometry is given, for particular inlet conditions.
- To compute the temperature distribution on the flame tube wall.
- To find out pressure loss in various components of an annular combustor, viz., diffuser, annuli, flame tube, and swirler etc.
- To analyze the mass flow split for inner annulus, outer annulus and flame tube.
- To analyze the mass flow distribution in cooling rings and cooling holes.

1.12 OUTLINE OF THE THESIS

The main work of this thesis has been described in various sections under Chapter 2 through Chapter 6. Chapter 2 is devoted to describe the methodology for the one-dimensional analysis of the combustor. It discusses computer model development in which the input data requirement and methods of the geometrical indexing are given for calculation at various axial locations of the combustor. Chapter 3 deals with the analysis of combustor diffuser. In this chapter different methods of diffuser calculation are discussed. An outline of the calculation procedure is explained in a detail. Chapter 4 discusses the methods for air flow analysis in the annuli and flame tube. Prediction of air mass flow split in the annuli and air mass flow distribution through various cooling holes and cooling rings are included. Chapter 5 is devoted to combustor heat transfer analysis. The primary objective of heat transfer analysis is

to establish the axial distribution of temperature along the flame tube wall. To serve this purpose, the heat balance equation is solved to determine the unknown temperature. Chapter 6 presents the overall result obtained from the computer simulation. The results are compared with the available experimental data and 3D analysis for validation of the model and the resulting program.

CHAPTER 2

MODELING METHODOLOGY AND PROGRAM DEVELOPMENT

2.1 INTRODUCTION

This chapter is an introduction to the combustor simulation and the assumptions made and the methodology used. It is intended to provide a frame work for the detailed discussion that follows in the succeeding sections.

2.2 MAJOR ASSUMPTIONS

The following assumptions are made for the present:

- Flow and combustion conditions are steady: no quantity varies with time. This assumption is reasonable, but it precludes the treatment of transient phenomena such as combustion oscillation.
- Combustors are of annular cross section. This precludes the direct simulation of tubo-annular (cannular) and tubular combustors. While flow conditions for these types may be approximated by appropriate selection of dimensions, other parts of the simulation (for example, radiation heat transfer) will be of reduced accuracy.
- Conditions are uniform around the circumference of the combustor; i.e. there is no circumferential variation in any quantity. This assumption is a major simplification; in practice, cyclic variations around the circumference occur, corresponding to the fuel-injection points. The result of this analysis would be useful, however, in indicating output parameters averaged around the circumference.
- The flow can be treated as quasi-one-dimensional. To represent the complex flow pattern existing in a real combustor is beyond the scope of the present work. Instead, the problem is broken down into two parts: flow in the main gas streams (one-dimensional) and flow and mixing of jets (predicted from correlated experimental data).
- Radial-flow or reversed-flow in the combustors is not analyzed.
- Flow conditions in the combustor are within the range of validity of the correlations used. The correlations are based on experimental data presently available. Outside their range of established validity, accuracy of prediction is likely to be reduced.

2.3 INPUTS TO THE COMPUTER PROGRAM

Input quantities required by the computer program are the following types:

(i) Combustor geometry data
(ii) Inlet flow conditions.

The following information must be supplied to specify the combustor geometry:

- Dimensions of diffuser walls, snout, dome, flame tube, and casing
- Hole and cooling-ring (equivalent cooling-slot) data:

a) Type of holes
b) Number of holes in a row
c) Axial locations; inner or outer wall
d) Area (or cooling-slot height)

- Identification of secondary-hole row (marks end of primary zone) and first hole row or slot in the flame-tube wall, as distinct from the dome (marks end of diffuser and start of combustor annulus)
- Specification of swirler (optional):
  a) No swirler
  b) Swirler designed within program
  c) Swirler dimensions supplied as input

2.4 GEOMETRICAL INDEXING SYSTEM

Four interrelated geometrical indexing system are used within the program-

1. Input stations (i.e. geometric input stations)
2. Hole rows stations and cooling rings (equivalent slots)
3. Diffuser stations
4. Flame tube calculation stations

These are illustrated by the sample numbering system on the Figure 2.1:

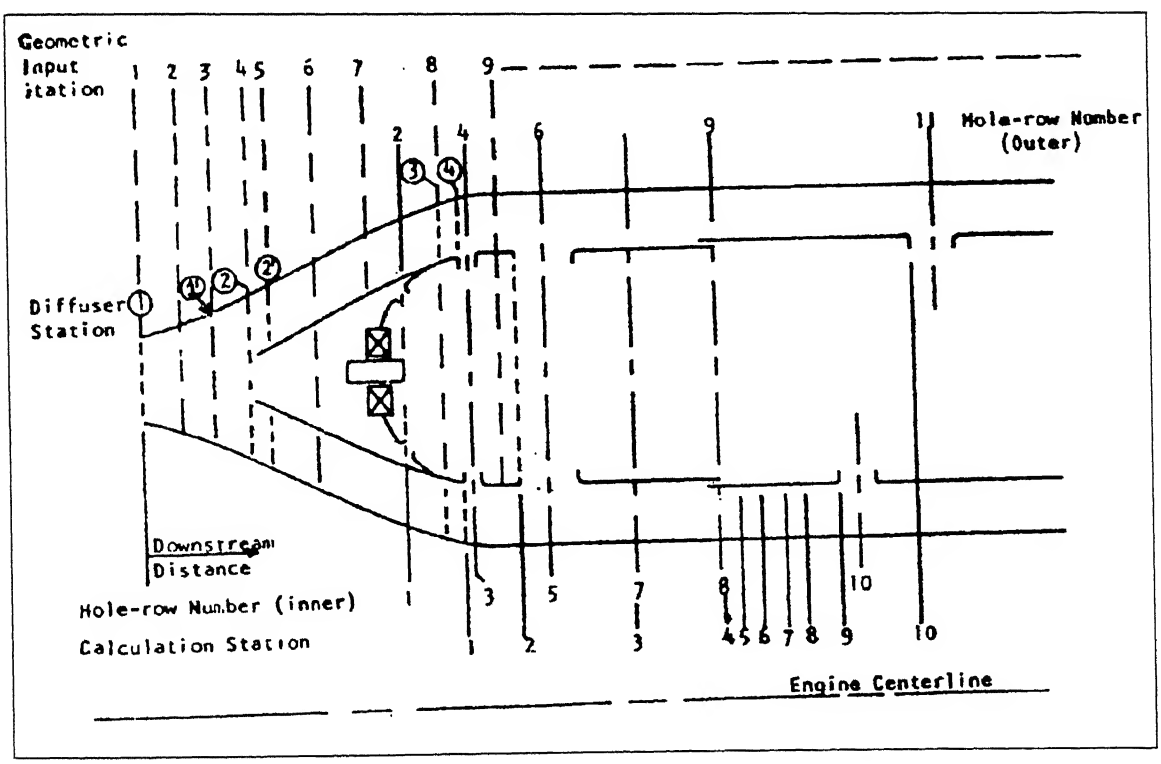

Figure 2.1 Geometrical indexing system.

2.4.1 Input Stations

The shapes of the walls of the diffuser, snout, dome, flame tube, and casing are described by their axial and radial dimensions at geometric input stations. Axial dimensions are measured from the diffuser inlet (compressor exit); radial dimensions from the engine center line. Station numbers begin with station 1 at the compressor exit.

2.4.2 Hole Rows

Holes are indexed in groups referred to as hole rows. A hole row comprises holes of identical size and shape, centered at the same axial location, and spaced at equal intervals around a single wall of the flame tube or dome. Up to six hole rows may be specified at a given axial location: hole rows may be interspersed on the same wall or paired on opposite walls of the flame tube. Indexing starts with the first hole row down stream of the compressor exit.

The indexing system for slots is similar to that for holes, except that slots are circumferentially continuous (as mentioned above) and hence only one slot may be placed on a given wall at any axial location. Non-continuous slots may be approximated by continuous slots of equal area. Slots and holes are indexed together.

Dummy hole rows (holes of zero diameter) may be specified as input, for purposes of arranging the location of calculation stations.

2.4.3 Diffuser Stations

The calculations in the diffuser make use of the input-station indexing system. In addition, labeled as follows in the above figure 2.1:

1→ Entrance to the diffuser (compressor exit).
1`→Outlet to the pre-diffuser or dump diffuser inlet.
2→ Last geometric input station upstream of the start of the snout (or cowl).
2`→First geometric input station on the snout.
3→ Last geometric station where diffusion takes place.
4→ Entrance to the annulus (diffuser exit). This station coincides with the upstream edge of the first hole row in the flame tube, as distinct from the dome.

2.4.4 Flame-Tube Calculation Stations

The primary zone of the flame tube is bounded by the dome and swirler, the flame-tube walls, and (at its down stream end) by a plane passing through the upstream edges of the secondary holes. This zone is treated as a homogeneous stirred reactor; no calculation stations are used.

Calculations in the annulus and in the flame tube down stream of the primary zone are related to a system of calculation stations located as follows.

1. At the upstream edge of each hole row that is centered at a distinct axial location. Thus, for hole rows paired on opposite flame-tube walls only one calculation station is assigned.
2. At each dummy hole row.
3. At the axial location of each cooling slot i.e. cooling ring having a distinct axial location.

4. At up to five axial locations spaced at a specified intervals down stream of each cooling-slot location.
5. One station at the very end of the combustor.

Indexing of calculation stations starts with the first hole row in the flame tube (as distinct from the dome) down stream of the compressor. The first calculation station thus coincides with the end of the diffuser annuli (Diffuser Station 4) and the start of the combustor annuli.

2.5 OVERALL STRUCTURE OF COMPUTER MODELING PROGRAM

The present computer model comprises many subprograms; these can be grouped by function into three major sections as follows:

1. Diffuser subprogram
2. Air flow subprogram
3. Heat-transfer subprogram

2.5.1 Diffuser Subprogram:

The diffuser subprogram receives inputs of geometry, inlet flow conditions and certain quantities related to the calculation procedure; it also asks a first estimate of mass flow among the cowl (i.e. snout) and the two annuli.

Using these inputs, the diffuser subprogram performs the following functions:

(a) Determines Diffuser Performance Parameters:
- Ideal pressure recovery coefficient
- Actual-pressure recovery coefficient
- Effectiveness

(b) Evaluate the mismatch at the snout or cowl

(c) Calculates flow conditions on the dome and at the end of diffuser annuli

Within the diffusing regions the three calculation methods may be used which are:

1. Stream tube method
2. Empirical data method
3. Mixing equation method

These methods will be described in detail in the next chapter.

2.5.2 Air Flow Subprogram:

The air flow subprogram receives the following inputs:

- Geometry of walls, holes and swirler at appropriate geometric stations.
- Fuel data
- Initial estimates of mass flow-split among snout and annuli
- Static pressure and static temperature on the dome and at the end of diffuser annuli.

With the use of these inputs, the air flow subprogram performs the following function:

- Calculates the flow conditions in the primary zone and at calculation station in the flame tube and annuli. These flow conditions are static pressure and temperature, mass flow rate and velocity
- Calculates the combustor total pressure loss
- Directs the iterative process by which the diffuser and air flow subprogram together arrive at the correct flow split among the snout and two annuli.

2.5.3 Heat-Transfer Subprogram:

The primary objective of heat transfer subprogram is to establish the axial distribution of temperature along the flame tube walls.

Geometry of the flame tube and casing, and the axial distribution of velocity and temperature of the flame tube gas are taken as input in the heat transfer subprogram from the air flow subprogram. The additional data may be specified as input to the program.

In operation, the subprogram evaluates various heat flux components at a point on the flame tube wall in terms of the wall temperature; the heat flux components which are considered include the following:

i) Convection from the flame tube wall gas
ii) Convection to the annulus air
iii) Radiation from the flame
iv) Radiation to the outer casing.

The heat balance equation is then solved to determine the unknown temperature. The operations are performed at calculation stations along the flame tube wall.

CHAPTER 3

COMBUSTOR DIFFUSER ANALYSIS

3.1 FUNCTION OF THE COMBUSTOR DIFFUSER

In the combustor inlet of an aircraft gas turbine engine, high velocity air from the compressor flows into the diffuser, where a considerable proportion of the inlet velocity head is converted to static pressure before the airflow enters the main combustor. Modern high through-flow turbine engine compressors are highly loaded and usually have high exit Mach numbers. With high compressor exit Mach numbers, the velocity head at compressor exit may be as high as 10% of the total pressure. The function of the diffuser is to recover a large proportion of this energy. Otherwise, the resulting higher total pressure loss would result in a significant loss of power and fuel efficiency. The diffuser performance must also be insensitive to inlet velocity profiles and geometrical variations of the combustor relative to the location of the pre-diffuser exit flow path.

Low diffuser pressure losses with high inlet Mach numbers are more readily achievable with increasing length. But diffuser length must be short to minimize engine length and weight. A good diffuser should have a well considered balance between the conflicting requirements for low pressure losses and short engine length.

3.2 DIFFUSER REQUIREMENTS

Important design requirements for combustor inlet diffusers that must accept high compressor exit Mach numbers are as follows:

(i) Low pressure losses. In general diffuser pressure loss should be less than 40% of the compressor exit velocity head.

(ii) Short length. Configurations that have special features, such as annular splitter vanes can be used, in some cases, to reduce length.

(iii) No flow separation, except in dump regions.

(iv) Uniform flow both circumferentially and radially.

(v) Dynamic flow stability at all operating conditions.

(vi) Insensitivity to changes in compressor exit flow patterns or exit flow conditions.

3.3 DIFFUSER TYPES

Diffusers are of different types based on requirements and engine operating conditions. The main types are:

3.3.1 Step Diffuser

This configuration is mechanically simple, aerodynamically efficient, and has a relatively high tolerance to distorted inlet velocity contours and dimensional tolerances. This type

of diffuser is also known as annular step diffuser. This thesis deals with only this type of diffuser keeping in view the indigenous **Kaveri** gas turbine aircraft engine (proposed to be used in LCA) development efforts, and will be discussed in detail

3.3.2 Controlled Diffuser

The controlled diffuser is designed to diffuse the compressor discharge flow smoothly with no flow separation at any operating conditions. This design characteristic imposes limitations on the overall diffuser area ratio and flow turning capability of the diffuser walls. This type of diffuser has a short pre-diffuser and long combustor cowling that extends upstream to the pre-diffuser exit plane. The controlled diffuser has low pressure losses in the inner and outer passages, but the center flow pressure losses are usually higher that those in the annular step diffuser. Advanced combustion system trends limit the use of controlled diffuser.

3.3.3 Multiple Passage Diffuser

An annular splitter vane is used in this concept to reduce the length required to obtain the desired diffuser area ratio and to provide high-energy flow to the combustor dome region. With a high area ratio pre-diffuser and low dumping losses, the overall pressure losses for this configuration are very low.

3.4 ANNULAR STEP DIFFUSER

This type of diffuser mainly has two flow regions to fulfill the requirement of short diffuser length and low diffuser losses. The configuration is illustrated in Figure 3.1.

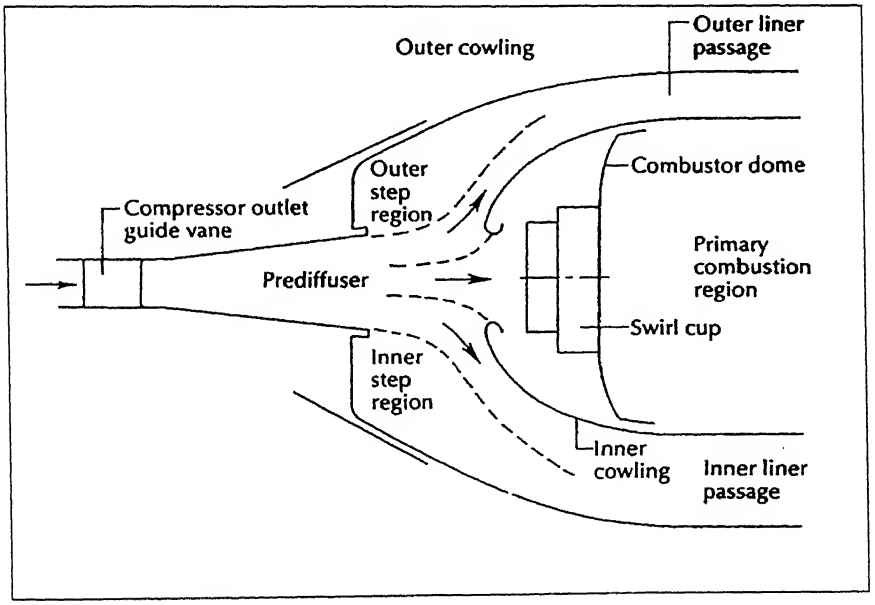

Figure 3.1 Annular step configuration.

The main regions are as follows:

3.4.1 Pre-diffuser

A large fraction of the compressor exit velocity head is recovered in the pre-diffuser sections of the combustor inlet diffuser. This reduction in velocity head results in reduced dumping losses at the end of pre-diffuser and reduced parasitic drag losses from frame support struts and fuel nozzle stems. The pre-diffuser must be carefully designed to avoid the possibility of flow separation ahead of the step regions. If flow separation occurs within the pre-diffuser section, the separated regions are usually unstable and occur at isolated locations around the annulus near the exit end of the pre-diffuser, sometimes at particular engine operating conditions. These randomly located flow separations cause severe circumferential distortions of the flow entering the combustor, which may result in hot streaks at the turbine inlet plane. These flow separations can also lead to dynamic instability.

Pressure losses in the pre-diffuser are relatively low and nearly all of the losses are caused by momentum deficiencies in the wall boundary layers. The velocity profile becomes more center-peaked and the boundary layers become weaker as the flow moves down stream. For the same average velocity, a center peaked profile has a higher mass-weighted velocity head than a flat profile. With more of the energy in the velocity head, the static pressure recovery is reduced below the ideal levels. High turbulence levels produce more uniform profiles and reduce the pressure losses.

3.4.2 Dump-diffuser (or Diffuser Step Regions)

Annular step diffusers are designed to have backward facing steps at the end of the pre-diffuser. The typical regions are illustrated in Figure 3.2. The flow at the pre-diffuser exit plane separates from the sharp corners at the trailing edge of the pre-diffuser and curves around the combustor cowling to the combustor liner passages. At the base of the dump region the flow is recirculating at low velocities. This low-momentum recirculating flow mixes with the higher energy flow leaving the pre-diffuser, resulting in momentum, mixing losses as the flow goes into the liner passages. Front of the reattachment point of the stagnation streamline, flow is reversed and goes into the recirculating region, and aft of this point, the flow goes downstream. If stable flow patterns exist in the recirculating region, the forward flow at the stagnation point is balanced by the flow mixes into the mainstream

A considerable proportion of the pressure loss in the annular diffuser is due to the mixing losses in the dump region. These losses are difficult to estimate because the geometry of this region is complicated. The theoretical dumping losses for step increase in passage area can be obtained by applying the momentum equation with the assumption of uniform, steady incompressible flow with negligible friction.

$$\frac{\Delta P}{P_{T3.1}} = \left[1 - \frac{P_{S3.1}}{P_{T3.1}}\right]\left[1 - \frac{A_{3.1}}{A_{3.2}}\right]^2$$

where $A_{3.1}$ and $A_{3.2}$ are the passage areas at stations 3.1 and 3.2, which are located upstream and downstream of the step respectively as shown in the Figure 3.2 .

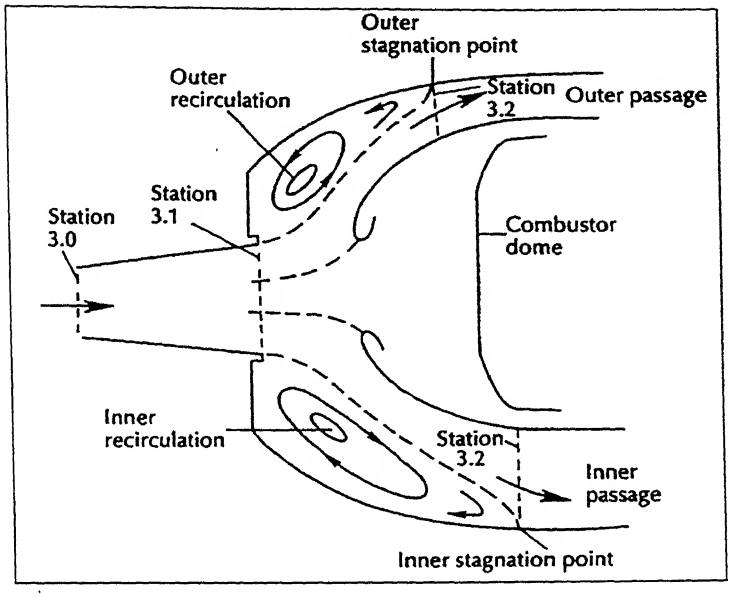

Figure 3.2 Recirculating flow patterns in dump diffuser region

One major difficulty in the analysis of dumping loss is to select an appropriate value for $A_{3.2}$, which is the effective cross-sectional area of the passage at the unknown point where the flow reattaches to the wall, i.e., the stagnation point. Dumping losses can also be affected by inlet velocity profiles and inlet turbulence levels, and by physical spacing between the exit plane of the Pre-diffuser and the cowling leading edges. If this spacing is too small, the flow into the dump region will be accelerated around the cowling leading edges and the pressure losses would be higher.

3.4.3 Dome Regions:

Ideally, the region within the combustor cowls, upstream of the dome, should be a plenum chamber with very low velocities and a uniform static pressure to provide uniform flow into the swirl cups and other openings. The upstream dome region of the annular step diffuser configuration, as shown in Figure 3.3, approaches this ideal concept. The area ratio of the center flow stream, from the exit plane of the pre-diffuser to the combustor dome region is very high, typically about ten to one. A large amount of diffusion occurs at upstream of the cowling opening as free stream diffusion. The remaining diffusion takes place inside of the cowling where the dome blockage effect spreads the flow out to the inner wall surfaces of the cowlings.

The cowling opening must be properly sized to achieve sufficient free stream diffusion without flow spillage from the cowling. If the opening is too small, the static pressure recovery in the dome region will be reduced. But if the opening is too large, some of the flow entering the cowling will turn around and flow out around the upper or lower cowling leading edge, as shown in Figure 3.3. This flow spillage from the cowling will reduce the pressure recovery in the dome region and will cause higher passages

losses, because the spillage flow, with low momentum, mixes with the higher velocity passage flow as this flow goes into the combustor liner passages. In some cases, this spillage flow may cause flow separation from the outer cowling surface. This depends on the cowling lip contours and on the contours around the outer surfaces of the cowling. The cowling contours should have smoothly accelerating flow on the outer surfaces from

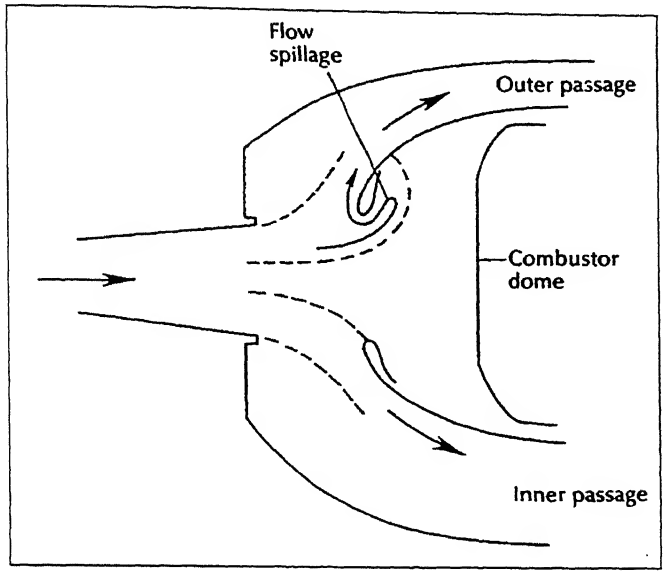

Figure 3.3 Diffuser with flow spillage around the outer cowling leading edge

the stagnation point at the leading edges of the combustor liner passages. A semi-elliptical shape, with the long axis horizontal approaches the ideal configuration.

Pressure losses in the flow that goes into the dome region are very difficult to determine. These losses are usually low and the shape of the inlet velocity profile heavily influences them.

3.4.4 Combustor Liner Passages:

Static pressure in the combustor liner passages should be as high as possible to provide the uniform flow in the combustion zone. The static pressures depend upon the passage area ratio and the velocity profile in the passages. If the passage area is too low, the velocity will be high and the static pressure would be lower. However, higher passage area ratio cause the dumping losses to be high and the flow leaving the dump region may not have reattached to the casing wall before entering the liner passage. In this case, the velocity profile in the passage would be much distorted, which would result in low static pressures. To avoid dynamic instability the flow should be reattached. If the flow in one passage is not attached, a disturbance which momentarily increases the flow in that passage would tend to fill the passage, resulting in reattachment. Under this condition, the passage static pressure would increase with increasing flow to the passage. This is an unstable situation that must be avoided.

Computer codes to analyze compressible viscous flow are continuously being improved and are being applied in diffuser analysis. This thesis is a bid in the same

direction and a computer program for one-dimensional analysis of diffuser and main combustor has been developed.

3.5 ANALYTICAL METHODS AND PROGRAM DEVELOPMENT FOR THE DIFFUSER

As mentioned in the Chapter 2, the three methods for diffuser analysis are:

3.5.1 Stream Tube Method

In this method the flow passage is divided into N stream tubes within each of which flow is assumed to be uniform and isentropic. In setting up the stream tubes, the distribution of boundary layer displacement thickness supplied as a program input is used to adjust the flow area. The development of the flow (static pressure and velocity) is computed for each stream tube at each station along the diffusing passage.

Boundary layer calculations are performed to obtain a revised estimate of boundary layer displacement thickness, which is then used in a revised stream tube analysis. This process is continued to convergence of the displacement thickness. The result of this method is the velocity distribution, static pressure and boundary layer blockage at the outlet from the diffusing passage.

3.5.2 Empirical Data Method

This method is based on the direct evaluation of the effectiveness of a particular diffusing passage. There are two ways this can be done-

a) Diffuser effectiveness may be supplied directly as a program input
b) Diffuser effectiveness may be calculated by the program from correlation of experimentally measured effectiveness versus diffuser geometry that is contained in the library data.

The remaining diffuser performance parameters like ideal and actual pressure recovery coefficients and the outlet conditions are calculated directly from the effectiveness, the geometry and the assumptions that the total pressure is constant.

3.5.3 Mixing Equation Method

The mixing- equation method is always used in the mixing regions. It takes into account the following effects occurring in these passages:

i) Pressure loss due to sudden expansion or contraction at the snout or cowl.
ii) Mixing in the diffusing passage from dome to the annulus diffusion region
iii) Pressure loss due to curvature of the flow passage from dome to the annulus diffusion region

Above three methods of diffuser analysis are separately useful in different part of the diffuser. Their usefulness and application in the model development is described in the succeeding sections of the diffuser analysis

3.6 OBJECTIVES OF THE DIFFUSER ANALYSIS SUBPROGRAM

The objectives of the subprogram are:

- To provide the necessary inlet flow conditions to the annuli; static pressure and temperature the specific properties calculated, although all others can be derived from these two and the mass flow.
- To determine the diffuser performance parameters of effectiveness, ideal pressure-recovery coefficient, and actual pressure-recovery coefficient.
- To determine whether separation occurs in the diffuser and, if so, at what points.
- To evaluate the magnitude of the flow mismatch (for diffusers with a snout).

3.7 MAJOR ASSUMPTIONS IN THE DIFFUSE SUBPROGRAM

The assumptions employed in the diffuser analysis common to all calculation options, referring to Figure 3.4, are that:

- The flow in the upstream part of the diffuser (1-1`, 1`-2) is unaffected by the flow downstream of Station 2.
- If there is a snout (or cowl), it is reasonably well matched to the flow; i.e., the streamlines in the portion 1-1`, 1`-2 which bound the flow required by the annular passages should have radial locations at Station 2 nearly equal to those of the snout as shown in the Fig. given below-

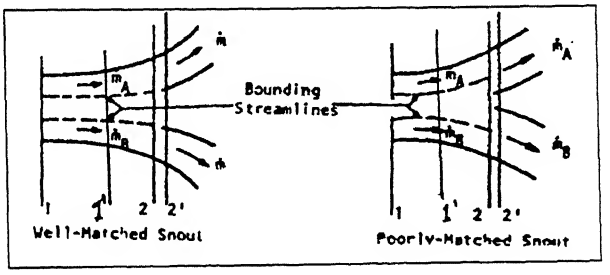

Figure 3.4 Flow match and mismatch at snout station

If the flow is not well matched, it is certain that the flow in the upstream part of the diffuser will be affected by flow in the down stream part, in which case the results of the diffuser subprogram are highly questionable.

- If there is a snout i.e. cowl, its performance as a diffusing passage is specified by an input value of the total-pressure-loss coefficient. This is based on the presumption that the flow in the snout (or cowl) will be dominated by either the colander (or orifice plate) or the downstream resistances supplied by the swirler and dome holes; in either case, it is not expected that the total-pressure loss due only to diffusion in the snout (or cowl) will be of sufficient magnitude to warrant a separate analysis.
- If there is no snout (or cowl), the performance of the passages 2-4A and 2-4B is specified by a single input value of total-pressure-loss coefficient between Stations 2 and 4 (i.e., ratio of total-pressure loss between stations 2 and 4 to the dynamic head at station 2). This is based on the presumption that in such cases the resemblance of these passages to a diffuser will be remote.

- The static pressure across any diffusing passage is constant across any section normal to the passage centerline. This assumes that the flow will be subjected to mild curvatures, and it seems to yield reasonable results for well-designed diffusers.

3.8 DEFINITION OF TERMS USED IN THE SUBPROGRAM

The terms fall in two categories: flow parameters, and diffuser-performance parameters.

3.8.1 Flow Parameters

The flow parameters which are most frequently used are the area-average velocity, the mass-average velocity, the ratio of equivalent free-flow area to total flow area, or blockage, and the dynamic head. All of these parameters refer to the flow at a given axial location, where the static pressure is assumed constant across any section normal to the passage centerline.

➢ Area-average velocity, $\bar{u}_a$, is defined by

$$\bar{u}_a = \frac{1}{A}\int_0^A u\,dA \qquad \text{---------- (3.1)}$$

where, u is the velocity component in the direction of the passage center-line (normal components are neglected) and 'A' is the passage cross-sectional area normal to the passage center line. For incompressible flow, $\bar{u}_a$ is the velocity the flow would have if the profile were uniform across the entire passage.

➢ Mass-average velocity, $\bar{u}_m$, is defined by

$$\bar{u}_m = \frac{\int_0^A u^2\,dA}{\int_0^A u\,dA} \qquad \text{---------- (3.2)}$$

For incompressible flow, it is the velocity which when multiplied by the mass flow would yield the total momentum flux.

➢ Blockage is 1-E, where E is defined by

$$E = \frac{\bar{u}_a}{\bar{u}_m} = \frac{1}{A}\,\frac{\left[\int_0^A u\,dA\right]^2}{\int_0^A u^2\,dA} \qquad \text{---------- (3.3)}$$

For incompressible flow, E is the ratio of the area which would be occupied by a uniform flow, with a total pressure equal to the mass-averaged total pressure of the actual flow, to the actual area of the passage. A related term which is frequently used is the profile

parameter, β, which is merely the reciprocal of E. a derivative of the general inlet blockage, 1-E, is the inlet boundary layer blockage, 1-E_{b1}, where E_{b1} is defined by

$$E_{b1} = \frac{A - A_{b1}}{A} \qquad \text{---------- (3.4)}$$

where A_{b1} is the area occupied by the boundary-layer displacement thickness. If the flow outside the boundary layer is uniform (i.e., u is constant across the passage) then $E_{b1} = E$

➢ Dynamic head based on mass-average velocity, $\bar{q}$, is defined by-

$$\bar{q} = \frac{1}{2}\bar{\rho}\,\bar{u}_m^{\,2} = \frac{1}{2}\bar{\rho}\,\beta^2\bar{u}_a^{\,2} \qquad \text{---------- (3.5)}$$

where $\bar{\rho}$ is the average density across the passage, mathematically

$$\bar{\rho} = \frac{\dot{m}}{u_m EA} \qquad \text{---------- (3.6)}$$

For incompressible flow, $\bar{q}$ the actual mass-average dynamic pressure; for compressible flow, it is treated as a reference quantity.

3.8.2 Performance Parameters

The diffuser performance parameters used herein are the ideal incompressible-flow pressure-recovery coefficient, the actual pressure-recovery coefficient, and the diffuser effectiveness.

➢ Ideal pressure-recovery coefficient is defined by

$$Cp_{,\,ideal} = \frac{(p_2 - p_1)_{max}}{\bar{q}_1} \qquad \text{---------- (3.7)}$$

where the subscripts 1 and 2 refer to inlet and exit, respectively.

➢ Ideal incompressible-flow pressure-recovery coefficient, C_{pi}, defined by

$$C_{p,i} = 1 - \left(\frac{A_1}{A_2}\right)^2 \qquad \text{---------- (3.8)}$$

where, $\frac{A_2}{A_1}$ is the passage area ratio. This expression in fact represents the maximum static-pressure rise that can be achieved in incompressible flow if the velocity profile at the diffuser inlet is uniform. If, however, the inlet velocity profile is non-uniform an additional increase in static pressure may be expected due to mixing process.

➢ Ideal pressure-recovery coefficient in presence of mixing, C_m, is given by

$$C_{pm} = \frac{1}{\beta_1^{\,2}}\left[2(\beta_1 - 1) + 1 - \left(\frac{A_1}{A_2}\right)^2\right] \qquad \text{---------- (3.9)}$$

where $\beta_1=\beta=1$ for uniform profile and $\beta_1>1$ for non-uniform profile.
The Equations (3.8) and (3.9) are more appropriate only for incompressible flow.

➢ Actual pressure-recovery coefficient, C_p, is defined by

$$c_p = \frac{p_2 - p_1}{\bar{q}_1} \qquad \text{---------- (3.10)}$$

➢ Diffuser effectiveness (ξ):

The diffuser effectiveness is defined as the ratio of the actual pressure-recovery coefficient to the ideal pressure-recovery coefficient. Corresponding to Equations (8) and (9), there are two definitions for pressure recovery coefficient as follows-

$$\xi = \frac{c_p}{c_{pi}} \qquad \text{---------- (3.11) and}$$

$$\xi = \frac{c_p}{c_{pm}} \qquad \text{---------- (3.12)}$$

3.9 PROCEDURE FOR DIFFUSER ANALYSIS

For the purpose of analysis diffuser is considered as four separate diffusing passages and two mixing passages as shown in Figure 3.5. These passages are as follows:

Diffusing passages → 1-1`, 1`-2, 2-3A, and 2-3B
Two mixing passages → 3A-4A and 3B-4B

The essential element of the diffuser analysis is the evaluation of the performance of a single diffusing passage, including the determination of both the performance parameters and the outlet conditions. Using one or the combination of the following three options listed below can carry out diffuser performance analysis for a single diffusing passage (the specific passages for which they can be used are indicated in the parenthesis):

Option 1: Empirical-Data Method (1-1`, 1`-2, 2-3A, 2-3B)
Option 2: Stream Tube Method (1-1`, 1`-2, 2-3A, 2-3B)
Option 3: Mixing-Equation Method (2-4A, 2-4B)

Out of the above three options mentioned, the stream tube method has been used to carry out the diffuser analysis between Stations 1-3A and 1-3B. Option 3, i.e., Mixing-Equation

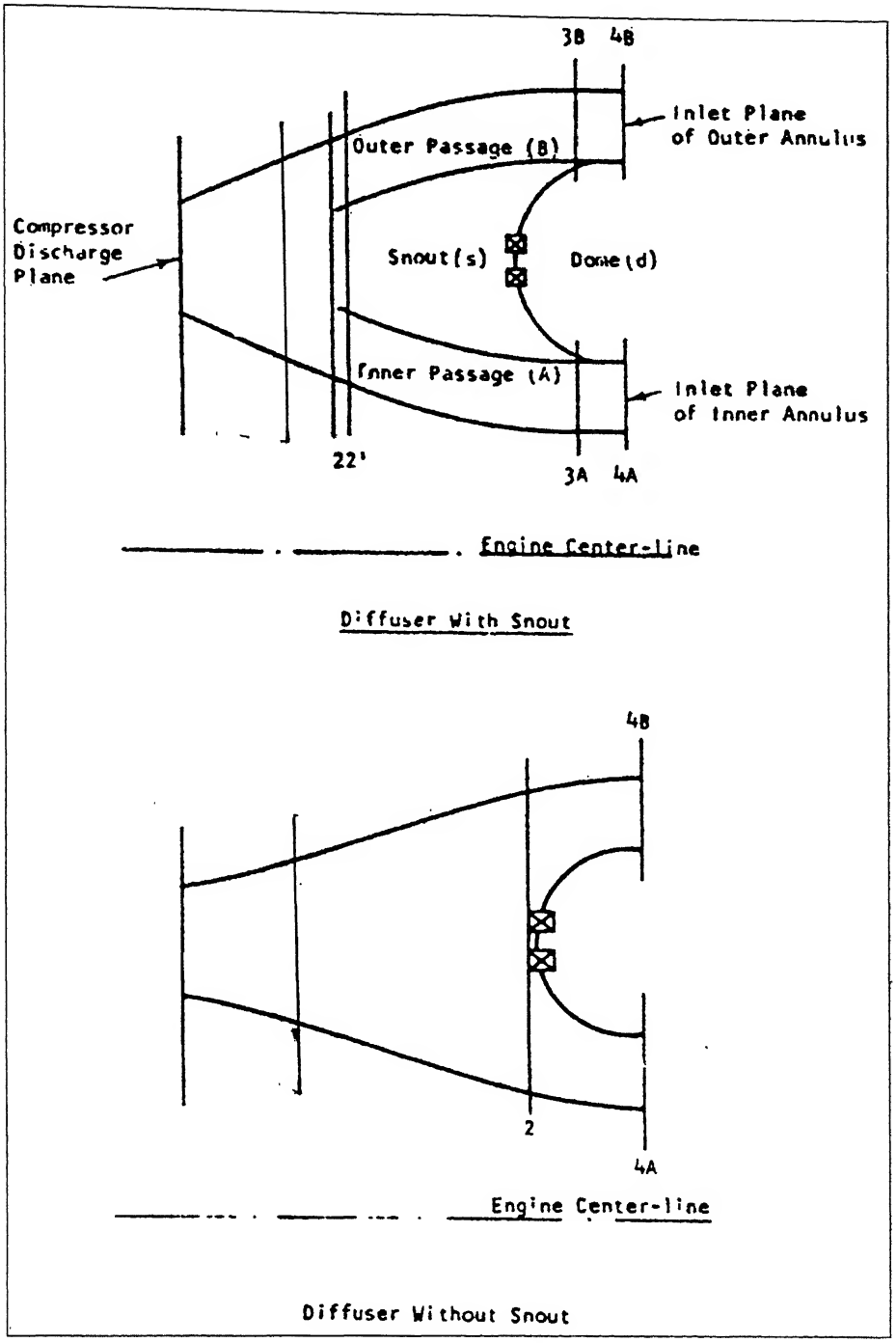

Figure 3.5 Main diffuser calculation stations

Method is always used in mixing passages 3A-4A and 3B-4B, regardless of the option(s) used up to Station 3A and 3B.

In the diffuser analysis, the Empirical-Data Method is not being used here due to lack of sufficient data and its less accuracy as compared the Streamtube method.

3.10 STREAM TUBE METHOD

This method involves a stream tube analysis to calculate development of the velocity profile within the diffuser, as well as an analysis of the wall boundary layer to provide the location of separation points, if any. The model is indicated schematically below. Here the subscripts U and L refer to the upper and lower wall of the passage respectively.

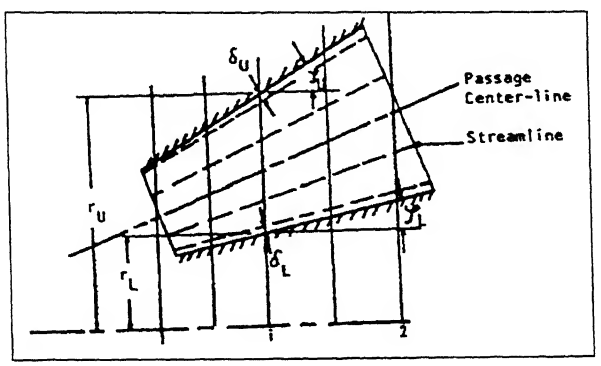

Figure 3.5 Stream tubes in the stream tube method calculation

3.10.1 Assumptions

The following assumptions specific to the stream tube method are made:

- The flow can be represented by a number of stream tubes in each of which the flow is uniform and isentropic.
- The boundary layer is identical to that of a flat plate with the same pressure gradient that exists in the diffuser and its effect on the inviscid flow is to produce an effective displacement of the diffuser wall equal to the displacement thickness of the boundary layer.
- The stream slope varies linearly from one wall to the other at any axial location.
- Separation of boundary layer is assumed to occur when the shape factor (i.e. form factor) H exceeds a critical value, H_{sep} which is an input to the program.
- Subsequent to boundary layer separation, no further static pressure rise occurs in the section of the diffuser being considered.

3.10.2 Input Information Required

The input information required for a stream tube analysis is:

1) The geometry of the diffuser in the form of radial position of each wall as function of axial distance.

2) The following inlet conditions:
   - i) Weighted mean total pressure, P_1.
   - ii) Uniform stagnation temperature, T_{01}.
   - iii) Mass flow rate, m.

iv) A velocity profile given by:

$$\frac{u}{U} = f(y)$$

where U= an arbitrary normalization velocity

f(y)= a tabulated function of $\frac{u}{U}$ against Y

Y = nondimensional annulus height.

v) The boundary layer displacement thickness, δ_1.

vi) The boundary layer shape factor, H_1.

3) The number of stream tubes into which the flow is to be divided, N.
4) An initial estimate of the boundary layer displacement thickness on each wall at every axial location of a geometric input point.

3.10.3 Outline of Method of Solution

The method of solution proceeds in the following steps:

1) The determination of the static pressure at the inlet, and the mass flow, stagnation pressure, and velocity in each stream tube.
2) The calculation of the static pressure at each down stream location (specified by the location of the geometric input points), and the resulting radial location of, and velocities in each stream tube. The first time this calculation is performed, the estimated values of boundary layer blockages at all axial locations (supplied as input) are used; subsequent calculation are based on revised estimates of this blockage.
3) The determination of the boundary layer displacement thickness on each wall, using the static pressure and wall stream tube velocities obtained in step 2.
4) Repeat step 2 and 3 until the displacement thickness determined in step 3 are within a specified tolerance of those used in step 2.

3.10.4 Inlet Conditions to the Stream-Tubes

The inlet conditions for each of N stream tubes are determined as follows (the subscript j refers to a particular stream tube):

1) Calculate the dimensionless coordinate Y_j of the mid point of each (equal area) stream tube from the relations

$$Y_j = \frac{\frac{R_j + R_{j+1}}{2} - R_1}{R_{N+1} - R_1} \qquad \text{---------- (3.13)}$$

where $R_{j+1} = \sqrt{\frac{A_j}{\pi} + R_j^2}$

$$A_j = \frac{\pi}{N}\left(R^2{}_{N+1} - R_1{}^2\right)\cos\left(\frac{\zeta_U + \zeta_L}{2}\right)$$

$$R_1 = r_L + \frac{\delta_L}{\cos\left(\frac{\zeta_L + \zeta_U}{2}\right)}$$

$$R_{N+1} = r_U - \frac{\delta_U}{\cos\left(\frac{\zeta_L + \zeta_U}{2}\right)}$$

At the compressor exit (Diffuser Station 1) it is assumed that

$$\cos\left(\frac{\zeta_U + \zeta_L}{2}\right) = 1$$

2) Find $\frac{u_j}{U}$ for each stream tube by interpolation from the velocity profile (tabulated as a function if Y) provided as input.

3) Calculate ρ_{ch}, a characteristic density to provide a first guess for ρ from

$$\rho_{ch} = \frac{p_1}{R\ T_{o1}} \qquad \text{----------(3.14)}$$

where p_1 is the weight mean total pressure at the inlet.

4) If the static pressure P_1 at inlet is not given, make a first guess at this pressure from

$$p`_1 = p_1 - \frac{1}{2}\rho_{ch}\left(\frac{\dot{m}}{\rho_{ch} A_1}\right)^2 \qquad \text{---------- (3.15)}$$

where $A_1 = NA_j$

5) Calculate the first guess at U from

$$U = \frac{\dot{m}}{\sum_j \frac{u_j}{U}\rho_{ch}\ A_j} \qquad \text{---------- (3.16)}$$

6) Using this value of U, calculate u_j from the results of step 2 and the temperature T_j, from

$$T_j = T_{01} - \frac{u_j^2}{2C_p} \qquad \text{----------} \quad (3.17)$$

7) calculate the density, ρ_j, from

$$\rho_j = \frac{P_j}{R\,T_j} \qquad \text{----------} \quad (3.18)$$

8) calculate U from

$$U = \frac{\dot{m}}{\sum_j \frac{u_j}{U}\rho_j A_j} \qquad \text{----------} \quad (3.19)$$

9) If this value of U is significantly different from the previous value of U return to step 6. If not continue.

10) Calculate the total pressure P_j in each stream tube from

$$\frac{P_j}{P_1} = \left(\frac{T_j}{T_{01}}\right)^{\frac{\gamma}{\gamma-1}} \qquad \text{----------} \quad (3.20)$$

11) Compute the mass flow in each stream tube from

$$\dot{m} = \rho_j u_j A_j \qquad \text{----------} \quad (3.21)$$

and the critical area of each stream tube A_j^* from the usual compressible flow relations.

$$\frac{A}{A^*} = \frac{1}{M}\left[\left(\frac{2}{\gamma+1}\right)\left(1+\frac{\gamma-1}{2}M^2\right)\right]^{(\gamma+1)/2(\gamma-1)} \qquad \text{----------} \quad (3.22)$$

12) If the static pressure at inlet is calculated in step 4, calculate the new value of weight mean total pressure from

$$(P_1)_{new} = \frac{1}{\dot{m}}\sum_j \dot{m}_j P_j \qquad \text{----------} \quad (3.23)$$

where $\dot{m}_j$ = mass flow in the jth stream tube.

13) If this new value of total pressure is significantly different from the given value of total pressure, calculate a new value of P_1 from

$$(P_1)_{new} = P_1 \frac{P_1}{(P_1)_{new}} \qquad \text{---------- (3.24)}$$

and return to step 7.

Hence, the quantities $\dot{m}_j, \rho_j, u_j, A_j^*, P_j$ are known at the inlet to each stream tube. The inlet dynamic head is calculated from

$$\bar{q}_1 = \frac{1}{2}\left(\sum_j \frac{\dot{m}_j}{\dot{m}} \rho_j\right)\left(\sum_j \frac{\dot{m}_j}{\dot{m}} u_j^2\right) \qquad \text{---------- (3.25)}$$

3.10.5 Determination of Stream-tube Properties at Downstream Axial Locations

The conditions in each stream tube at each downstream axial location are determined in an iterative manner by estimating the static pressure at the axial location, computing the resulting total area of the stream tubes, and repeating the procedure until the computed total flow area equals the actual flow area normal to the passage center-line. The actual flow area is determined from the effective wall geometry obtained from the actual wall position and the estimate of boundary-layer displacement thicknesses.

(a) Calculation Procedure:

Subscripts, i → refers to axial location of a geometric input point, and
j → refers to a stream tube.

i) As a first estimate, assume that the relative mid-stream tube streamline slope at i :

$$(\zeta_{rj})_{i+1} = (\zeta_{rj})_i \qquad \text{---------- (3.26)}$$

where $\zeta_{rj} = \zeta_j - \frac{\zeta_L + \zeta_U}{2}$

ζ_j = mid-stream tube streamline slope.

For the first axial location downstream of the inlet, assume

$$(\zeta_{rj})_{i+1} = \left[\zeta_{rL} + \frac{1}{N}(\zeta_{rU} - \zeta_{rL})\right]_{i+1}$$

since the relative streamline slope at the inlet is always assumed to be zero.

ii) Estimate the pressure at the next axial location (i+1) from

$$TA_{i+1} = \sum_{j=1}^{N} \left[\frac{\dot{m}_j^{\,2}/2\rho_j}{\dot{m}_j^{\,2}/\rho_j A_j^{\,2} - \Delta P} \right]_i^{\frac{1}{2}} \left(\cos \zeta_{rj}\right)_i \qquad \text{(3.27)}$$

and $p_{i+1} = p_i + \Delta p$

where TA_i = effective total area at axial location i

$$TA_i = \pi \left[\left\{ \left(r_U - \delta_U \frac{\cos\zeta_{rL}}{\cos\frac{\zeta_U + \zeta_L}{2}} \right)^2 - \left(r_L + \delta_L \frac{\cos\zeta_{rL}}{\cos\frac{\zeta_L + \zeta_U}{2}} \right)^2 \right\} \cos\frac{\zeta_U + \zeta_L}{2} \right]_i$$

iii) Calculate the static to total pressure ratio for each stream tube, p_{i+1}/P_i and determine T_j/T_{o1}, u_j, and A_j at i+1 each from the usual compressible relations.

iv) Compute total flow area based on initial estimate of streamline slope from

$$(TA)'_{i+1} = \left(\sum_{j=1}^{N} A_j \cos \zeta_{rj} \right)_{i+1} \qquad \text{(3.28)}$$

v) Re-estimate the relative slope of each mid-stream tube streamline from

$$\left(\zeta_{rj}\right)_{i+1} = \left[\zeta_{rL} + Y_j(\zeta_{rU} - \zeta_{rL})\right]_{i+1} \qquad \text{(3.29)}$$

where $Y_j = \dfrac{\sum_{k=1}^{j} (A_k \cos\zeta_{rk}) - \frac{A_j}{2}\cos\zeta_{rj}}{\sum_{k=1}^{N} (A_k \cos\zeta_{rk})}$

and k is a dummy index.

vi) Compute revised total flow area based on new estimate of streamline slope from Equation (3.29). Repeat Step 5 until two consecutive values of $(TA)'_{i+1}$ are equal.

vii) If $(TA)'_{i+1}$ does not equal TA_{i+1} obtained from Equation (3.27), then repeat entire process from Step 2 with P_i, ρ_{ji}, A_{ji}, ζ_{ji} in Equation (3.26) being replaced by the current values of p_{i+1}, $\rho_{j,i+1}$, $A_{j,i+1}$, $\zeta_{j,i+1}$.

viii) Continue the preceding process until $p_2, \rho_{j2}, A_{j2}, \zeta_{j2}, u_{j2}$ are obtained at the exit station of the diffuser.

(b) Determination of Boundary Layer Displacement Thickness

With the velocity, u_i, and density, ρ_i, in the bounding stream tubes (j=1 and j=N) known, a new estimate of the boundary layer displacement thickness along each wall is made in the following way:

i) The momentum thickness at each axial Station i is computed from the following relation, using the momentum integral equation for boundary layers:

$$\theta_{j,i+1} = \left[\theta_{j,i}^{1/6} \left(\frac{u_{j,i}}{u_{j,i+1}} \right)^{25/6} \left(\frac{\rho_{j,i}}{\rho_{j,i+1}} \right)^{7/6} + \frac{0.0076\, \nu^{1/6}}{\rho_{j,i}^{7/6}\, u_{j,i+1}^{25/6}} \int_{x_o}^{x} u_j^{4}\, \rho_j^{7/6}\, dx` \right]^{6/7} \quad \text{---------- (3.30)}$$

where j=1 or N referring to L and U walls, respectively. And

$$x`_{i+1} - x`_i = (x_{i+1} - x_i) \frac{1}{\cos\left[\left(\frac{\zeta_U + \zeta_L}{4} \right)_i + \left(\frac{\zeta_U + \zeta_L}{4} \right)_{i+1} \right]} \quad \text{---------- (3.31)}$$

ii) The shape factor, H, of the boundary layer along each wall is computed from the relationship Dussord [30]:

$$\Delta H_{j,i+1} = H_{j,i} + 70(H_{j,i} - 1.05) \frac{d\theta_j}{dx} \quad \text{---------- (3.32)}$$

H_j is never permitted to be less than 1.1, since this relationship is not valid for highly accelerating flows, and since the characteristics of the boundary layer when subjected to highly favorable pressure gradient are of little interest in the present application. H_j is also not permitted to exceed 3.5 as this value exceeds any reasonable separation value.

iii) For all axial location at which H does not exceed H_{sep} (critical value of H at which separation takes place) on either wall, calculate the resulting displacement thickness along each wall from:

$$\delta`_{j,i} = H_{j,i}\, \theta_{j,i}$$

For axial location where $H > H_{sep}$ on either wall, proceed to step v.

iv) Since this value of displacement thickness tends to interact substantially with the bounding stream tube velocity, a new estimate of the displacement thickness is determined from the following relation:

$$\delta_{j,i} = \delta_{oj} + 0.2\frac{\delta`_{j,i} - \delta_{0j,i}}{\left|\delta``_{j,i} + \delta_{oj,i}\right|} \qquad \text{----------} \quad (3.33)$$

where the subscript o refers to the initial estimate supplied as input to the boundary layer calculation. $\delta``_{j,i}$ and $\delta``_{N,i}$ are determined from the solution to the following equations as shown below [35]:

$$\left(\psi_{j,i}+1\right)\delta``_{j,i} + \psi_{j,i}\,\delta``_{N,i} = \delta`_{j,i}\left[1-\psi_{j,i}\right] + \psi_{j,i}\left(\delta_{o1}+\delta_{oN,i}\right)$$

$$\left(\psi_{N,i}+1\right)\delta``_{N,i} + \psi_{N,i}\,\delta``_{j,i} = \delta`_{N,i}\left[1-\psi_{N,i}\right] + \psi_{N,i}\left(\delta_{o1,i}+\delta_{oN,i}\right)$$

where,

$$\psi_{j,i} = \frac{\delta`_{j,i}}{r_U - r_L}\left[240\frac{\left(H_{oj,i}-1.05\right)}{H_{j,i}}\cdot\frac{\theta_{j,i}}{x`_i - x`_{i-1}} + \frac{24}{7}\right]$$

$$\psi_{j,i} = 70\frac{\left(H_{oj,i}-1.05\right)}{H_{j,i}}\cdot\frac{\Delta\theta_{j,i-1}}{x`_i - x`_{i-1}}$$

$$\Delta\theta_{j,i-1} = -3.3\;\theta_{j,i-1}\frac{\delta``_{j,i-1}+\delta``_{N,i-1}-\delta_{o1,i-1}-\delta_{oN,i-1}}{r_{U,i-1}-r_{L,i-1}}$$

if no separation occurs along either wall at any axial location, proceed to Step vii.

v) If $H>H_{sep}$ on either wall at any axial location, set H=3.5 on the separated wall for reference purposes, and calculate the displacement thickness along the separation wall from, for example:

$$\left(r_L\cos\zeta_{c1}+\delta_1\cos\zeta_{rL}\right)_i = \sqrt{\left(r_U\cos\zeta_{c1}-\zeta_N\cos\zeta_{rU}\right)_i^2 - \frac{(TA)_{sep}\cos\zeta_{c1,i}}{\pi}}$$

where, $(TA)_{sep}$= effective flow area at the separation point

$$= \pi\left\{\frac{\left(r_U\cos\zeta_{c1}-\delta_N\cos\zeta_{rU}\right)^2 - \left(r_L\cos\zeta_{c1}+\delta_1\cos\zeta_{rL}\right)^2}{\cos\zeta_{c1}\cos\frac{\left(\zeta_{rL}+\zeta_{rU}\right)}{4}}\right\}_{sep}$$

and $$\zeta_{c1} = \frac{\zeta_U + \zeta_L}{4}$$

This assumes that the static pressure and the flow area remain constant after separation.

vi) In the separated flow region, estimate the new value of displacement thickness from:

$$\delta_{j,i} = \frac{1}{2}\left(\delta_{0j,i} + \delta`_{j,i}\right)$$

vii) If the newly estimated values of $\delta_{j,i}$ are not equal to the originally estimated ones, $\delta_{oj,i}$, return to the stream tube calculation with the newly estimated value. Repeat both stream tube and boundary- layer calculations until agreement is obtained.

3.10.6 Determination of Diffuser Performance Parameters and Outlet Conditions

The diffuser performance parameters are calculated in the following way:

- Ideal pressure-recovery coefficient

$$c_{pi} = 1 - \left(\frac{A_1}{A_2}\right)^2 \qquad \text{---------- (3.34)}$$

- Actual pressure recovery coefficient

$$c_p = \frac{p_2 - p_1}{\bar{q}_1} \qquad \text{---------- (3.35)}$$

where $\bar{q}_1$ is the inlet dynamic head.

- Diffuser effectiveness

$$\xi = \frac{c_p}{c_{pi}} \qquad \text{---------- (3.36)}$$

- The blockage due to displacement thickness

$$E_{bl} = 1 - \frac{\left(r_{U2} - \delta_{U2}\cdot\frac{\cos\zeta_{rU2}}{\cos\zeta_{c12}}\right)^2 - \left(r_{L2} + \delta_{L2}\cdot\frac{\cos\zeta_{rL2}}{\cos\zeta_{c12}}\right)^2}{r_{U2}^{\,2} - r_{L2}^{\,2}} \qquad \text{-------- (3.37)}$$

- The outlet conditions of p_2, ρ_2, $u_2(r)$ are directly available from the procedure, as well as ρ_j , u_j , m_j, A_j , for each stream tube.

➢ **Pressure Loss for a Dump Diffuser**

The pressure loss for a dump diffuser was can be estimated in the range $0.2<Ai/A_e<1$ by the equation(Barclay, 1972),

$$\frac{P_{te}}{P_{ti}} = EXP\left\{-\frac{\gamma}{2}M_i^2\left[\left(1-\frac{A_i}{A_e}\right)^2+\left(1-\frac{A_i}{A_e}\right)^6\right]\right\} \qquad \text{---------- (3.38)}$$

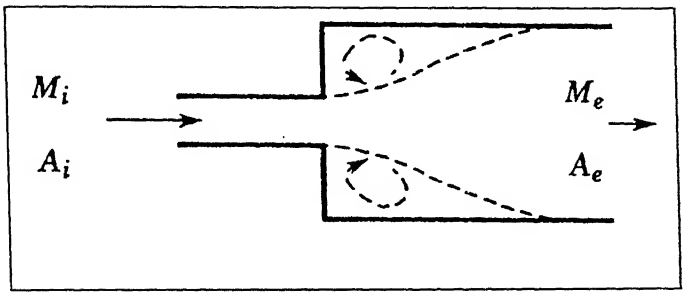

Figure 3.6 Model dump diffuser

For example, given the following dump diffuser data:
$A_e/A_i = 5.0$, $M_i = 0.5$, and $\gamma = 1.4$. Using above equation (3.41) gives

$$P_{te}/P_{ti} = 0.854$$

3.11 LIMITATIONS OF THE METHOD

The major limitations of the method are as follows:

i) Diffusers which are highly curved or in which streamline curvature effects are otherwise important cannot be treated. In these cases, the static pressure gradients across the passage are significant.

ii) The results of the method tend to be quite sensitive to the inlet boundary layer properties; an accurate estimate of these properties at the diffuser inlet is difficult in practical situations.

iii) The determination of location of separation is subject to error.

iv) Dump diffuser analysis is difficult to carryout in this method as flow becomes turbulent. Assumption that the nature of flow being one-dimensional is no more valid in this region. Vortex formation and eddy losses are the dominant phenomena in this case. Two-dimensional analysis or the use of empirical correlation is capable of predicting dump losses.

The method does, however, represent a substantial improvement over the empirical data method.

3.12 MIXING EQUATION METHOD

The mixing equation method can only be applied to the diffusing passages 2-4A and 2-4B.

3.12.1 Assumptions

The assumptions employed in the method are:

i) The losses in the diffusing process can be represented as the some of mixing losses, losses due to curvature of the passage, and expansion or contraction losses at the snout or cowl lip.

ii) The mixing losses can be evaluated from the determination of the pressure recovery coefficient for incompressible flow.

3.12.2 Input Information Required

The information required in the mixing- equation method is:

i) The geometry of the passage, in terms of inlet area, exit area, the total angle difference between the slope of the passage center-line at inlet and that at exit, and the mean radius of curvature of the passage center-line.

ii) The inlet conditions defined by $\dot{m}$, p_1, q_1, and β_1; the subscript 1 here refers to condition determined at diffuser Station 2.

iii) The ratio of the area at diffuser station 2 occupied by the mass flow in the annulus under consideration to the annulus area normal to the engine center line at diffuser station 2`, A_{th}/A_2, i.e., for inner annulus

$$(A_{th})_{2A} = \pi\left[(r_{th})_{2A}^{\ 2} - (r_{2A})^2\right] \qquad \text{---------- (3.39)}$$

where, $(r_{th})_{2A}$ is determined from

$$\dot{m} = \int_{r_{2A}}^{(r_{th})_{2A}} 2\pi r \rho u dr \qquad \text{---------- (3.40)}$$

where, $\dot{m}$ = mass flow in inner annulus

r_{2A}= radius of inner casing at station 2A

ρ, u = properties form diffuser solution at Station 2A

A similar calculation may be performed for the outer annulus.

3.12.3 Development of Mixing Equation for Incompressible flow

(a) Solution Procedure

The method of solution proceeds in the following steps:

i) Calculate diffuser performance between Stations 1 and 2, and the outlet conditions at 2, by either the empirical data or stream tube method.

ii) Determine inlet conditions for the second stage of diffusion in a form suitable for the diffuser analysis methods to be used between Stations 2-3A and 2-3B and the inlet conditions to the snout (if any).

iii) Determine the stagnation pressure on the dome or cowl.

iv) If the diffuser has no snout, determine the inlet conditions to the annuli by assuming an isentropic expansion around the dome.

v) If the diffuser has a snout, calculate the diffuser performance between Stations 2-4A and 2-4B and the outlet conditions at 4A and 4B, by using the empirical data method or stream tube method between Stations 2-3A and 2-3B and a mixing analysis between stations 3A-4A and 3B-4B, or by using the mixing equation method between Stations 2-4A and 2-4B.

When the stream tube or empirical data methods are used between stations 2-4, it is always implied that the methods are used between Stations 2-3 followed by a mixing analysis between Stations 3-4.

For diffusers without snouts (or cowl), the analysis of the flow between Stations 2-4 is independent of the option employed between Stations 1-2.

(b) Inlet Conditions for the Second Stage of Diffusion

For diffusers without snout or cowl, the only additional information required is the mass flow split, $\dot{m}_A$, $\dot{m}_B$, $\dot{m}_S$. This is supplied as input from the airflow subprogram.

For diffusers with snout, the information required in addition to the mass flow split, consist of the flow properties A_{th}, u_a, β (or E) to be associated with the flows into the inner annulus, the outer annulus, and the snout or cowl. **Using stream tube method these can be obtained, between Stations 1-2, as below:**

i) The area of the passage at station 2, $A_{th,2A}$ and $A_{th,2B}$, which are occupied by the mass flow $\dot{m}_A$ and $\dot{m}_B$ are determined from Equations

$$(A_{th})_{2A} = \pi\left[(r_{th})_{2A}^2 - (r_{2A})^2\right] \text{ and } \dot{m} = \int_{r_{2A}}^{(r_{th})_{2A}} 2\pi r \rho u dr \qquad \text{---------- (3.41)}$$

applied to both mass flows. Then $A_{th,2S}$ is determined from the equation:

$$A_{th,2S} = A_2 - A_{th,2A} - A_{th,2B} \qquad \text{---------- (3.42)}$$

where, A_2 is the total mass flow at the combustor inlet.

ii) The inlet area average velocities are determined from

$$\bar{u}_{a,2A} = \frac{1}{A_{th,2A}} \int_0^{A_{th,2A}} u dA \qquad \text{---------- (3.43)}$$

and a similar equation for $\bar{u}_{a,2B}$.

iii) The inlet velocity profile parameters are calculated from

$$\beta_{2A} = \frac{\int_0^{A_{th,2A}} u^2 dA}{A_{th,2A}\,\bar{u}_{a,2A}} \qquad \text{----------} \quad (3.44)$$

and a similar equation for β_{2B}. It is assumed that $\beta_{2S}=1$.

For the purpose of the diffuser analysis between Stations 2 and 3, the areas of diffusing passages at Station 2` are assumed to be

$$A_{th,2A} = A_{th,2A} \cos \varsigma_{C,A} \qquad \text{----------} (3.45)$$

and

$$A_{th,2B} = A_{th,2B} \cos \varsigma_{C,B\ A} \qquad \text{----------} (3.46)$$

where ς_C angle of the slope of the passage centerline relative to the axis of the combustor. This assumes in effect that the inlet areas to the annular diffusing passages are the areas occupied by respective flows at Station 2, projected normal to the passage centerline.

iv) The inlet dynamic head at the diffusing passages are calculated from:

$$\bar{q}_{2A} = \frac{1}{2}\frac{\dot{m}_A (\beta_{2A})^2 \bar{u}_{a,2A}}{A_{th,2A}} \qquad \text{----------} (3.47)$$

and a similar equation for $\bar{q}_{2B}$. The inlet dynamic head at the snout or cowl is determined from:

$$\bar{q}_{2S} = \frac{1}{2}\frac{\dot{m}_s \bar{u}_{m2}}{A_{th,2S}} \qquad \text{----------} (3.48)$$

(c) Conditions on the Dome

If the diffuser has no snout or cowl, the stagnation pressure on the dome is assumed to be constant and is determined by

$$P_d = P_2 + (1 - K_d)\bar{q}_{2A} \qquad \text{----------} (3.49)$$

where $\bar{q}_2 = \frac{1}{2}\bar{\rho}_2 (\bar{u}_{m2})^2$

The coefficient K_d is an input quantity representing the number of dynamic heads lost in the mixing and flow processes occurring around the dome. The magnitude of K_d will depend upon the shape of the dome and the effectiveness of the diffuser between Station 1

and 2, and is difficult to determine a priori. It is expected that its value would be in the range 0.2 – 0.5.

For diffusers with snout (or cowl), the static pressure just inside the snout, $P_{2S`}$, is determined by assuming a sudden contraction or expansion process between the areas $A_{th,2s}$ and $A_{2S`}$ (the actual geometric areas of the snout entrance)

$$\bar{q}_{2S`} = \left(\frac{A_{th,2s}}{A_{2s`}}\right)^2 \bar{q}_{2s} \qquad \text{---------- (3.50)}$$

The total pressure on the dome is then calculated from

$$P_d = P_{2s`} + (1-K_d)\bar{q}_{2s`\,A} \qquad \text{---------- (3.51)}$$

where K_d is an input quantity representing the number of dynamic heads lost.

(d) Diffuser Performance between diffuser outlet and Annuli diffusion region (Stations 2 and 4)

The procedure for determining the performance of the diffusing passage between Stations 2 and 4 depends upon the diffuser analysis method employed. **Using stream tube method the procedures are as follows:**

In the stream tube method, three steps are involved since the basic stream tube analysis is only applicable between Stations 2 and 3, and do not consider any loss due to expansion or contraction of the flow at the snout lip.

The steps are as follows:

1) A basic stream tube analysis, as previously described, is performed between Stations 2A-3A and 2B-3B. The inputs required for this analysis are $\dot{m}$, $A_{th_{2A`}}$, P_2, $u_2(r)$, δ_{2A}, H_{2A} and similar set for the outer annulus. In addition it is assumed that the boundary layer properties on the snout lip are δ=0 and H=1.4. The only calculated quantities which are used subsequently are the static pressure, P_{3A} and P_{3B} and the profile parameters, β_{3A} and β_{3B} which are computed from Equation (3.47) applied to the Stations 3A and 3B.
2) It is assumed that the profile mixes to a uniform one between Stations 3 and 4. The static pressure at Station 4 in the absence of area mismatch at the snout lip is accordingly obtained from Equation:

$$\frac{P`_{4A} - P_{3A}}{\bar{q}_{3A}} = \frac{1}{\beta_{3A}^{\,2}}\left(1+\frac{A_{3A}}{A_{4A}}\right)\left(\beta_{3A} - \frac{A_{3A}}{A_{4A}}\right) \qquad \text{---------- (3.52)}$$

3) The effects of any area mismatch at the snout are crudely approximated by assuming that the total-pressure loss between Stations 2 and 4 due to this process is given by the sudden expansion or contraction relations, and that this loss may be applied directly at Station 4; i.e., for example, in the inner annulus:

$$\frac{P_{4A} - P`_{4A}}{q_{2A}} = \frac{1}{2}\left(1 - \frac{A_{2A`}}{A_{th,2A`}}\right)\left(\frac{A_{th,2A`}}{A_{2A`}}\right)^2 \qquad \text{---------- (3.53)}$$

if $\frac{A_{2A`}}{A_{th,2A'}} < 1$, then $P`_{4A}$ is the total pressure corresponding to $P`_{4A}$, T_o, $\dot{m}_A$, and A_{4A}.

3.13 LIMITATIONS OF THE DIFFUSER SUBPROGRAM

The analytical methods used in the diffuser subprogram contain several limitations:

- Flow in the diffuser is assume to be unaffected by downstream conditions. If the flow is well matched at the cowl, this assumption is expected to be valid. Otherwise, serious errors will undoubtedly result. Cowl design should, therefore, receive careful attention.
- No provision is made for including splitter vanes in the diffuser analysis.
- The program does not attempt to treat flow after separation.

3.14 STRUCTURE OF THE SUBPROGRAM

The diffuser subprogram consists of:

- A subroutine which sets up starting conditions and directs the diffuser calculation through the other subroutines in the appropriate sequence.
- A group of subroutines which perform the stream tube analysis.
- A group of library subroutines which provide gas properties and interpolation procedures.

Subroutines and flowchart of the diffuser subprogram is given in the Appendix A2.

CHAPTER 4

AIR-FLOW ANALYSIS OF MAIN COMBUSTOR

4.1 COMBUSTION CHAMBER FLOW PATH ANALYSIS

Analysis of the combustion chamber flow path is closely related to, and proceeds in parallel with, the inlet diffuser analysis. These analyses must be coordinated because the combustor cowl and passage contours are very important to successful diffuser operation. Conversely, diffuser pressure recoveries must be known in order to select appropriate cooling and dilution hole sizes to get the specified flow distribution.

For most applications, the preferred flow path is the shortest one that meets all design requirements. Increased length adds weight to the engine and requires more liner cooling flow, which reduces available combustor air.

4.2 PERFORMANCE PARAMETERS

The main performance parameters for an annular combustion chamber are (see Figure 4.1):

- **Combustor dome height (H_d):** the dome height of the combustor is important because it has a significant effect on altitude relight capability. The dome height must be large enough to permit the combustion system to satisfy the altitude relight requirements of the engine.

- **Combustor dome velocity (V_d):** the combustor dome velocity is defined as the average velocity for all of the combustor dome flow, immediately downstream of the dome, between the inner and outer combustor liners. In general, combustion flame stability is reduced as dome velocity is increased.

- **Combustor length to dome height ratio (L_c/H_d):** all combustors must have sufficient volume and length to accommodate a low-velocity flame stabilization region and a higher velocity mixing region, where the hot combustion products are mixed with the excess dilution air. The total necessary volume depends on space rate, residence time and other loading parameters, but the overall flow pattern required is well established. The desired flow patterns determine, to a large extent, the overall shape of the combustor, as defined by the combustor length to dome height ratio (L_c/H_d). Since the basic flow patterns can be scaled to larger and smaller sizes, L_c/H_d is essentially independent of engine size. Therefore, L_c/H_d provides a useful means of comparing the combustors of different engine models.

- **Combustor passage velocity (V_p):** liner passage velocity for a combustion system is the velocity of the flow between the inner and outer annulus of the system. The passage velocities depend on the mass flow rate and passage flow area, but it is defined as the velocity at the dome exit plane with the total passage air flow. The passage velocities should be low enough to provide a uniform flow to the

combustor with high static pressures and low total pressure losses in the passages, and high enough to provide good convective cooling of the combustor liner.

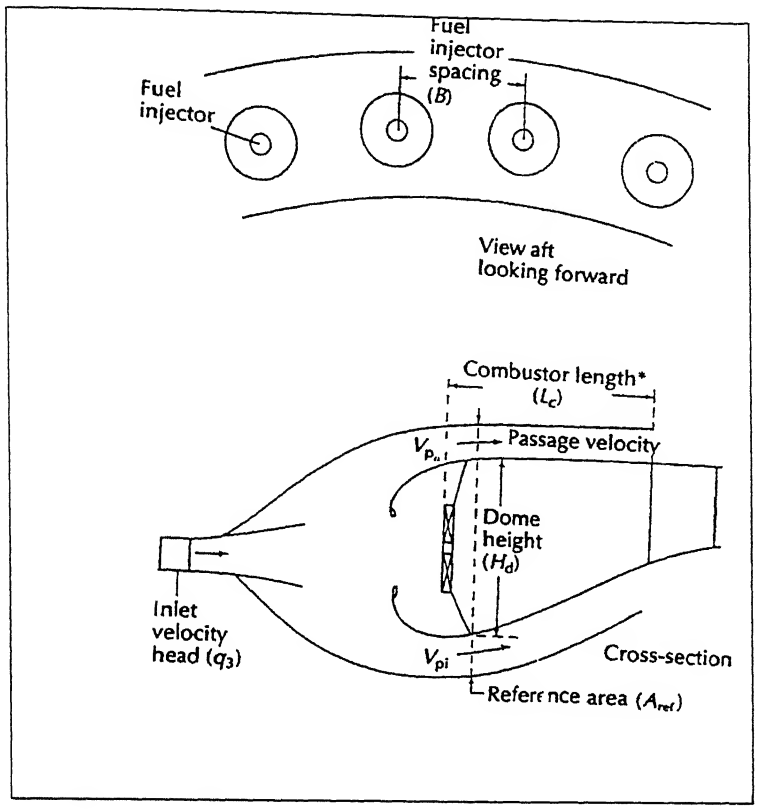

Figure 4.1 Combustor chamber variables

- **Fuel injector spacing (B):** ideally, for good combustion system performance, the fuel should be injected at an optimum number of points. However, practical considerations usually limit the number of fuel injectors to a few only than optimum number. Fuel injectors along with the swirl cups which are used with each injector, are costly and heavy. Also, a large number of injectors increases maintenance time and costs. The ratio of combustor length, L_c, to circumferential spacing of fuel injectors, B, is a critical design parameter. If the fuel injectors are too widely spaced and the L_c/B parameter is too low, high-temperature regions may appear downstream of each fuel injector at the turbine inlet plane which may cause the pattern factor to be too high to meet requirements.

- **Space rate (SR):** the combustion system space rate is a measure of the fuel energy released per unit volume of the combustion chamber.
- **Reference area (R_{ref}):** it is the area at the point of maximum flow area between the combustor casings.

- **Reference velocity (V_{ref}):** it is a measure of an "average" velocity through the entire cross-section area between the inner and outer casing walls of the combustion chamber. This velocity affects the residence time of fuel-air mixtures in the burner

and the basic flame stability of the system. Although the reference velocity does not describe a physical velocity at any particular place in the system, this parameter provides a convenient method of comparing different designs. The reference velocity is calculated based on compressor exit flow, and air density calculated using compressor exit total pressure and total temperature.

Reference velocity can also be defined in terms of the maximum combustor cross-sectional area.

- **Reference velocity head (q_{ref}):** the reference velocity head is the difference between total and static pressure at the inlet air density and velocity.

$$q_{ref} = \tfrac{1}{2}(\rho_3 V^2_{ref})$$

The magnitude of q_{ref} relative to pressure drop across the combustor dome and liners is important to uniform air distribution and good dilution jet penetration.

- **Inlet velocity head (q_3):** it is the difference between total and static pressure at the compressor discharge.

$$q_{ref} = \tfrac{1}{2}(\rho_3 V^2_3) = P_{T3} - P_{S3}$$

4.3 AIRFLOW DISTRIBUTION

Combustor airflow is distributed to different combustor locations to achieve different design goals. Flows are generally specified as a percentage of total combustor airflow. The airflow distribution does not vary significantly with combustor operating conditions.

The most important airflows are:

1) Compressor exit flow.
2) Turbine cooling airflow which bypasses the combustor.
3) Combustor air flow (1-2)
4) Fuel atomizing airflow admitted through the fuel injectors to the fuel into small drops.
5) Swirler airflow admitted through a swirler around the atomizer to provide a strong, well-mixed recirculation zone within the primary zone.
6) Primary air jets which interact with the swirler flow to close the primary, zone provide rapid fuel-air mixing and oxygen to complete combustion reaction in the secondary zone.
7) Dilution air jets down stream of the primary zone to provide the desired exit temperature profile.
8) Dome cooling airflow.
9) Liner cooling airflow.
10) Combustor dome flow (4+5+8)

4.4 DOME AIR FLOW

Dome flow consist of fuel atomizing flow, swirler flow and dome cooling air flow

a. **Fuel atomizing flow**: the atomizer airflow should be at least two to three times atomizer fuel flow. Lower levels of atomizing flow will reduce the atomization. Higher levels will tend to reduce lean blow out capability.

b. **Swirler flow:** the swirler is used to set up a recirculation zone for stability and to provide good fuel/air mixing for low smoke. For the sake of low power combustor efficiency and lean stability, a swirler flow level much higher than the nominal 11% is not recommended.

c. **Dome cooling flow:** the last component of dome flow is dome cooling air flow. Dome cooling flow is estimated based on the total area to be cooled (dome area less exit area), and a cooling rate based on previous experience. For a typical combustor, dome-cooling flow will be 10 – 15% of combustor airflow.

4.5 COMBUSTOR LINER AIRFLOWS

The combustor liner flows are mainly through primary, secondary and dilution holes. The primary holes are typically located at an axial location about one dome height downstream of the dome. Primary air serves two purposes. First, part of the primary air interacts with the atomizing and swirler airflows and a portion of the dome cooling air to prevent smoke formation in the primary zone. Second, all of the primary air, along with all atomizing, swirler and dome cooling air is needed to reduce the overall equivalence ratio down stream of the primary holes to less than stoichiometric, thereby providing oxygen to complete the combustion reactions initiated in the primary zone. The zone immediately downstream of the primary zone is called the secondary zone. Secondary hole airflows ensures the complete combustion of the combustible mixture that was burnt in the primary zone. The remainder of combustor airflow is available for liner dilution holes down stream of the secondary zone. Dilution airflow helps in getting desired temperature profile at the combustor outlet or turbine inlet.

4.6 DETAILED FLOW ANALYSIS

As a minimum, a detailed one-dimensional flow analysis is needed to determine pressure distributions within the liner passages and combustion chamber. Total and static pressure distributions throughout the system are required to determine dilution and cooling hole sizes necessary to obtain desired airflow distribution.

For one-dimensional analysis, combustor is divided into a large number of short segments. The start of each segment is defined by two axial positions or stations as shown in Figure 4.2. The first station is normally at combustor dome. An additional station is located on the centerline of each row of liner dilution or cooling holes.

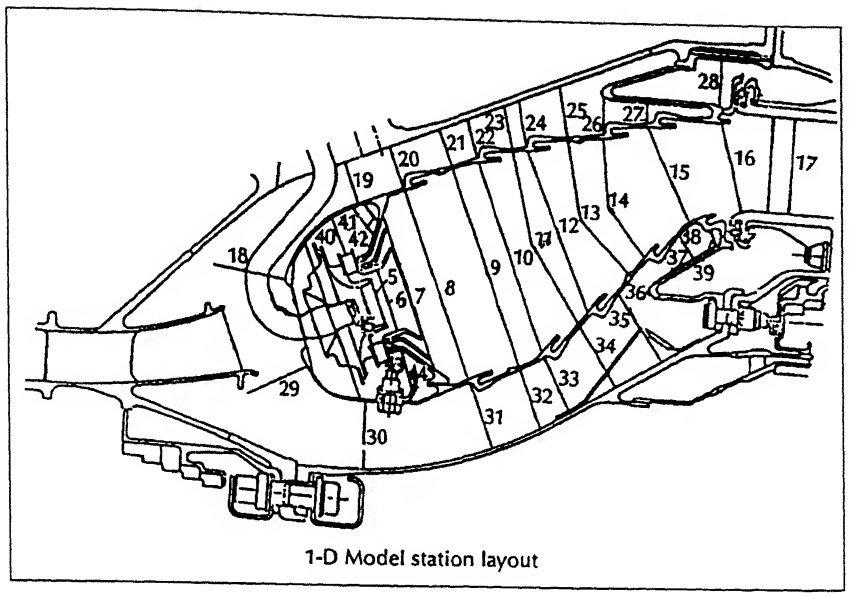

Figure 4.2 Layout for one-dimensional combustor analysis

The basic compressible equations are solved at each station. The initial pressures are based on passage recoveries calculated on diffuser analysis. Between calculation stations, the effects of friction losses and momentum exchange between the dilution jets and internal flows are calculated and results are reflected in calculations at the next station. An interactive solution procedure is used to balance flow and pressure distribution.

4.7 ANALYTICAL METHODS AND PROGRAM DEVELOPMENT

4.7.1 Objective of the Airflow Subprogram

The main objectives of the airflow subprogram are:

- To calculate the air mass flow and pressure distribution in the flame tube and annuli and, hence, the overall pressure loss.
- To provide a starting point for the heat transfer calculation by working out the temperature and velocity distribution of the gases in the flame tube and annuli.

To facilitate analysis, flow in the combustor is broken down into distinct but interacting streams:

1. The annulus air (inner and outer annuli).
2. The air flowing into the flame tube through:
   (a) Swirler.
   (b) Dome holes.
   (c) Penetration holes in the flame tube.
   (d) Wall cooling slots in the flame tube.
3. The mixture of fuel, air, and combustion products flowing through the primary zone (the flame tube up stream of the secondary holes).
4. Parallel streams flowing through the flame tube down stream of the primary zone:
   (a) The hot stream, a mixture of combustion products, unburned fuels, and air.

(b) The cold streams, those portions of the penetration jets and wall cooling films, originating upstream, that remain unmixed at a given axial position.

The following sections give a detailed description of the calculation methods.

4.7.2 Assumptions

The air flow calculation rests on the following main assumptions:

- The primary zone can be treated as a stirred reactor:
  a) Static pressure, temperature, and fuel air ratio are uniform through out the zone.
  b) Mixing and burning occur instantaneously.
  This is one of the major simplifications in this work. It is particularly invalid at low pressures.
- The flow can be considered to be one-dimensional. This represents a considerable simplification, particularly in the case of the gases in the flame tube.
- The rate of fuel burning as a function of axial length can be specified as input. This assumption makes the calculations easier but a realistic estimate of the fuel burning rate will be difficult to make, particularly (as mentioned above) at low pressures. If the fuel air ratio at any axial position, which will not be known in advance, exceeds the stoichiometric value, the excess fuel is assumed to be available for burning at the next downstream position.

4.7.3 Calculation Procedure

In calculating the flow conditions throughout the combustors, the air flow subprogram goes through the following routine for each iteration on the mass flow split:

1. The mass flow rate through the dome is obtained from the flow split, and the total pressure on the dome is obtained from the diffuser calculation.
2. The pressure drop across the dome to the primary zone is found by equating the combined swirler and the dome hole flows (functions of pressure drop) to the total dome flow.
3. With the primary zone static pressure established, flow conditions in the annulus and the flow through flame tube holes into the primary zone are computed for calculation stations up to secondary holes (the end of primary zone).
4. The portion of the secondary hole flow that recirculates into the primary zone is calculated, either directly by the program or from a fraction specified as input.

All of the contributions to the primary zone air flow (through the swirler, dome holes, and flame tube holes up to the secondary holes) are now known. In addition, the fuel flow into the primary zone is known from input.

5. The temperature rise due to combustion is calculated for the primary zone treated as a stirred reactor. (Excess fuel above stoichiometric is carried downstream). Flow conditions at the end of the primary zone are then found.

For the remainder of the calculation the combustor is divided into axial control volumes bounded by adjacent calculation stations k and k+1.Calculations proceed down stream

from station to station. In general, the flow conditions at the upstream station, k, are known from the results of the previous calculation step. **Conditions at the downstream station are found as follows:**

6. From the annulus to flame tube pressure drop at station k the mass flow rate through the holes just downstream of k is found. The mass flow remaining in the annulus is then known.
7. For the annulus, the equations of continuity, momentum, energy, and state are solved for the pressure, temperature, velocity, and density at station k+1.
8. Correlations for flow and mixing of wall and penetration jets are used to compute the fluxes of mass, momentum and enthalpy contained in the jets entering the control volume (through holes at stations k and in the form of residual jets originating upstream of k) and leaving the control volume (residual jets at k+1). The net transfer of mass, momentum, and enthalpy from the jets into the main gas stream in the flame tube may thus be found.
9. The equations of momentum, energy, continuity, and state are written for the hot stream in the flame tube (excluding residual jets) between stations k and k+1. Heat addition is included for fuel burned, up to stoichiometric; any excess fuel is carried downstream. The solution of these equations yields the temperature, pressure, density, and mass flow at station k+1.

The sections that follow describe the detailed calculations that are performed in each of the above steps.

(a) Flow through Holes and Swirler

The mass flow rates through the holes in the dome and in the flame tube walls are calculated from the discharge equation:

$$m_h = C_d A_h \left(2 \rho_{an} \left(p_{an} - p_{ft}\right)\right)^{\frac{1}{2}} \qquad \text{---------- (4.1)}$$

where P_{an} = total pressure in annulus

$= P_{an} + q_{an}$

$q_{an} = \rho_{an} u^2_{an}/2$

C_d = discharge coefficient

= 0.6 for dome holes; for other holes types the data are drawn from [10], [11], [12], [13], [14], and [15].

(b) Pressure- Ratio Correction

The effect of flame tube velocity on discharge coefficient can be predicted by [14]:

$$C_d = C_d^1 \left(0.75+0.25\ p_{an}/p_{ft}\right) \qquad \text{---------- (4.2)}$$

where C_d = actual discharge coefficient which is a function of pressure ratio.

C_d^1 = corrected discharge coefficient which is independent of pressure ratio.

(c) Swirler Flow

The equation used in the program to determine the flow through a swirler is given [16]:

$$\frac{\Delta P_{sw}}{q_{ref}} = \left[\frac{A_{ref}^2}{A_{sw}^2} \sec^2 \beta_{sw} - \frac{A_{ref}^2}{A_{ft}^2} \right] \frac{m_{sw}^2}{m_{ref}^2} \qquad \text{---------- (4.3)}$$

where A = area
m = mass flow
q = dynamic head
β = swirler angle
sw = swirler
ref = reference conditions
ft = flame tube
K_{sw} = constant
= 1.3 for straight bladed swirlers; and 1.15 for curved wall swirlers.

(d) Recirculation

In an actual combustor a complex pattern of recirculating flow exists, particularly in the primary zone. The fraction of secondary hole air flowing into the primary zone, $m_{sy,p}/m_{sy}$, may be specified as input to the computer program; $m_{sy,p}/m_{sy} = 0$ if not specified as input to the program. It may be generated in the program from the following empirical formula [17]:

$$\frac{m_{sy,p}}{m_{sy}} = 0.5 \sin \varphi \left[\frac{T_{an}}{T_{ft}} \right]^{1/2} \qquad \text{---------- (4.4)}$$

The air entering the primary zone by recirculation from the secondary holes is treated in exactly the same way as air entering through swirler, dome and wall holes. Air going down stream is treated as ordinary penetration jet air.

(e) Primary Zone of Flame Tube

The pressure in the primary zone, p_1, is found from the pressure in the diffuser upstream of the dome, obtained by the diffuser subprogram, and the pressure drop across the dome, which is a function of the flow through the dome and the characteristics of the swirler and the dome holes:

$$P_d - p_1 = \frac{m_d^2}{2\rho_{ref} \left[A_{dh} C_{dh} + 1 \Big/ \sqrt{K_{sw} \left[\frac{\sec^2 \beta_{sw}}{A_{sw}^2} - \frac{1}{A_{ft}^2} \right]} \right]^2} \qquad \text{---------- (4.5)}$$

where m_d = total flow through dome
= $m_{sw} + m_{dh}$
m_{dh} = flow through dome holes
C_{dh} = discharge coefficient of dome holes.
K_{sw} = coefficient in swirler pressure drop equation.
β_{sw} = blade angle of swirler
A_{ft} = cross-sectional area of primary zone

(f) Temperature Rise

The energy equation for combustion in the primary zone is given by (neglecting the velocity terms as mean velocities in the primary zone are quite small):

$$m_1 h_{air,T_1} + \dot{q} = (m_1 + m_{fb})\, h_{prod,T_2} \qquad \text{---------- (4.6)}$$

where m_1 = air mass flow rate
m_{fb} = fuel burning rate
$\dot{q}$ = heat release rate
h_{air} = enthalpy of air
h_{prod} = enthalpy of combustion products
The subscripts 1 and 2 refer to conditions before and after combustion, respectively.

The enthalpies of air and combustion products are calculated from the expression (neglecting the dissociation effects):

$$h = \int c_p dT \qquad \text{---------- (4.7)}$$

where the specific heat of air as a function of temperature is correlated by:

$$c_p = 0.2419 - 0.8181\times10^{-5}T + 17.91\times10^{-9}T^2 - 2.743\times10^{-12}T^3 \qquad \text{---------- (4.8)}$$

The specific heat of combustion products is given by [18]:

$$c_p = 0.2419 + .103f - (0.8181 - 22.6f)\times10^{-5}T + (17.91 - 29.6f)\times10^{-9}T^2 - (2.743 - .35f)\times10^{-12}T^3$$
$$\text{---------- (4.9)}$$

where f = local fuel air ratio.
This equation is suitable up to stoichiometric values of the fuel-air ratio which can be obtained from the relation:

$$f_{stoich} = 0.0867\left(\frac{1+H/C}{1+3H/C}\right) \qquad \text{---------- (4.10)}$$

where H/C = fuel hydrocarbon ratio by mass.

The combustion of fuel in a vitiated gas, when the enthalpies don't include the effects of dissociation, the heat release rate, $\dot{q}$, is adjusted to account for dissociation and recombination. In general, for combustion between conditions 1 and 2:

$$\dot{q} = m_{fb} h_p + 3\times10^{-26}\left[\frac{m_1 T_1^{7.5}}{1+f_1} - \frac{m_2 T_2^{7.5}}{1+f_2}\right] \qquad \text{---------- (4.11)}$$

where m_{fb} = rate of burning of fuel

For combustion in the primary zone the temperature, T_2, is very large and the $T_1^{7.5}$ term in Equation (4.11) may be ignored. Equation (4.6) is now solved for T_2, the primary zone temperature.

(g) Density and Velocity

The density is found from the equation of state:

$$\rho_2 = \frac{p_2}{RT_2} \qquad \text{---------- (4.12)}$$

and the velocity from the continuity equation:

$$U_2 = \frac{m_2}{\rho_2 A_2} \qquad \text{---------- (4.13)}$$

where $m_2 = m_1$

(h) Hot Loss

The "hot loss" of total pressure, which is the change in total pressure due to heat addition, is given by:

$$\Delta P = P_1 - P_2$$

$$= \frac{\rho_2 U_2^2}{2}\left(1 - \frac{\rho_2}{\rho_1}\right) \qquad \text{---------- (4.14)}$$

4.7.4 Flow in Annulus

The equation of continuity, momentum, energy, and state are set up for a section of one annulus between adjacent calculation stations, shown as 1 and 2 in the sketch below (Figure 4.3):

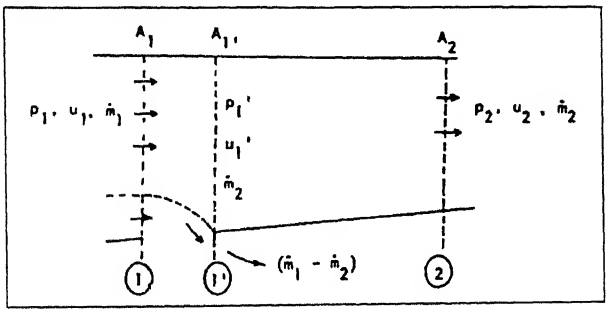

Figure 4.3 Calculation stations in annulus

The resulting equations are then used to calculate conditions at Station 2 from the conditions at Station1.

(a) Continuity Equation:

The continuity equation for flow in the annulus between Stations 1 and 2 is written as follows:

$$\frac{\rho_{an,1} u_{an,1} A_{an,1} m_{an,2}}{m_{an,1}} = \rho_{an,2} u_{an,2} A_{an,2} \qquad \text{---------- (4.15)}$$

(b) Momentum Equation

Due to the presence of annulus wall holes between stations 1 and 2, the equation for the conservation of momentum becomes complicated. To deal with this complication the calculation is carried out in three steps.

1) The flow through the hole, m_h, is found from the hole type and size, the pressure drop across the hole, and discharge coefficient data.

2) It is assumed that the air remaining the air remaining in the annulus at station 1`, immediately downstream of hole, undergoes a sudden expansion. The resulting total pressure loss given by the following empirical expression [19], from which $P_{an,1`}$ the pressure at station 1` may be calculated:

$$P_{an,1} - P_{an,1`} = 1.85 \frac{\rho_{an,1} u_{an,1}^2}{2} \left[\frac{m_h}{1.36 m_{an,1}} \right]^{1/(.5+.242M_{an,1}^{2.21})} \qquad \text{---------- (4.16)}$$

With the total pressure at Station 1` known, the other flow conditions at Station 1` may be found from the equations for the isentropic flow of a perfect gas between Stations 1 and 1`. The approach is first to calculate the Mach number at Station 1`, $M_{an.1`}$ from the following equation:

$$\frac{m_{an,1`}}{A_{an,1`}} = \frac{m_{an,2}}{A_{an,1}} = \left[\frac{\gamma}{R} \right]^{1/2} \frac{P_{an,1`}}{T_o^{1/2}} \frac{M_{an,1`}}{\left[1 + \frac{\gamma - 1}{2} M_{an,1`}^2 \right]^{\frac{\gamma+1}{2(\gamma-1)}}} \qquad \text{---------- (4.17)}$$

where T_o = stagnation temperature and assumed to be constant across the expansion

$$= T_{an,1} + \frac{u_{an,1}^2}{2 C_p}$$

The static temperature and static pressure are then determined from:

$$\frac{T_{an,1`}}{T_o} = \left[ 1 + \frac{\gamma - 1}{2} M_{an,1`}^2 \right]^{-1}$$

$$\frac{p_{an,1`}}{p_o} = \left[\frac{T_{an,1`}}{T_o}\right]^{\gamma/\gamma-1}$$

Then from the equation of state the density at 1` is:

$$\rho_{an,1`} = \frac{p_{an,1`}}{RT_{an,1`}}$$

From continuity equation, the velocity is:

$$u_{an,1`} = \frac{m_{an,1`}}{\rho_{an,1`} A_{an,1`}}$$

Thus, the assumption of a sudden expansion at Station 1` permits all of the necessary flow quantities at that station to be completed.

3) Now apply the momentum equation for flow between Stations 1` and 2:

$$p_{an,1`} A_{an,1} + m_{an,2} u_{an,1`} + \int_{x_{1`}}^{x_2} p_{an} \frac{dA}{dx} dx - \int_{x_{1`}}^{x_2} \frac{FA_W \rho_{an} u_{an}^2}{2} dx = p_{an,2} A_{an,2} + m_{an,2} u_{an,2} \quad \text{---------- (4.18)}$$

where F= fanning friction factor [20]
$= 0.0035+0.264\ (Re)_{an,1}^{-.42}$
A_W = Wetted wall area per unit length.

A simplified form of equation (4.18), on ignoring small pressure losses due wall slope and friction, is as follows:

$$\int_{x_{1`}}^{x_2} \frac{FA_W \rho_{an} u_{an}^2}{2} dx = \frac{1}{2} F(C_A + C_B) \rho_{an,1`} u_{an,1`}^2 (x_2 - x_{1`}) \quad \text{---------- (4.19)}$$

where, C_A and C_B are the inner and outer wall areas/ unit length between 1` and 2.

The integral pressure term can be evaluated if it is assumed that flow between Stations 1` and 2 is incompressible and that the mixing rate will be delayed by diffusion. With these assumptions the integral pressure term may be integrated as follows:

The integral pressure term in the annulus momentum equation (Eq. 4.18) may be integrated by parts to get:

$$\int_{x_{1`}}^{x_2} p_{an} \frac{dA}{dx} dx = (p_{an,1`} - p_{an,2}) \frac{2A_{an,1} A_{an,2}}{A_{an,1} + A_{an,2}} + p_{an,2} A_{an,2} - p_{an,1`} A_{an,1}$$

Now, the final momentum equation thus becomes:

$$\frac{2A_{an,1}A_{an,2}}{A_{an,1}+A_{an,2}}(p_{an,1`}-p_{an,2})-F(C_A+C_B)\frac{\rho_{an,1`}u_{an,1`}^{2}}{2}(x_2-x_{1`})=m_{an,2}(u_{an,2}-u_{an,1`})$$

------ (4.20)

(c) Energy Equation

The energy equation for flow in the annulus between stations 1` and 2 is:

$$\left[h(T_{an,1})+\frac{u_{an,1}^{2}}{2}\right]m_{an,2}+\int_{x_1}^{x_2}\dot{q}_w C_A dx=\left[h(T_{an,2})+\frac{u_{an,2}^{2}}{2}\right]m_{an,2}$$

where h(T)= static enthalpy of annulus air at temperature T

$\dot{q}_w$ = heat transfer rate from unit area of the flame tube wall to the annulus air.

The casing temperature is normally assumed to be equal to the compressor delivery temperature because the heat transfer rate between casing and annulus air is assumed to be negligibly small.

Since the variations in the annulus air temperature are normally small, h (T) may be assumed equal to c_p (T-T_b), where c_p is a mean specific heat. If mean values are assumed for $\dot{q}_w$ and C_A, the simplified energy equation becomes:

$$\left(c_pT_{an,1}+\frac{u_{an,1}^{2}}{2}\right)m_{an,2}+\dot{q}_w C_A(x_2-x_1)=\left(c_pT_{an,2}+\frac{u_{an,2}^{2}}{2}\right)m_{an,2}$$ -------- (4.21)

(d) Equation of State:

The equation of state for the annulus air is:

$$\frac{p_{an,1}}{\rho_{an,1}T_{an,1}}=\frac{p_{an,2}}{\rho_{an,2}T_{an,2}}=R$$ ---------- (4.22)

4.8 METHOD OF SOLUTION OF ANNULUS EQUATIONS

Since the mass flow through the holes between stations 1 and 2, m_h, is known, the down stream flow in the annulus, $m_{an,2}$ is simply:

$$m_{an,2}=m_{an,1`}=m_{an,1}-m_h$$

There remaining four unknowns, $u_{an,2}$, $p_{an,2}$, $\rho_{an,2}$ and $T_{an,2}$, which can be found by solving equations (4.15), (4.20), (4.21) and (4.22).

These equations can be easily reduced to a quadratic in $u_{an,2}$:

$$B_2 u_{an,2}^2 + B_1 u_{an,2} - B_o = 0 \qquad \text{---------- (4.23)}$$

where $B_2 = 1 - \frac{c_p}{R}\frac{A_{an,1} + A_{an,2}}{A_{an,1}}$

$$B_1 = 2\frac{c_p}{R}\left[p_{an,1'}\frac{A_{an,2}}{m_{an,2}} + u_{an,1'}\left(\frac{A_{an,1} + A_{an,2}}{2A_{an,1}}\right)\left(1 - \frac{f(C_A + C_B)(x_2 - x_{1'})}{2A_{an,1}}\right)\right]$$

$$B_o = u_{an,1}^2 + 2c_p\left[T_{an,1} + \frac{\dot{q}_w C_A (x_2 - x_1)}{c_p m_{an,2}}\right]$$

The solution of Equation (4.23) gives,

$$u_{an,2} = \frac{-B_1 + \sqrt{B_1^2 + 4B_0B_2}}{2B_2} \quad \text{(+ve root)} \qquad \text{---------- (4.24)}$$

With $u_{an,2}$ known, Equations (4.15), (4.20), and (4.22) are solved for $p_{an,2}$, $\rho_{an,2}$, and $T_{an,2}$:

$$p_{an,2} = p_{an,1'} + \frac{m_{an,2}}{A_{an,2}}\left(\frac{A_{an,1} + A_{an,2}}{2A_{an,1}}\right)\left[u_{an,1'}\left(1 - \frac{f(C_A + C_B)(x_2 - x_1)}{2A_{an,1}}\right) - u_{an,2}\right]$$

$$p_{an,2} = \frac{m_{an,2}}{A_{an,2}u_{an,2}}$$

$$T_{an,2} = \frac{p_{an,2}}{R\rho_{an,2}}$$

4.9 CHARACTERIZATION OF JET FLOW AND MIXING

The flow characteristics of jets entering the flame tube through holes and cooling slots or rings is treated by the use of empirical correlations for:

- The length of the jet (measured along its center line).
- The cross-sectional area of the spreading jet as a function of jet length.
- The jet center-line velocity and temperature as functions of jet length.
- The development of the non-dimensional velocity and temperature profiles across the jet with jet length.

Two sets of correlations are provided, one for wall jets (where the air enters the flame tube through a cooling slot or ring in a direction parallel to the wall) and one for penetration jets. These two types of jet are shown below (Figure 4.4):

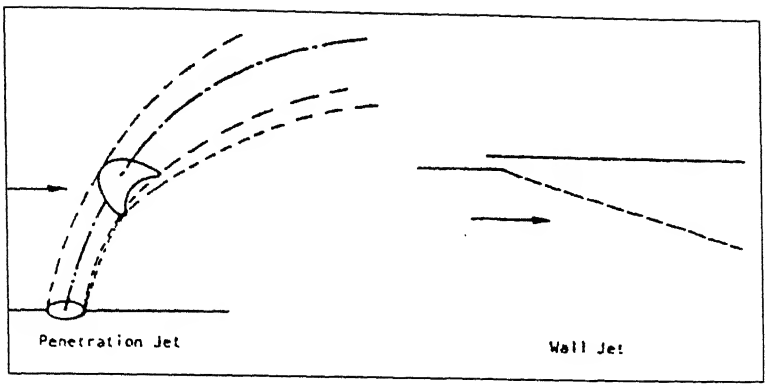

Figure 4.4 Combustor penetration and wall jet.

The characteristics of penetration and wall jets and of the three mixing models (any one of them can be used in the program) are as follows:

4.9.1 Penetration Jets:

The dimensions used in the describing jet behavior are shown in the sketch below:

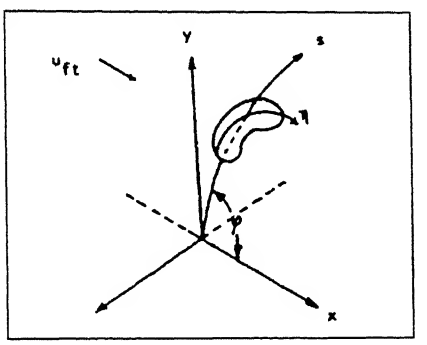

Figure 4.5 Penetration jet parameters

Where x, is the direction of flow of main-stream gas in the flame tube
y, is the jet penetration distance normal to the flame-tube wall
s, is the distance along the jet center line
η, is transverse width of the jet (measured normal to the jet center line along lines of constant s), and
φ, is the angle between the initial jet trajectory and the flame tube wall at the entry hole.

(a) Initial Jet Angle Data

The jet mixing correlations, and the momentum equations in the flame tube, make use of the initial jet angleφ. This is available as a function of pressure-loss factor for different hole types in the library data. Where data do not exist, the following correlation is used:

$$\sin^2 \varphi = \frac{C_d}{C_{dn}} \qquad \text{---------- (4.25)}$$

where C_{dn} is the asymptotic value of C_d as $1+\frac{\Delta p_h}{q_{an}}$ tends to infinity.

This approximation gives reasonable results for round flush holes.

(b) Penetration Distance:

The penetration distance y, measured from the wall to the jet center line, is calculated by an empirical correlation [21] through [23].

$$y = 0.87 d_h \left(\frac{\rho_{an}}{\rho_{ft}}\right)^{0.47} \left(\frac{u_{j,o}}{u_{ft}}\right)^{0.85} \left(\frac{x}{d_h}\right)^{0.32} \sin\varphi \qquad \text{---------- (4.26)}$$

where d_h = effective axial length of hole
$= (C_d)^{1/2} \times$ axial length
$u_{j,o}$ = initial jet velocity
$$= \frac{m_h}{\rho_{an} C_d \times \text{hole area}}$$

It is assumed that there is no change in density of the jet as the air passes through the hole.

(c) Jet Center Line Velocity

An empirical equation for the jet center line velocity is, Keffer and Baines [22]:

$$u_{j,CL} = u_{j,o}, \qquad \text{for } \frac{s`}{d_j} < 3.45$$

$$u_{j,CL} = u_{ft} + \left[1 - .229\left(\frac{s`}{d_j} - 3.45\right)\right](u_{j,o} - u_{ft}), \qquad \text{for } 3.45 < \frac{s`}{d_j} < 5.2$$

$$u_{j,CL} = u_{ft} + \left[3.6\, e^{-.344 s`/d_j}\right](u_{j,o} - u_{ft}), \qquad \text{for } 5.2 < \frac{s`}{d_j} \qquad \text{--------- (4.27)}$$

The effective distance along the jet center line, s`, used in the above equations, is calculated [22] from;

$$s` = s + \left(2.93 - 0.279\frac{u_{j,o}}{u_{ft}}\right) d_j \qquad \text{--------- (4.28)}$$

where
$$s = \int \left[1 + \left(\frac{dy}{dx}\right)^2\right]^{1/2} dx \qquad \text{--------- (4.29)}$$

d_j = effective initial jet diameter.
$$= \sqrt{(C_d \times \text{hole area} \times 4/\pi)}$$

(d) Transverse Velocity Profile:

The correlating equation for the jet velocity profile, expressed in terms of the transverse coordinate,η, are obtained from [22]:

$$u_{j,\eta} = u_{ft} + \left[0.5\cos\left(\frac{\pi}{2}\frac{\eta}{\eta_{1/2}}\right) + 0.5\right]\left(u_{j,CL} - u_{ft}\right), \quad \text{for } 0 < \eta < \eta_{1/2}$$

$$u_{j,\eta} = u_{ft} + 1.74e^{-1.25\eta,2}{}^{1}\!/_{2}\left(u_{j,CL} - u_{ft}\right), \quad \text{for } \eta > \eta_{1/2} \text{ ------- (4.30)}$$

where, from [22]; $\eta_{1/2} = 0.215s$`

(e) Transverse Temperature Profile:

The transverse temperature profile is assumed to be similar in form to the transverse velocity profile. The expressions relating temperature to velocity are:

$$\frac{T_{j,\eta} - T_{ft}}{T_{j,CL} - T_{ft}} = \frac{u_{j,\eta``} - u_{ft}}{u_{j,CL} - u_{ft}} \qquad \text{---------- (4.31)}$$

$$\frac{T_{j,CL,s`} - T_{ft}}{T_{j,o} - T_{ft}} = \frac{4.8}{6.5}\left(\frac{u_{j,CL,s`} - u_{ft}}{u_{j,o} - u_{ft}}\right) \qquad \text{---------- (4.32)}$$

where $\eta`` = \eta/1.4$

The constants are taken from Forstall and Shapiro [24], and Squire [25]

(f) Calculation of Jet Properties:

The cross-sectional area of a jet in a plane normal to its center line may be represented by [24]:

$$A_{j,cs} = 0.12\eta^{*1.8} \qquad \text{---------- (4.33)}$$

where η^* = the value of η at the assumed jet boundary.

The jet area normal to the combustor axis is then given by:

$$A_j = \frac{0.12\ \eta^{*1.8}}{\cos\varphi_j} \qquad \text{---------- (4.34)}$$

where φ_j = local jet angle

$$= \cos^{-1}\left[1 + \left(\frac{dy}{dx}\right)^2\right]^{-1/2} \qquad \text{---------- (4.35)}$$

Other jet properties needed for solution of the flame tube equations may be calculated as follows:

Mass flow rate, $$m_j = \int_0^{\eta^*} \rho_j u_{j,\eta} 0.12 \times 1.8 \eta^{0.8} \, d\eta \qquad \text{---------- (4.36)}$$

Axial component of jet momentum flux,

$$M_j = \int_0^{\eta^*} \rho_j u_{j,\eta}^{\ 2} \, 0.12 \times 1.8 \eta^{0.8} \, d\eta \, \cos\varphi_j \qquad \text{--------- (4.37))}$$

Enthalpy, $$h_j = \int_0^{\eta^*} \rho_j u_{j,\eta} \left[c_p \left(T_{j,\eta} - T_b \right) + \frac{1}{2} u_{j,\eta}^{\ 2} \right] 0.12 \times 1.8 \eta^{0.8} \, d\eta \qquad \text{--------- (4.38))}$$

4.9.2 Wall Jets:

The symbols used are defined by the Figure 4.6:

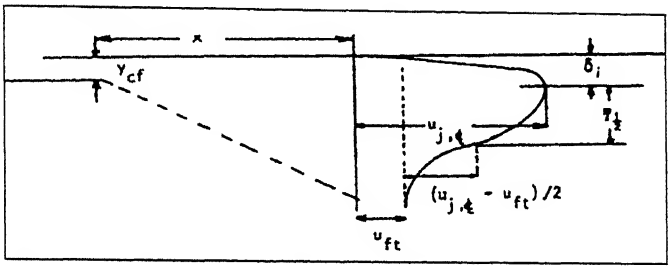

Figure 4.6 Wall jet parameters

(a) Maximum Velocity:

The maximum velocity in the wall jet is given by [26]

When (i) $x = 0$, $s` = 0$

$$u_{j,CL} = u_h$$

(ii) $x = x + dx$, $$s` = s` + \left(1 - \frac{u_{ft}}{u_{j,CL}} \right) dx$$

$$u_{j,CL} = u_{ft} + \frac{0.0287 y_{cf}}{\nu (12 s`)^{\alpha}} \left(u_h - u_{ft} \right) \qquad \text{---------- (4.39)}$$

where u_h = initial jet velocity

$$= \frac{m_h}{\rho_{an} C_d \times \text{slot area}}$$

and $$\alpha = \left[\frac{1.06}{1 - u_{ft}/u_h} - 0.5 \right]$$

The above equations apply for values of $u_{j,CL}$ between u_h and u_{ft} . Otherwise, $u_{j,CL}$ is set equal to u_h.

(b) Velocity Profile:

For analysis purposes, the velocity profile is divided into two sections about its maximum.

i) Near the wall ($\eta<\delta_1$) the equation from [26] is used:

$$\frac{u_{j,\eta}-u_{ft}}{u_{j,CL}-u_{ft}}=C\left(\frac{\eta}{\delta_1}\right)^{1/n}, \qquad \eta\le\delta_1 \qquad \text{---------- (4.40)}$$

where η= perpendicular distance from wall

$C\cong 1.0$

$n\cong 10$

$\delta_1 = 0.0109s`$

Since n is so large, we can ignore the precise shape of the profile and to assume:

$$\int_0^{\delta_1}\frac{u_{j,\eta}-u_{ft}}{u_{j,CL}-u_{ft}}d\eta = 0.95\delta_1 \qquad \text{---------- (4.41)}$$

ii) In the outer region ($\eta>\delta_1$) the equation from [27] is given by:

$$\frac{u_{j,\eta}-u_{ft}}{u_{j,CL}-u_{ft}}=e^{-k\,\eta`^2} \qquad \text{---------- (4.42)}$$

where $k=0.693$

$$\eta`=\frac{\eta-\delta_1}{\eta_{1/2}-\delta_1}$$

$$\eta_{1/2}=0.065s` \qquad [36]$$

(c) Calculation of Jet Properties:

The equations for the properties of wall jets are similar to the penetration jets from Equations (4.43-4.38). The major difference is in the expression for elements of area.

$$A_j = C_A\eta^* \qquad \text{(on the inner wall) ---------- (4.43)}$$

$$m_j = C_A\int_0^{\eta^*}\rho_j\,u_{j,\eta}\,d\eta \qquad \text{---------- (4.44)}$$

$$M_j = C_A \int_0^{\eta^*} \rho_j \, u_{j,\eta}{}^2 \, d\eta \qquad \text{---------- (4.45)}$$

$$h_j = C_A \int_0^{\eta^*} \rho_j \, u_{j,\eta} \left[c_p \left(T_{j,\eta} - T_b \right) + \frac{1}{2} u_{j,\eta}{}^2 \right] d\eta \qquad \text{---------- (4.46)}$$

4.9.3 Jet Mixing Model:

There are many jet mixing models that can be used. In this program following models has been used.

(a) Mass-Loss Model:

In this model a specified fraction of the initial mass flow in the jet is assumed to mix with the main stream for each unit of distance along the jet.
The mass flow remaining in the jet, m_j , is given by:

$$m_j = m_h \left(1 - \frac{C s`}{d_j} \right) \qquad \text{---------- (4.47)}$$

The entrainment constant, C, may be assigned any value between zero (no mixing) and one (instantaneous mixing).
The other jet flow quantities are calculated directly from the residual mass flow, with the jet velocity, density, and temperature assumed uniform:

$$A_j = \frac{m_j}{\rho_{an} u_{j,o} \cos \varphi_j} \qquad \text{---------- (4.48)}$$

$$M_j = m_j u_{j,o} \cos \varphi_j \qquad \text{---------- (4.49)}$$

$$h_j = m_j \left[c_p \left(T_{an} - T_b \right) + \frac{1}{2} u_{j,o}{}^2 \right] \qquad \text{---------- (4.50)}$$

(b) Equivalent-Entrainment Model:

This model starts with the actual mass flow in the jet, $m_{j,act}$, as estimated from Equation (4.36) for penetration jets or (4.44) for wall jets. In these equations the integration of mass flow is carried across the jet to a value of the jet width, η^*, large enough that virtually all of the jet is included. The excess of this mass flow over the initial flow through the hole, $(m_{j,act}-m_h)$, is the mass flow of gases that have been entrained into the jet from the main stream. It is then assumed that a fraction C of this entrained mass flow represents the jet mass flow that has been mixed into the main stream. The residual mass flow in the jet is then given by:

$$m_j = m_h - C\left(m_{j,act} - m_h \right) \qquad \text{---------- (4.51)}$$

where C= 0 , no mixing
C=1 , complete mixing when the computed flow of the actual jet reaches twice the initial jet flow.
C= large number, implies instantaneous mixing

4.10 COMBUSTION ANALYSIS OF THE FLAME TUBE

The equation of continuity, momentum, energy, and state are solved for a section of the flame tube between adjacent calculation Stations 1 and 2. Following sketch shows the flow contributions:

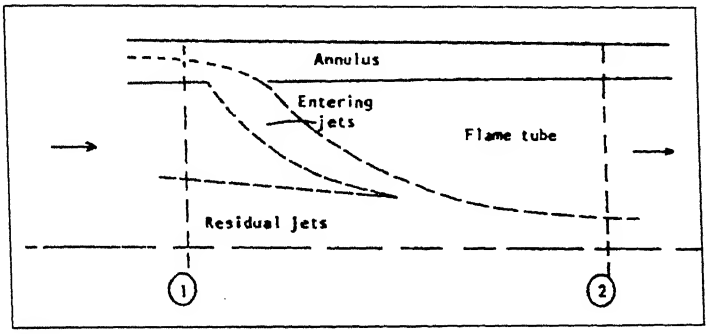

Figure 4.7 Flame tube section

4.10.1 Continuity Equation:

The equation expressing the conservation of mass in the flame tube is:

$$\rho_{ft,1}u_{ft,1}\left[A_{ft,1} - \sum_{\text{residual jets}} A_{j,1}\right] + \sum_{\text{residual jets}} m_{j,1} + \sum_{\text{entering jets}} m_h + m_{fb}$$

$$= \rho_{ft,2}u_{ft,2}\left[A_{ft,2} - \sum_{\text{all jets}} A_{j,2}\right] + \sum_{\text{all jets}} m_{j,2} \text{ -------- (4.52)}$$

where m_{fb} = fuel burning rate

4.10.2 Momentum Equation:

The flame tube equations include terms for the entering and residual jets. Since the gas velocity in the flame tube is quite low, the friction loss has been ignored.

The equation expressing the conservation of momentum within a control volume bounded by the flame tube wall and by transverse planes at Station 1 and 2 is then:

$$p_{ft,1}A_{ft,1} + m_{ft,1}u_{ft,1} + \sum_{\text{entering jets}} M_{j,o} + \sum_{\text{residual jets}} m_{j,1} + \int_{x_1}^{x_2} p_{ft}\frac{dA}{dx}dx$$

$$= p_{ft,2}A_{ft,2} + m_{ft,2}u_{ft,2} + \sum_{\text{all jets}} M_{j,2}$$

where Mj = axial component of jet momentum

$= m_j u_j \cos\varphi_j$

φ_j = local angle between jet axis and flame tube center line

m_{ft} = mass flow of hot gases in flame tube. (This excludes unmixed air in the residual jets but includes the mass of fuel burned between Stations 1and 2)

The integral pressure term is approximated by:

$$\int_{x_1}^{x_2} p_{ft} \frac{dA}{dx} dx = \frac{1}{2}\left(A_{ft,2} - A_{ft,1}\right)\left(p_{ft,1} + p_{ft,2}\right)$$

The final form of flame tube momentum equation is then:

$$p_{ft,1}A_{ft,1} + m_{ft,1}u_{ft,1} + \sum_{\text{entering jets}} M_{j,o} + \sum_{\text{residual jets}} m_{j,1} + \frac{1}{2}\left(A_{ft,2} - A_{ft,1}\right)\left(p_{ft,1} + p_{ft,2}\right)$$

$$= p_{ft,2}A_{ft,2} + m_{ft,2}u_{ft,2} + \sum_{\text{all jets}} M_{j,2} \qquad \text{---------- (4.53)}$$

4.10.3 Energy Equation:

The equation expressing conservation of energy between adjacent calculation stations in the flame tube is written as follows,

$$\left[h\left(T_{ft,1}\right) + \frac{1}{2}u_{ft,1}^{\,2}\right] m_{ft,1} + \sum_{\text{entering jets}} h_{j,o}\, m_{j,o} + \sum_{\text{residual jets}} h_{j,1}\, m_{j,1} + \int_{x_1}^{x_2} \dot{q}\, dx$$

$$= \left[h\left(T_{ft,2}\right) + \frac{1}{2}u_{ft,2}^{\,2}\right] m_{ft,2} + \sum_{\text{all jets}} h_{j,2} m_{j,2} \qquad \text{--------- (4.54)}$$

where the enthalpy of hot gasses is defined by:

$$h\left(T_{ft}\right) = \int_{T_b}^{T_{ft}} c_p(T)\, dT$$

The specific heat c_p is correlated as a function of temperature by Equation (4.11); the enthalpy of jets, h_j , is obtained from the jet mixing calculation, Equations (4.38), (4.46); and the heat release rate, $\dot{q}$, from Equation (4.11).

Heat loss from the hot gases to the flame tube walls has been ignored in Equation (4.49) to avoid the complications in the calculation procedure.

The jet areas and mass flow rates are obtained from the results of jet mixing calculations, Equations (4.34), (4.36), (4.43), (4.44), (4.47), (4.48), and (4.51).

4.10.4 Equation of State:

The equation of state may be written as follows:

$$\frac{p_{ft,1}}{\rho_{ft,1}T_{ft,1}} = \frac{p_{ft,2}}{\rho_{ft,2}T_{ft,2}} = R \qquad \text{---------- (4.55)}$$

R= gas constant for air

4.10.5 Method of Solution

The mass flow at Station 2 is known from jet mixing results:

$$m_{ft,2} = m_{ft,1} + \sum m_{j,o} + \sum m_{j,1} - \sum m_{j,2} \qquad \text{---------- (4.56)}$$

Since Equation (4.54) can not be solved explicitly for $T_{ft,2}$, an iterative technique is used to arrive at a solution. In this equation the velocity terms make a small contribution to the total enthalpy. For the first stage in the iterative process, therefore, $u_{ft,2}$ is set equal to $u_{ft,1}$. In addition, the specific heat and heat release rate are computed for $T_{ft,2} = T_{ft,1}$. With these simplifications Equation (4.54) can be solved explicitly for a first estimate of $T_{ft,2}$. New values of the specific heat and heat release rate are then computed for the new $T_{ft,2}$ and Equation (4.54) is solved again. The process is repeated until $T_{ft,2}$ converges to an acceptable accuracy.

Using the value of $T_{ft,2}$ so obtained equations are solved to obtain a quadratic equation in $\rho_{ft,2}$:

$$\rho_{ft,2}{}^2 RT_{ft,2}\left(\frac{A_{ft,2} + A_{ft,1}}{2}\right) - \rho_{ft,2}K_1 + \frac{m_{ft,2}{}^2}{\left(A_{ft,2} - \sum A_{j,2}\right)} = 0 \qquad \text{---------- (4.57)}$$

where $K_1 = \frac{1}{2}p_{ft,1}\left(A_{ft,2} + A_{ft,1}\right) + m_{ft,1}u_{ft,1} + \sum m_{j,o} + \sum m_{j,1} - \sum m_{j,2}$

the resulting value of $\rho_{ft,2}$ is substituted in the following continuity equation to obtain $u_{ft,2}$:

$$u_{ft,2} = \frac{m_{ft,2}}{\rho_{ft,2}\left(A_{ft,2} - \sum A_{j,2}\right)}$$

this value of $u_{ft,2}$ is substituted in Equation (4.54) and a new value of $T_{ft,2}$ is found. This process is repeated until both $T_{ft,2}$ and $u_{ft,2}$ have converged to within specified tolerances.

4.11 LIMITATIONS OF THE AIR-FLOW SUBPROGRAM

The more important limitations of the air-flow subprogram are as follows:

1) The treatment of the primary zone as stirred reactor.
2) The program does not calculate the fuel burning rate directly, but receives it as input and only serves to keep it below stoichiometric at any location.
3) The jet mixing models suffer from a lack of experimental data upon which the choice of models and entrainment constants are based; in addition, the program does not relate the mixing rate of wall jets to the film cooling analysis carried out in the heat transfer section.

4.12 STRUCTURE OF THE SUBPROGRAM

The air-flow subprogram consists of:

1) A subroutine which steps up starting conditions and directs the air flow calculation through the other subroutines in the appropriate sequence.
2) Subroutines for solving the equations for flow in the annulus and flame tube.
3) Subroutines for calculating the heat addition due to fuel burning and the temperature in the primary zone.
4) A subroutine for calculating the rate of mixing of the entering jets.

The subroutines and flowcharts of air-flow subprogram are given in the Appendix A3.

CHAPTETR 5

COMBUSTOR HEAT- TRANSFER ANALYSIS

5.1 INTRODUCTION

The basic functions of the combustor dome and liners are to contain and guide the burning fuel-air mixture from the point of fuel injection to the turbine nozzle inlet, to meter airflow to the various zones within the combustor chamber and to protect engine structural components from the burning gases. Protection of the combustor dome and liners from the hot gases within the combustor is extremely important and challenging. The structure must be protected using cooling air at combustor inlet temperature.

5.2 LINER COOLING APPROACHES

The established method for protecting combustor components from the hot products of combustion is to use film cooling, where a film of air at combustor inlet temperature is injected along the liner surface. Several different types of liner construction have been used for film-cooled liners as described below:

5.2.1 Louvred liners

This method of liner construction uses a simple sheet metal wall with a series of called louvres installed at intervals along the surface (Figure 5.1).

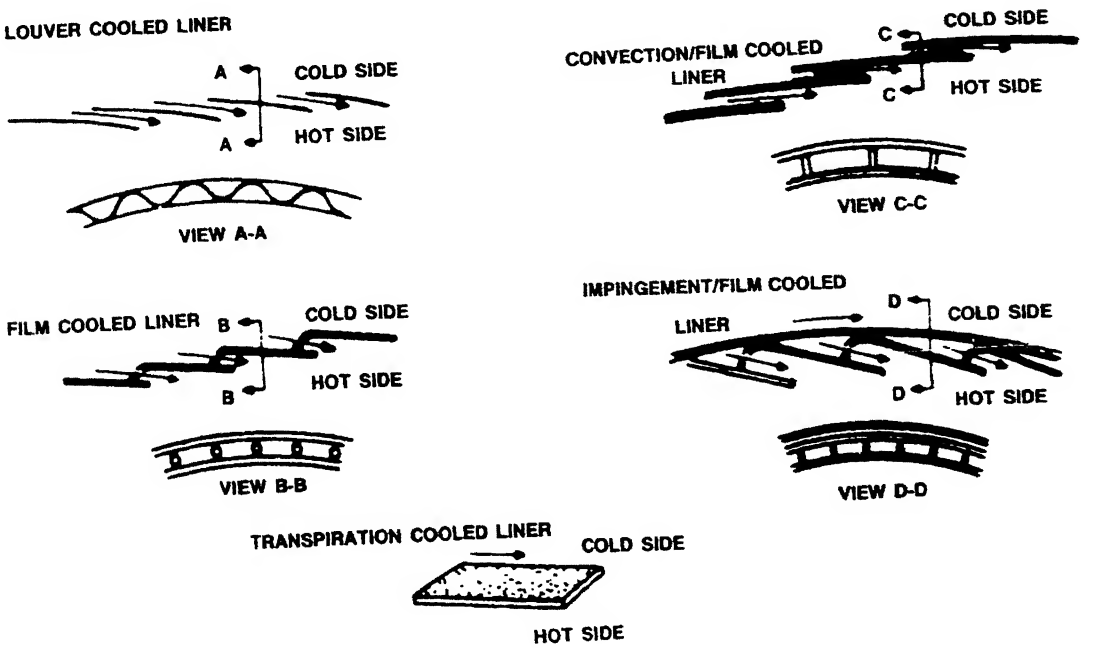

Figure 5.1 Liner cooling techniques

Liners of this type are lightweight, inexpensive and easily fabricated.

Drawbacks associated with the louvred liner construction include short life due to cracking and poor control of cooling air flow. The base of the louvres is a prime location for crack initiation due to very high stress concentration at the point where the liner has been sheared during louvre installation.

5.2.2 Cooling slots

A majority of current combustors designs use some type of continuous circumferential annular slots spaced axially at intervals along the liner to inject a cooling film along the inner surface of the liner. Seven different slot configurations are shown in Figure 5.1 below.

5.3 ONE-DIMENSIONAL ANALYSIS

Once the internal flow conditions are known, cooling flows are selected, and detailed geometry is specified, one-dimensional heat transfer analysis can be conducted at several different axial locations to determine whether peak liner temperatures are acceptable. If not, cooling flow and liner geometry are adjusted, and analysis is repeated until a satisfactory temperature profile is obtained.

5.4 ANALYTICAL METHODS AND PROGRAM DEVELOPMENT

The principal operations in the heat-transfer subprogram comprise the formation of the various heat flux components at the flame tube walls in terms of the wall temperature, the solution of the heat balance equation to determine the wall temperature and the evaluation of the wall heat fluxes. The heat transfer subprogram receives as input the geometry of the flame tube and casing from the control subprogram and the axial distributions of velocity and temperature of the flame tube gases from the air flow subprogram.

The primary objective of the heat transfer subprogram is to establish the axial distribution of temperature along the flame tube walls for various program options.

5.4.1 Assumptions Made in Heat-Transfer Analysis

- Conditions are assumed to be constant in the circumferential direction for the annular geometry.
- Steady-state conditions prevail.
- The quantities supplied by the air flow subprogram are reasonable approximations to real conditions.
- Flame and walls are gray radiators, i.e., spectral effects can be ignored.
- Wall emissivities and absorptivities are constant.
- Effect of wall to bulk temperature ratio can be neglected; fluid properties used in the heat transfer relations are evaluated at the bulk fluid temperature.

- One dimensional radiation option assumes that the temperature gradients in the flame tube are small.
- The temperature gradients along the walls are small and that the two walls are at approximately the same temperature.
- Unless the outer casing temperature distribution is specified in the program input, it is assumed that the casing temperature is close to the compressor discharge temperature.

5.4.2 Heat Balance in Flame Tube

The heat flux balance is performed on an elemental length of the flame tube wall. Conditions in the circumferential direction are assumed to be uniform. The heat flux components considered in the heat balance are:

a) Radiation from the flame to the flame tube wall, R_1.
b) Convection in the flame tube gases at the wall, C_1.
c) Radiation from the flame tube wall to the outer casing, R_2.
d) Convection in the annulus air at the outside surface of the flame tube wall, C_2
e) Longitudinal conduction in the flame tube wall, ΔK
f) Radiation interchange between the flame tube walls, R_3.

Equating the heat gained by the element of wall to the heat lost, the following equation can be written:

$$R_1 + C_1 + \Delta K = R_2 + C_2 + R_3 \qquad \text{----------} (5.1)$$

5.4.3 Radiation from the Flame to the Flame-Tube Wall (1-D Model)

The one-dimensional radiation model describes the case where each element of wall receives radiation only from element of flame at the same axial position. This model is accurate when axial temperature gradients and end effects are small and the length-to-diameter ratio of the flame tube is large.

The usual expression for radiant heat transfer between a gray flame at temperature T_{ft} and a black container at temperature at T_w is:

$$R_1 = \sigma\left(\varepsilon_{ft} T_{ft}^4 - \alpha_{ft} T_w^4\right) \qquad \text{----------} (5.2)$$

where, σ = Stefan-Boltzmann constant
ε_{ft} = emissisvity of flame at flame temperature
α_{ft} = absorptivity of flame to radiation at temperature T_W

Sine the wall is not black, but has an absorptivity α_w which will normally be between 0.8 and 1.0 a correction should be made for absorption, reflection, re-absorption and so on. McAdmas [31] suggests a factor $(1-\alpha_w)/2$ to allow for this effect.

A further simplification is suggested by Lefebvre and Herbert [4]:

$$\frac{\alpha_{ft}}{\varepsilon_{ft}} = \left[\frac{T_{ft}}{T_w}\right]^{1.5}$$

Then $$R_1 = \frac{1}{2}\sigma(1+\alpha)\varepsilon_{ft} T_{ft}^{1.5}\left(T_{ft}^{2.5} - T_w^{2.5}\right) \quad \text{----------} (5.3)$$

5.4.4 Volume of Flame Element

The elements of flame considered have element length in the axial direction of ΔX_{ft} and inner and outer (flame-tube-wall) radii of r_2 and r_1 respectively. Thus, the volume of each flame element is:

$$\Delta X_{ft} - \pi(r_1^2 - r_2^2) \quad \text{----------} (5.4)$$

5.4.5 Emission per Unit Volume

The radiation emitted by unit volume of flame temperature T_{ft} is, Hottel [31]:

$$4\sigma\sigma_{ft}^4 p_G \left(\frac{d\varepsilon_{ft}}{dp_G^1 b}\right)_{P_G l_b = 0} \quad \text{----------} (5.5)$$

where, p_G = partial pressure of radiating gas (i.e., water vapor and carbon dioxide).

The quantity $\left(\frac{d\varepsilon_{ft}}{dp_G l_b}\right)_{P_G l_L = 0}$ is mainly a function of temperature. For a typical value of $p_G/p_{ft} = 0.05$ and for a non-luminous flame it can be approximated by [31],

$$\left(\frac{d\varepsilon_{ft}}{dp_G l_b}\right)_{P_G l_L = 0} = \frac{3.6}{T_{ft}} \quad \text{----------} (5.6)$$

5.4.6 View Factor

The sketch below illustrates the nomenclature of the axially symmetric configuration considered.

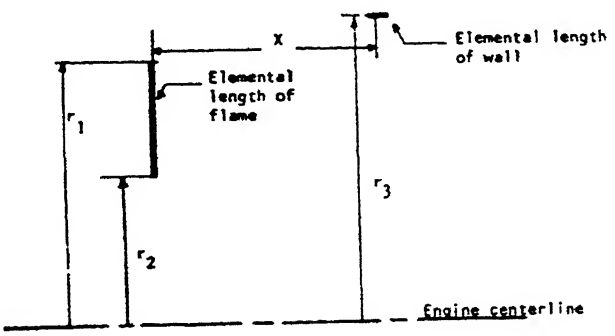

Figure 5.2 Flame tube view factor nomenclature

The following equation was obtained for the view factor of the flame element radiating to an element of length ΔX_w [28],

$$F_{FW} = \frac{1}{4}\frac{\Delta X_w}{(r_3 - r_2)}\left[1 - \frac{X}{\sqrt{X^2 + (r_3 - r_2)^2}}\right] - \frac{1}{4}\frac{\Delta X_w}{(r_3 - r_1)}\left[1 - \frac{X}{\sqrt{X^2 + (r_3 - r_1)^2}}\right] \quad \text{--------- (5.7)}$$

5.4.7 Transmittance

The transmittance accounts for the radiative energy which is not absorbed by the intervening gas. It is a function of the distance the radiation travels through the gas, the gas composition and the gas temperature. The expression for transmittance, [18], is:

$$\Gamma = \frac{14.82}{p_G s + 14.82} \quad \text{---------- (5.8)}$$

where s is the distance from element at considered point on the wall to element of the flame.

Mean value of the transmittance for each axial location of the flame element to an outer wall element is given by:

$$\Gamma_{mean} = \frac{1}{20}\sum_{i=1}^{20} \frac{14.82}{14.82 + p_G\sqrt{X^2 + \left[r_3 - r_2 - \left(\frac{1}{20} - \frac{1}{40}\right)(r_1 - r_2)\right]^2}} \quad \text{------- (5.9)}$$

5.4.8 Total Radiation

Introduction of wall temperature, T_w, and effective wall absorptivity, $(1+\alpha_w)/2$, the radiation absorbed by the wall element from the flame element is given by:

$$4\sigma\Gamma_{mean}\frac{(1+\alpha_w)}{2}p_G\left(\frac{d\varepsilon}{dp_G L}\right)_0 \Delta X_{ft}\pi(r_1^2 - r_2^2)F_{FW}(T_{ft}^4 - T_w^4) \quad \text{------- (5.10)}$$

Hence, the total radiation per unit time at a point on the outer flame-tube wall receiving radiation from all positions of the flame is:

$$4\pi\pi\frac{(1+\alpha_w)}{2}\sum_{\substack{\text{all flame}\\ \text{positions}}}\left[\Gamma_{mean}\, p_G\left(\frac{d\varepsilon}{dp_G L}\right)_0 \Delta X_{ft}\,(r_1^2 - r_2^2)F_{FW}(T_{ft}^4 - T_w^4)\right] \quad \text{------- (5.11)}$$

The radiative heat flux per unit time and area of flame tube is therefore, given by:

$$R_1 = \frac{(1+\alpha_w)\sigma}{\Delta X_w R_3}\sum_{\substack{\text{all flame}\\ \text{positions}}}\left[\Gamma_{mean}\, p_G\left(\frac{d\varepsilon}{dp_G L}\right)_0 \Delta X_{ft}\,(r_1^2 - r_2^2)F_{FW}(T_{ft}^4 - T_w^4)\right] \quad \text{------- (5.12)}$$

A similar expression applies for radiation to the inner flame-tube wall.

5.4.9 Radiation from Flame-Tube Wall to the Outer Casing

The radiant heat flux from flame-tube wall to the outer casing is given by equation:

$$R_2 = F_{wc}\sigma\left(T_w^4 - T_c^4\right) \qquad \text{-------- (5.13)}$$

where T_c = temperature of casing.
F_{wc} = overall interchange factor.

For the case where only two surfaces are involved and where both surfaces have high emissivities, the overall interchange factor is approximately given by, [31]:

$$\frac{1}{F_{wc}} = \left(\frac{1}{\varepsilon_w} - 1\right) + \frac{A_w}{A_c}\left(\frac{1}{\varepsilon_c} - 1\right) + \frac{1}{F_{wc}} \qquad \text{---------- (5.14)}$$

where, $\overline{F}_{wc}$ = black-surface overall interchange factor
ε_c = emissivity of casing (assumed equal to absorptivity)
A_w = surface area of flame-tube wall
A_c = surface area of casing

For radiation across an annular space, the black-surface exchange factor can be assumed to be equal to unity. With this simplification Equation (5.14) becomes.

$$F_{wc} = \frac{\varepsilon_w \varepsilon_c}{\varepsilon_c + \varepsilon_w\left(1 - \varepsilon_c\right)\dfrac{A_w}{A_c}} \qquad \text{---------- (5.15)}$$

Thus, from Equations (5.13) and (5.15) the radiation heat flux from the wall to the outer casing is:

$$R_2 = \sigma\left[\frac{\varepsilon_w \varepsilon_c}{\varepsilon_c + \varepsilon_w\left(1 - \varepsilon_c\right)\dfrac{A_w}{A_c}}\right]\left(T_w^4 - T_c^4\right) \qquad \text{---------- (5.16)}$$

5.4.10 Radiation Exchange Between Flame-Tube Walls

The net rate of heat transfer to a section of the flame-tube walls from all other "visible" parts of the flame-tube wall is derived using the nomenclature shown in the sketch:

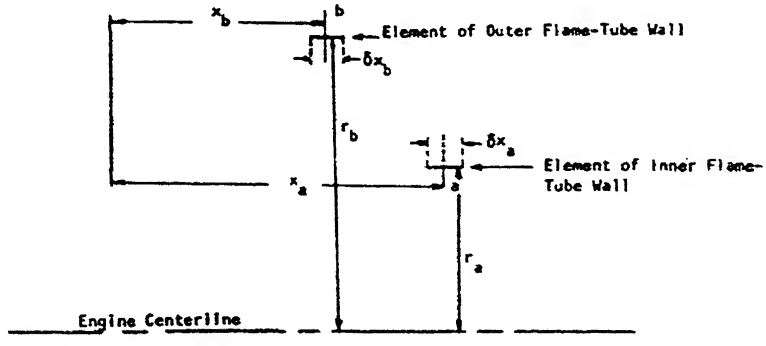

Figure 5.3 View factor nomenclatures

Radiation emitted by an element δx_b which is received by element δx_a (neglecting any reflections) is:

$$\sigma \varepsilon_w^2 2\pi r_b \delta x_b F_{ba} \Gamma\left(T_{wb}^4 - T_{wa}^4\right) \qquad \text{---------- (5.17)}$$

where, F_{ba} = View factor for radiation from b to a

$$= \frac{\delta x_a (r_b - r_a)^2}{2\left[(r_b - r_a)^2 + (x_a - x_b)^2\right]^{3/2}}$$

Γ = transmittance between b and a

$$= \frac{14.82}{p_G \sqrt{(x_a - x_L)^2 + (r_a - r_b)^2} + 14.82} \qquad \text{---------- (5.18)}$$

Radiation exchange per unit time and area of inner wall is given by:

$$\Delta R_3 = \frac{\sigma \varepsilon_w^2 \; r_b \delta x_b (r_b - r_a)^2 \Gamma\left(T_{wb}^4 - T_{wa}^4\right)}{r_a^2 \left[(r_b - r_a)^2 + (x_a - x_b)^2\right]^{3/2}} \qquad \text{---------- (5.19)}$$

Thus the net rate of heat transfer per unit areas to the point on the inner wall under consideration, from all parts of the outer wall is:

$$R_3 = \frac{\sigma \varepsilon_w^2}{2} \sum_{\substack{\text{all b-wall} \\ \text{positions}}} \frac{r_b (r_b - r_a)^2 \Gamma\left(T_{wb}^4 - T_{wa}^4\right) \delta x_b}{r_a \left[(r_b - r_a)^2 + (x_a - x_b)^2\right]^{3/2}} \qquad \text{---------- (5.20)}$$

A similar expression applies for radiation from all parts of the inner wall to a point on the outer wall.

5.4.11 Convection at the Inner Surface of the Flame-Tube Wall

The correlation employed for the internal convective heat transfer at the flame-tube wall for subsonic flow through smooth tubes at high surface and fluid temperatures is [29],

$$C_1 = 0.023 \frac{k}{D_{ft}^1} Re^{0.8} Pr^{0.4} \left(T_{ft} - T_w\right) \qquad \text{---------- (5.21)}$$

where K = thermal conductivity of gas

D_{ft}^1 = hydraulic diameter of the flame tube, equal to twice the distance between flame-tube walls.

5.4.12 Entry-Length Effect

When starting conditions on the wall are uniform, there is a developing boundary layer and the expression for the Nusselt number is usually multiplied by a factor for the entry-length effect. This is given as [31]:

$$\left[1 + \left[\frac{L}{D_{ft}^1}\right]^{-0.7}\right] \qquad \text{---------- (5.22)}$$

5.4.13 Internal Convection with Film Cooling

The contribution of internal convection to the wall heat balance is computed from Equation (5.21) only when film cooling and transpiration cooling are absent. For the case in which film cooling is employed. Equation (5.21) is modified by replacing the hot-gas temperature. T_{ft} by an adiabatic wall temperature, T_{ad} Thus:

$$C_1 = 0.023\frac{k}{D_{ft}^1}Re^{0.8}Pr^{0.4}(T_{ad} - T_w) \qquad \text{---------- (5.23)}$$

The adiabatic wall temperature can be obtained from the following equations [8]:

$$\tau \equiv \frac{T_{ft} - T_{ad}}{T_{ft} - T_{cf}} \qquad \text{---------- (5.24)}$$

$$X = 0.91\left(\frac{U_{ft}}{\overline{U}_{ft}}\frac{x}{Y_{cf}}\right)^{0.8}(Re_{cf})^{-0.2} + 1.41\left[\frac{x}{Y_{cf}}\left|1 - \frac{U_{ft}}{\overline{U}_{ft}}\right|\right]^{0.5} \qquad \text{---------- (5.25)}$$

where, T_{cf} = inlet temperature of cooling film
Y_{cf} = slot width
x = downstream distance of wall element from the cooling slot.

5.4.14 Convection at the Outer Surface of the Flame-Tube Wall

External convection from the flame-tube walls to the annulus air is governed by equation similar to Equation (5.21):

$$C_2 = 0.023\frac{k}{D_{ft}^1}Re_{an}^{0.8}Pr^{0.4}(T_w - T_{an}) \qquad \text{---------- (5.26)}$$

5.4.15 Longitudinal Conduction Along flame-Tube Wall

The longitudinal conduction effect can be estimated on the basis of average temperature gradients. For the inner flame-tube wall, the rate of heat flow to the section of wall (n) under consideration to an adjacent section (n+1) is given by:

$$q = \frac{k_w t_w C_\Lambda (T_{w.n+1} - T_{w.n})}{x_{n+1} - x_n} \qquad \text{---------- (5.27)}$$

where k_w = thermal conductivity of wall material
t_w = wall thickness
Per unit area the heat gain is:

$$K = \frac{k_w t_w C_\Lambda (T_{w.n+1} - T_{w.n})}{x_{n+1} - x_n}\quad\frac{2}{x_{n+1} - x_{n-1}}$$

Combining this with a corresponding quantity for heat flow from the (n-1) element, the net heat received becomes:

$$\Delta K = \frac{2k_w t_w}{x_{n+1} - x_{n-1}}\left[\frac{T_{w.n+1} - T_{w.n}}{x_{n+1} - x_{n-1}} - \frac{T_{w.n} - T_{w.n-1}}{x_n - x_{n-1}}\right] \qquad \text{---------- (5.28)}$$

5.5 SOLUTION OF THE HEAT-BALANCE EQUATION

When all of the heat-flux terms are considered, the heat-balance equation for an element of the flame-tube wall is:

$$R_1 + C_1 + \Delta K = R_2 + C_2 + R_3 \qquad \text{---------- (5.29)}$$

The longitudinal conduction term, ΔK, and the radiation exchange term, R_3, are functions of the wall temperature distribution (rather than the local temperature of the wall element) and, therefore, an iterative method of solution of Equation (5.29) is required when these terms are considered.

5.5.1 Non-Iterative Solution

If we don't consider ΔK and R_3 then a non-iterative solution of Equation (5.29) is possible. In this case Equation (5.29) becomes:

$$R_1 + C_1 = R_2 + C_2 \qquad \text{---------- (5.30)}$$

Substituting for R_1 from Equation (5.2) or (5.12); C1 from Equation (5.21), (5.22); for R_2 from Equation (5.16); for Equation (5.25); then equation (5.30) becomes:

$$D_1 T_w^4 + D_2 T_w^{2.5} + D_3 T_w = D_4 \qquad \text{---------- (5.31)}$$

where, D_1, D_2 ,D_3 and D_4 are known. Newton's approximation is used to solve Equation (5.31).

For use in Newton's approximation, a first estimate of T_w is obtained from one of the following equations:

$$D_1 T_w^4 = D_4$$
$$D_2 T_w^{2.5} = D_4$$
$$D_3 T_w = D_4$$
$$T_w = T_{ft}$$

The chosen T_w is that which leads to the smallest value of ε when Equation (5.31) is written in the form:

$$D_1 T_w^4 + D_2 T_w^{2.5} + D_3 T_w = \varepsilon \qquad \text{---------- (5.32)}$$

With this initial estimate of T_w, Newton's approximation is used to find a value of T_w that satisfies Equation (5.31).

5.5.2 Iterative Solution

The iterative heat-balance solution is only called for after a non-iterative calculation; an approximate wall-temperature distribution will therefore always be available. The iterative heat balance is repeated until the maximum temperature change between any two iteration cycles is less than specified tolerance.

5.6 LIMITATIONS OF THE HEAT TRANSFER SUBPROGRAM

There are several significant limitations of the heat transfer subprogram:

- The film cooling model is idealistic; there is a serious lack of experimental data upon which to base choice of the characteristic distance X_o used in the correlation; in addition, as mentioned above, the film cooling and wall jet mixing models are not related.
- Data are lacking on the emissisvity of luminous flame.
- No heat balance is performed to calculate the temperatures of the inner and outer casing walls.

5.7 STRUCTURE OF THE SUBPROGRAM

The heat-transfer subprogram consists of:

1. A subroutine for solving the non-iterative heat balance.
2. A subroutine for solving the iterative heat balance.
3. A group of library subroutines which provide gas properties, correlation for wall cooling and flame emissivity, and the solution of the fourth-power heat-balance equation.

The subroutines and flowcharts of heat-transfer subprogram are given in the Appendix A4.

CHAPTER 6

RESULTS AND DISCUSSION

6.1 INTRODUCTION

This chapter presents the results obtained from the computer simulation of a gas turbine combustor. These results were the outcome of the techniques and methodology used in the previous chapters to analyze the combustor for flow and performance parameters. The results were compared with the available experimental data and 3D analysis for annular combustors of a modern fighter aircraft engine (Kaveri engine for LCA).

There are many design aspects of a modern combustor and effort was to incorporate all these for the satisfactory operation of the engine, but this was not possible due to the complex nature of flow and heat transfer in the combustor. So a compromise was made between them. As for as 1-D analysis is concerned, the main parameters of interest are the pressure loss, the flow distribution and the heat transfer. As described in previous chapters, the analysis was carried out in three major sets, namely diffuser, main combustor, and heat transfer analysis. The results of the computer simulation program for various test runs and their comparison with the experimental data and 3D analysis illustrating aspects of the program are presented in the following three sections.

6.2 DIFFUSER ANALYSIS RESULTS

The diffuser analysis is mainly concerned with the checking of the validity of the analytical "stream tube" method. The results obtained in this subprogram were compared with the experimental data and 3D analysis on annular diffusers.

Two types of combustor diffusers are taken into consideration, namely, K1 and K4 for the validation of the present diffuser subprogram. The analysis was carried out for two conditions, first for known mass flow split and second for unknown mass flow split. The inlet conditions and results are as follows:

6.2.1 K1 -Combustor:

Table 6.1 -Inlet Conditions

Total Pressure (MPa)	2.17
Total Temperature (K)	756.50
Air mass flow rate (kg/s)	63.34
Mach No.	0.34
Length (pre-diffuser) (m)	0.087
Critical Shape Factor	2.28
Included Angle (degrees)	6
Mass flow inner annulus (%)	42
Mass flow outer annulus (%)	45
Mass flow core (%)	13

Table 6. 2 -Results of Pressure Loss and Mach number

Pressure Loss	1-D	Known flow Split (13% core)	0.14
		Unknown flow split	0.15
	3-D		0.18
Mach No.	1-D	Known flow Split (13% core)	0.2
		Unknown flow split	0.2
	3-D		0.17
Ideal Pressure Recovery Coefficient (Cpi)			0.971
Pressure Recovery Coefficient (Cp)			0.645
Diffuser Effectiveness (ξ)			0.656

6.2.2 K4 -Combustor:

Table 6.3 - Inlet Conditions

Total Pressure (MPa)	2.17
Total Temperature (K)	756.50
Air mass flow rate (kg/s)	63.34
Mach No.	0.34
Length (pre-diffuser) (m)	0.065
Critical Shape Factor	2.28
Included Angle (degrees)	7
Mass flow inner annulus (%)	42
Mass flow outer annulus (%)	45
Mass flow core (%)	13

Table 6.4 – Results of Pressure Loss and Mach number

Pressure Loss	1-D	Known flow Split (13% core)	0.17
		Unknown flow split	0.18
	3-D		0.2
Mach No.	1-D	Known flow Split (13% core)	0.23
		Unknown flow split	0.23
	3-D		0.216
Ideal Pressure Recovery Coefficient (Cpi)			0.972
Pressure Recovery Coefficient (Cp)			0.945
Diffuser Effectiveness (ξ)			0.983

Tables 6.2 and 6.4 show the pressure loss, outlet Mach number, pressure recovery coefficient, and effectiveness of the diffuser as obtained from diffuser calculations. These results are in good agreement with the 3D analysis, which had been verified and validated with the experimental data for the same diffuser under same inlet conditions. The differences among, 3D analysis, experimental data and 1D is due to the fact that when the stream tube method is used between the annuli, the calculated boundary layer blockage decreases considerably between the outlet of pre-diffuser and inlet to the annulus which results in lower mixing losses.

The pressure losses in the diffusing passages influence the mass flow split at the snout or cowl. The flow split at the snout in turn influences the temperature level in the flame tube. The diffuser analysis has been carried out by the 'stream tube method' assuming a uniform inlet velocity profile; to account for the fact that the actual velocity at the wall was about 20 per cent greater than that in the mid stream, the test cases were run with a blockage of 0.8, and a corresponding shape factor of 1.24. Since the deceleration of the flow between the diffuser walls is greater for the non-uniform velocity profile, a larger boundary layer blockage should be used with a uniform velocity profile to simulate this effect. The only effect which the computations apparently do not accurately predict is the effect of high Mach numbers on the pressure-loss factor.

6.3 COMBUSTOR FLOW ANALYSIS RESULTS

The combustor flow analysis is mainly concerned with the analysis for air mass flow split, inner and outer annulus pressure losses, flow distribution through various cooling holes and slots and outlet Mach numbers in annuli and flame tube. The inlet conditions are the same as given in the Table 6.1 for K1 combustor and Table 6.3 for K4 combustor. The results pertaining to the combustor flow for K1 and K4 type of combustors are given below.

6.3.1 K1- Combustor: (same inlet conditioned as mentioned in Table 6.1)

Table 6.5 – Results of Liner Mass Flow Distribution

	1-D		3-D
	Known Split(13% Core)	Unknown Split	
Outer Annulus	%	%	%
Primary Zone	10.92	10.97	10.9
Cooling Ring No.3	2.71	2.72	2.9
Secondary Zone	2.43	2.44	3.2
Cooling Ring No.5	2.68	2.68	2.7
Dilution Zone	8.31	8.34	10.5
Cooling Ring No.7	2.91	2.92	2.9
Cooling Ring No.9	2.85	2.86	2.6
Cooling Ring No.11	2.84	2.85	2.9
Inner Annulus			
Primary Zone	11.34	11.28	12.5
Cooling Ring No.4	1.92	1.92	1.6
Secondary Zone	2.59	2.59	3.0
Cooling Ring No.6	1.94	1.94	1.5
Dilution Zone	10.04	10.02	10.1
Cooling Ring No.8	2.02	2.02	2.2
Cooling Ring No.10	2.28	2.28	2.0
Cooling Ring No.12	2.45	2.46	2.2

Table 6.6 – Results of Pressure Loss and Mach number

			Inner Annulus	Outer Annulus	Overall (Flame Tube Exit)
Pressure Loss	1-D	Known Split (13%Core)	2.04	2.7	6.8
		Unknown	2.05	2.7	6.86
	3-D		1.29	1.97	6.83
Mach No	1-D	Known Split (13%Core)	0.111	0.096	0.124
		Unknown	0.112	0.095	0.123
	3-D		0.105	0.0984	0.119

Table 6.7 - Results of Mass Flow Split

		Inner Annulus (%)	**Outer Annulus (%)**	**Core (%)**
1-D	Known Split (13%Core)	41	44	15
	Unknown	41.4	43.6	15
3-D		42.3	44.7	13

6.3.2 K4- Combustor: (same inlet conditions as given in Table 6.3)

Table 6.8 – Results of Liner Mass Flow Distribution

	1-D		Experimental	3-D
	Known Split(13% Core)	Unknown Split		
Outer Annulus	%	%	%	%
Primary Zone	11.00	10.840	12.40	10.7
Cooling Ring No.3	2.790	2.760	2.764	3.1
Secondary Zone	2.434	2.400	2.450	3.2
Cooling Ring No.5	2.764	2.740	2.764	2.7
Dilution Zone	8.474	8.380	8.840	10.6
Cooling Ring No.7	3.016	3.000	2.764	2.9
Cooling Ring No.9	2.905	2.880	2.764	2.7
Cooling Ring No.11	2.856	2.830	2.764	2.9
Inner Annulus				
Primary Zone	12.030	11.910	14.640	12.4
Cooling Ring No.4	1.923	1.910	2.234	1.6
Secondary Zone	2.342	2.320	2.900	3.0
Cooling Ring No.6	1.923	1.910	2.234	1.5
Dilution Zone	9.463	9.360	10.18	10.1
Cooling Ring No.8	2.014	2.000	2.234	2.2
Cooling Ring No.10	2.167	2.150	2.234	1.9
Cooling Ring No.12	2.344	2.330	2.234	2.2

Table 6.9 - Results- Total Pressure Loss and Mach number

			Inner Annulus	Outer Annulus	Overall (Flame Tube Exit)
Pressure Loss	1-D	Known Split (13%Core)	2.14	3.12	8.44
		Unknown	2.14	3.12	8.43
	3-D		2.32	2.71	9.17
Mach No	1-D	Known Split (13%Core)	0.125	0.108	0.16
		Unknown	0.125	0.109	0.16
	3-D		0.1343	0.118	0.1373

The results shown in Tables 5, 6 and 7 pertain to the K1 combustor. The results are in agreement with the 3D analysis and hence with experimental results since the 3D analysis have already been validated with the experimental results. There is a little difference in the dome mass flow split. This variation may be due to the fact that 1D analysis calculates the mass flow split based on the flow area. Since the discharge coefficient of holes have influence over the flow mass rate, its effect on flow split can not be overlooked. An accurate value of discharge coefficient for different types of holes under different flow conditions would surely increase the accuracy of the results obtained from the computer program.

Table 6.8 and 6.9 show the results of K4 combustor. Table 6.8 compares 1D and 3D predictions with the well established experimental data. One can clearly see that the1D predictions are as close to the experimental results as the 3D predictions.

6.4 HEATS-TRANSFER RESULTS

There are many heat transfer parameters that affect the functioning of an aircraft engine combustor like flame tube wall temperature, film cooling effectiveness and the heat transfer to the annulus air mainly due to convection and radiation. The flame tube wall temperature is the most critical and important parameter for a combustor design. It imposes a certain limit on the maximum temperature rise of liner wall material to avoid distortion and to keep the mechanical strength adequate enough.

1-D analysis has been carried out for various heat transfer and cooling parameters of the combustion chamber. Here only flame tube wall temperature results are presented due to its importance over other parameters.

The predictions of the heat-transfer subprogram for K1 and K4 have been compared with data presented by NASA [35]. The casing temperature was calculated assuming natural convection and radiation using room-temperature as the reference. (The actual heat transfer coefficients were obtained from McAdams [31]). Heat transfer from the casing to the annulus air was ignored. The flame tube wall absorptivities and emissivities were taken as 0.85; the casing emissivity was taken as 0.8

Figure 6.1 shows the temperature distribution of flame tube wall for a NASA combustor. The geometric configuration of this combustor is quite simple as compared to K1 and K4 combustors. Unlike K1 and K4, this combustor doesn't have any dump region in the diffuser part. Its inlet conditions are also different. Still this result has been used for the validation of the computer program for heat transfer in the absence of other experimental data. This comparison, at least, gives a trend and range of predicted values from the present simulation.

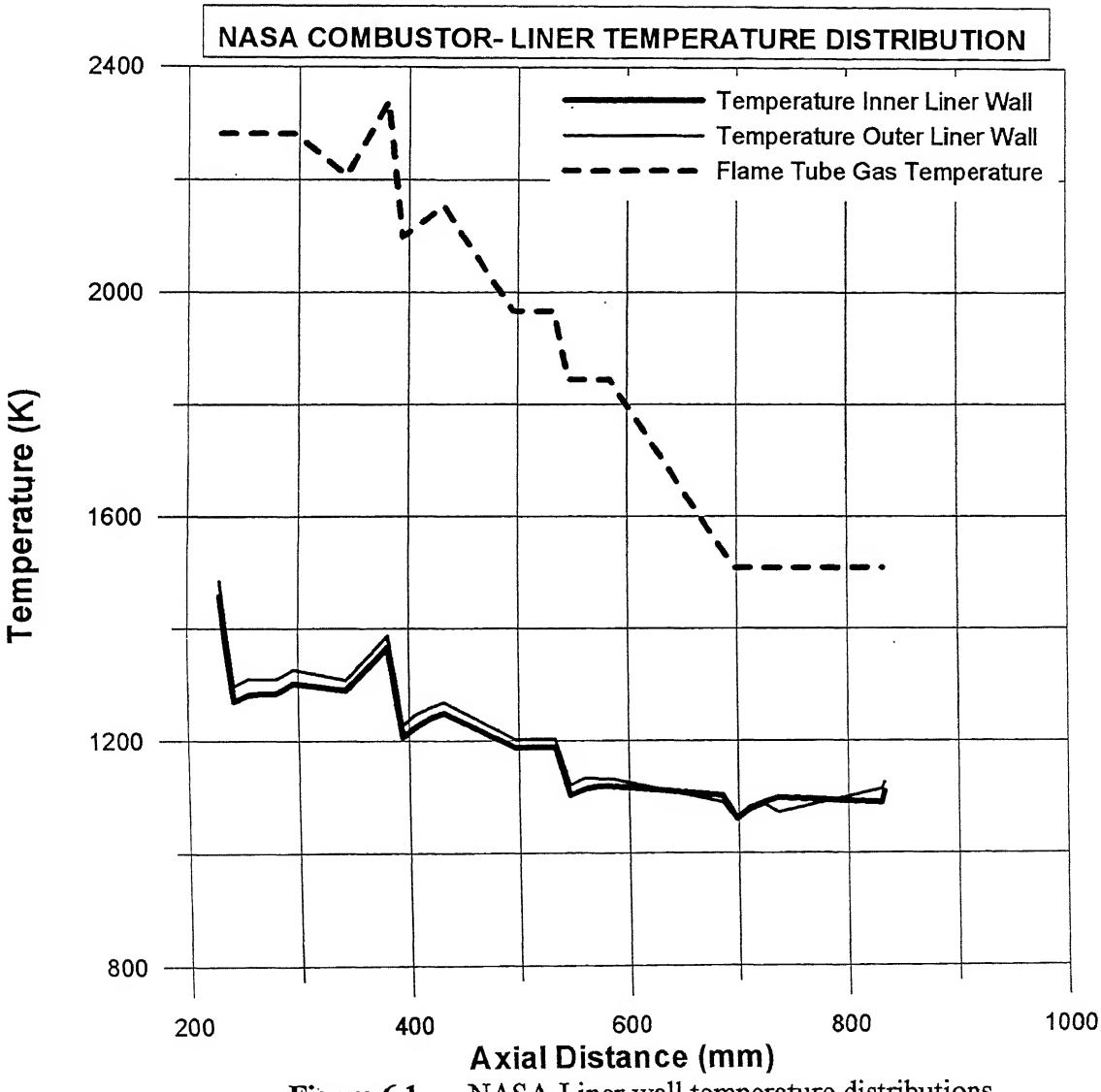

Figure 6.1 NASA-Liner wall temperature distributions.

Figures 6.2 and 6.3 pertain to the K1 and K4 combustors, respectively, and give the linear temperature distribution obtained from 1D prediction. In spite of different geometry and inlet conditions of NASA combustor, agreement of these results with Fig. 6.1(NASA) is reasonably good. The virtually instantaneous mixing of the penetration jets results in a sharply falling flame temperature immediately downstream of each hole row. As the wall jets don't mix at all, the amount of gas available in the tube is reduced by the contents of the wall jets and the resulting spatial variation of flame-temperature is considerably higher than it would have been, had the wall jets mixed with the main stream in the flame tube.

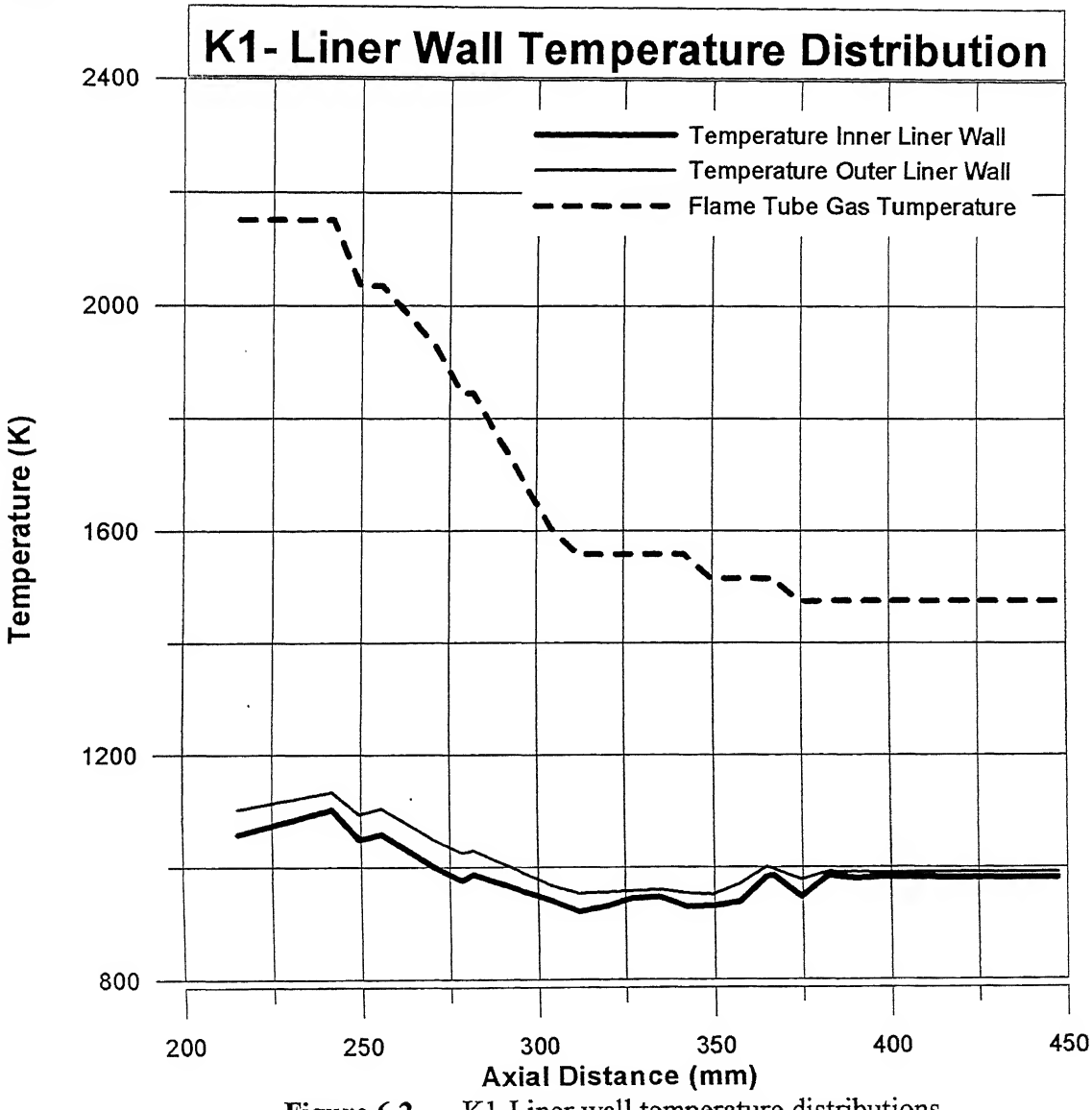

Figure 6.2 K1-Liner wall temperature distributions.

As evident from the plots, the temperatures of the flame tube walls follow the general variation of the flame temperature reasonably closely up to an axial position of about 370 mm. as it would be expected with a 1-D calculation of radiation from the flame tube walls. Downstream of this position, the sharply dropping radiative heat transfer from the flame is roughly balanced by a drop in convective heat transfer in the annuli caused

by the sharply reduced air velocities in the annuli downstream of the dilution holes. Near the end of the combustor the air velocities in the annuli fall nearly to zero, causing the wall temperature to rise sharply.

A closer look on the curves of Fig. 6.2 and 6.3 shows certain variations of the predicted values with NASA results of Fig. 6.1. The inconsistency may be due to:

1 The difference in geometry and inlet condition although the basic shape is same.
2. Simpler assumptions about the dimensions of the test combustor.
3. Simpler assumptions about the heat loss from the casing.
4. Two-dimensional effects which become increasingly important as the convective heat transfer components are reduced.

The casing temperature exerts an important influence on the flame tube wall temperature, since radiation from the flame tube wall to the casing becomes significant in the absence of film cooling.

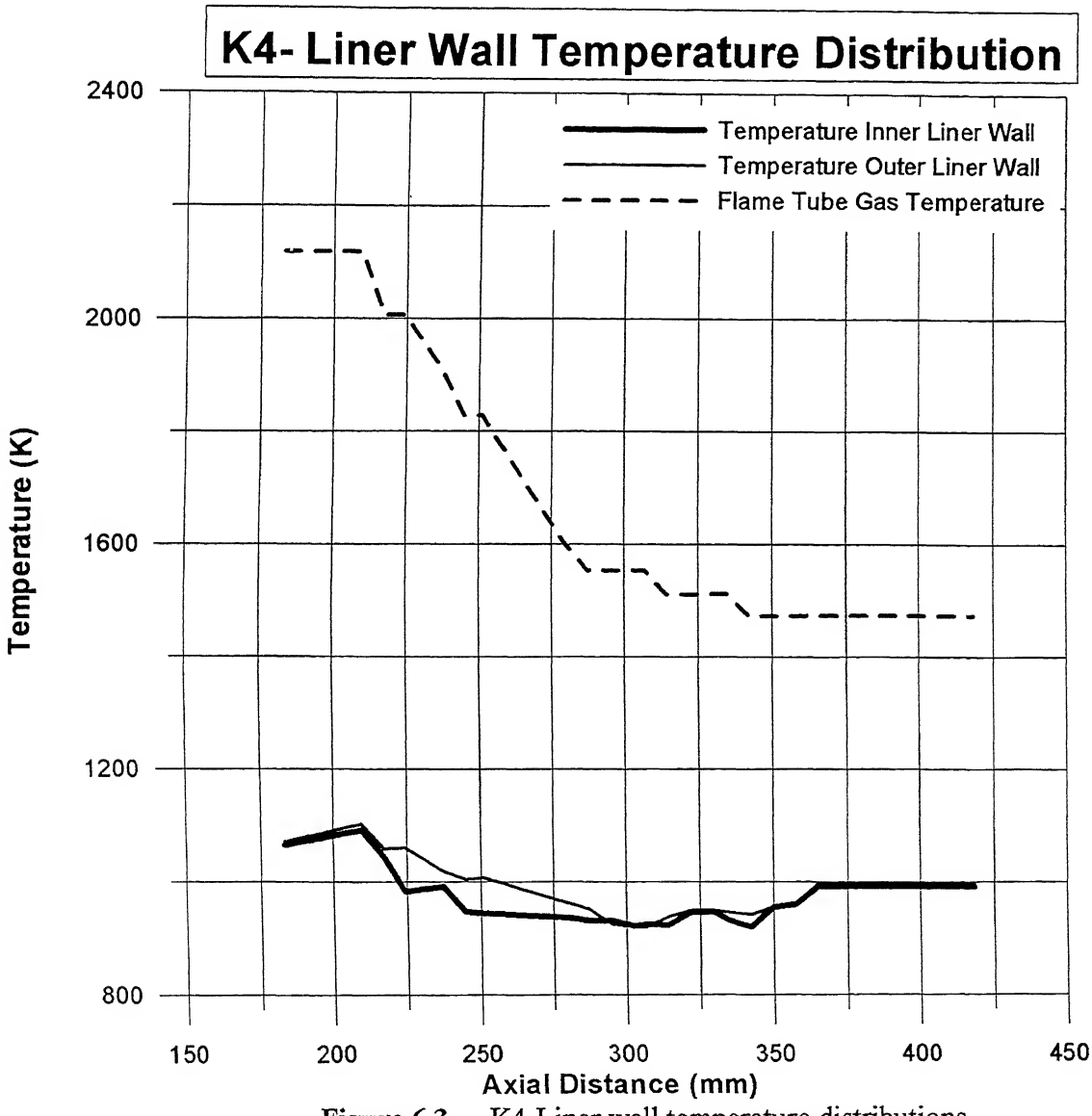

Figure 6.3 K4-Liner wall temperature distributions.

The most striking differences between the above curves are in their slopes. There appears to be a dominant two-dimensional heat transfer mode that is causing the experimentally measured wall temperatures to fall off rapidly with distance downstream. This effect is most apparent in the radiation-only results. As the amount of fuel available for burning in the primary zone does not vary from case to case, and the total temperature of the entering air is almost constant, the effect of a decrease in the flow through the dome into the primary zone is to raise the temperature of the combustion products. From the results of the present computer calculations, it is concluded that the film and convective cooling models used are producing results that agree with the NASA values.

6.5 CONCLUSIONS

Operation of the complete computer program has been checked by running two test cases having different geometry, but identical inlet conditions. The results of the diffuser, airflow and heat transfer test cases have been discussed in their respective sections separately. The comparison of results with well established data reveals the accuracy and validity of the computer program for 1D analysis of a modern annular combustor.

The attempt was to predict the maximum number of flow and performance parameters for an annular combustor using 1D analysis for reasonably accurate results. The results obtained from analysis are presented graphically and in Tabular forms. The main conclusions of this work are as follows:

1. A computer program for analyzing the airflow and heat transfer characteristics of annular gas turbine combustors has been developed.

2. The diffuser, air-flow, and heat-transfer sections of the computer program were tested individually by comparing their predictions for appropriate quantities with available experimental data and 3D analysis in the open literature. The correlation between calculated and experimental values is judged to be reasonably good.

3. The complete computer program was tested for satisfactory operation by running it for two test cases, using different geometry, but same inlet conditions and program options as specified by GTRE. The main trends of the results, as inferred by comparing changes in pressures, flows, and temperature distributions from case to case, are also in agreement with the 3D analysis as well as with the available experimental data.

6.8 SUGGESTIONS FOR FUTURE WORK

Present computer modeling can be made more powerful and accurate by introducing the analysis for those regions in which sudden expansion or eddy losses are predominant. Dump diffuser region analysis comes in the same category. As 1D model is not capable of capturing the eddy and turbulence losses, which are at least 2D in nature; therefore 1D computer simulation could be coupled with 2D or 3D modeling specifically for the dump region. This would help in providing more realistic input conditions for the air-flow and heat-transfer subprograms.

The results of the stream tube diffuser calculation are quite good in view of the gross assumptions made. If the equations are examined further and the potentialities and limitations of the method explored, this technique could prove to be a powerful new tool for more general applications.

It would be useful to make a more exhaustive survey of the influence of certain program input parameters. For example, critical shape factor, boundary layer blockage, entrainment function and constant, hole discharge coefficient, etc, are few parameters to which program results are very sensitive. By experiment, a "most reasonable" choice of these parameters may be found and accuracy of the simulation results can be increased significantly.

REFERENCES

1. Graves, C.C. and Grobman, J.S., Theoretical Analysis of Total Pressure Loss and Airflow Distribution for Tubular Turbojet Combustors with Constant Annulus and Liner Cross-sectional Areas (NACA Rep. 1373), National Advisory Committee for Aeronautics, 1958.
2. Grobman, J.S., Comparison of Calculated and Experimental Total-Pressure Loss and Airflow Distribution in Tubular Turbojet Combustors with Tapered Liners (NASA Memo 11-26-58E), National Aeronautics and Space Administration, 1959.
3. Samuel, B.P., A Jet Engine Combustor Design Analysis Suitable Electronic Computers (ASME Preprint 61-WA-305), American Society of Mechanical Engineers,1961.
4. Lefebvre, A.H. and Herbert, M.V., "Heat-Transfer Processes in Gas-Turbine Combustion Chambers", Proc. Inst. Mech. Engrs., England, Vol. 174,1960.
5. Tipler, W., "Combustion Chambers and Control of the Temperature at Which They Operate", Inst. Mech. E. – ASME Joint Conference on Combustion, Institution of Mech. Engrs., England,1955.
6. Sovran, G. and Klomp, E.D., Experimentally- Determined Optimum Geometries for Rectilinear Diffusers with Rectangular, Conical, or Annular Crossed-Section, presented at the Symposium "Fluid Mechanics of Internal Flow", General Motors Research Laboratories, Michigan, Sep, 1965.
7. Reneau, L.R., Johnston, J.P., and Kline, S.J., Performance and Design of Straight, Two-dimensional Diffusers (ASME Prep. 66-FE-10), American Society of Mechanical Engineers, May 1966.
8. Spalding, D.B., "Prediction of Adiabatic Wall Temperatures in Film-cooling Systems", AIAA Journal, Vol. 3, no. 5, May 1965, pp. 965-967.
9. Schirmer, R.M. and Quigg, H.T., Effect of JP Fuel Composition on Flame Radiation and Hot Corrosion (Res. Div. Rep. 4230-65R), Phillips Petroleum Company, Bartlesville, Okla., 1965.
10. Venneman, W.F., Flow Coefficient and Jet Deflection Angles for Combustor-liner Air-entry Holes, Part-1, G.E. Company, Schenectady, New York, 1959.
11. Venneman, W.F., Flow Coefficient and Jet Deflection Angles for Combustor-liner Air-entry Holes, Part-II, G.E. Company, Schenectady, New York, 1960.
12. Marshal, L.A., Aerodynamic Characteristics of Combustor-liner Air-entry Passages (Rep. R58 AGT 558), Aircraft Gas Turbine Division, G.E. Company, Cincinnati, 1958.
13. Kaddah, K. Sh., Discharge Coefficient and Jet Deflection Studies for Combustor-liner Air-entry Holes, Thesis No. 17/10, College of Aeronautics, Cranfield, England, June 1964.
14. Dittrich, R.T. and Graves, C.C., Discharge Coefficients for Combustor-liner Air-entry Holes, I-Circular Holes (NACA TN 3663), National Advisory Committee for Aeronautics, 1956.
15. Dittrich, R.T. and Graves, C.C., Discharge Coefficients for Combustor-liner Air-entry Holes, II-Flush Rectangular Holes, Step Louvers, and Scoops (NACA TN 3924), National Advisory Committee for Aeronautics, 1958.

16. Knight, M.A., and Walker, R.B., "The Component Pressure Losses in Combustion Chambers", ARC R& M 2987, 1957.
17. Rosenthal, J., Exploratory Methods for the Determination of Gas Flow and Temperature Patterns in Gas Turbine Combustors (ARL ME Note 235), Aeronautical Research Laboratory, Dept. of Supply, Australia, 1959.
18. Fielding, D. and Topps, J.E.C., Thermodynamic Data for the Calculation Gas Turbine Performance (ARC R&M 3099), Aeronautical Research Council, England, 1959.
19. Flow Through a Sudden Enlargement in a Pipe (Aerodynamic Data Sheet 00.03.29), Royal Aeronautical Society, London, January 1964.
20. Wilson, R.E., McAdams, W.H., and Seltzer, M., "The Flow of Fluids Through Commercial Pipe Lines", Ind. Eng. Chem., Vol. 14, No. 2, 1922, pp 105-119.
21. Gandamihardja, O., Jet Deflection (Thesis 15/16/C), College of Aeronautics, Cranfield, England, 1962.
22. Keffer, J.F., and Baines, W.D., " The Round Turbulent Jet in a Cross Wind", J. Fluid Mech., Vol. 15, April 1963.
23. Jordinson, R., Flow in a Jet Directed Normal to the Wind (ARC R&M 3074), Aeronautical Research Council, England, 1958.
24. Forstall, W., and Shapiro, A.H., "Momentum and Mass transfer in Co-axial Jets", J. Appl. Mech., December, 1950, pp 399-408.
25. Squire, H.B., "Jet Flow and Its Effects on Aircraft", Aircraft Eng., England, Vol. 22, March, 1950.
26. Kruka, V. And Eskinazi, S., " The Wall-jet in a Moving Stream", J. Fluid Mech., Vol. 20, Part-4, 1964, pp 555-579.
27. Harris, G.L., The Tubulent Wall Jet in a Moving Stream, "Recent Developments in Boundary Layer Research" (AGARDograph 97), North Atlantic Treaty Organization, May 1965, pp 125-158.
28. Hamilton, D.C. and Morgan, W.R., Radiation- Interchange Configuration Factors (NACA TN 2836), National Advisory Committee for Aeronautics, 1953.
29. Humble, L.V., Lowdermilk, W. H. And Desmon, L.E., Measurement of Average Heat Transfer Coefficients for Subsonic Flow of Air in Smooth Tubes at High Surface and Fluid Temperatures (NACA Rep. 1020), National Advisory Committee for Aeronautics, 1951.
30. Dussourd, J.L., et al., Aerodyanmic Criteria for Optimum Design of Mixed-flow Impellers-experimental Results for Impellers 1 and 1B (WADC TN 58-88), AiResearch Manufacturing Company, June, 1960.
31. McAdams, W.H., Heat Transmission, 3rd Ed, McGraw-Hill Book Company, New York, 1954.
32. Peters, J.E., and Hammond, D.C., "Design of Modern Turbine Combustors", 1987.
33. Boyce, Mecherwan P., " Gas Turbine Engineering Hand Book", 1997
34. Doods, W.J., and Bahr, D.W., "Combustor System Design", Academic Press Ltd, 1990.
35. Grobman, Jack S., NASA Report No. 1111-1, NASA-Lewis Research Center, 1969.
36. Spalding, D.B., A Unified Theory of Friction, Heat Transfer and Mass Transfer in the Turbulent Boundary Layer and Wall Jet (ARC CP No. 829), Aeronautical Research Council, England, 1965.

APPENDIX

SUBROUTINES AND FLOWCHARTS

A1 INTRODUCTION

This section is meant to show how the modeling methods described in Chapter 2 through Chapter 5 are fitted into the computer program. As already explained that the computer modeling program consist of three independent subprograms, viz., diffuser, airflow and heat transfer subprograms, each of which contains a family of the subprograms

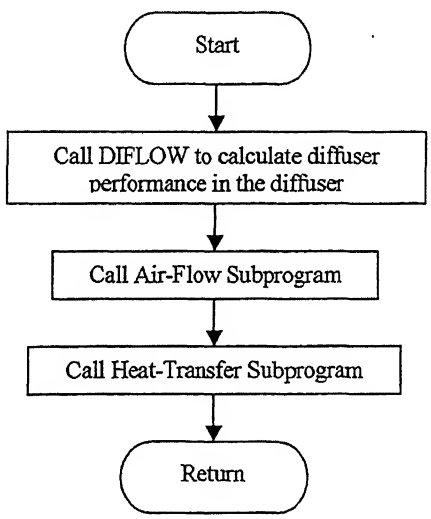

Figure A1 Flowchart for Main Program

Figure A1 shows the main program flowcharts. It calls subroutine DIFLOW for the diffuser portion of calculation under diffuser subprogram, subroutine AIRFLOW for the air-flow calculation under airflow subprogram and subroutine HEAT for heat transfer calculation of combustor under heat transfer subprogram. Figure A2 presents flowchart for overall program including as a whole including reading of input data and writing out it to make sure that the input data are read in correctly. Geometrical calculations of the combustor are also carried out to supply required geometric input data to various subroutines in appropriate form for further calculations in the subroutine. The subroutines and respective flowcharts are given in brief in the succeeding sections.

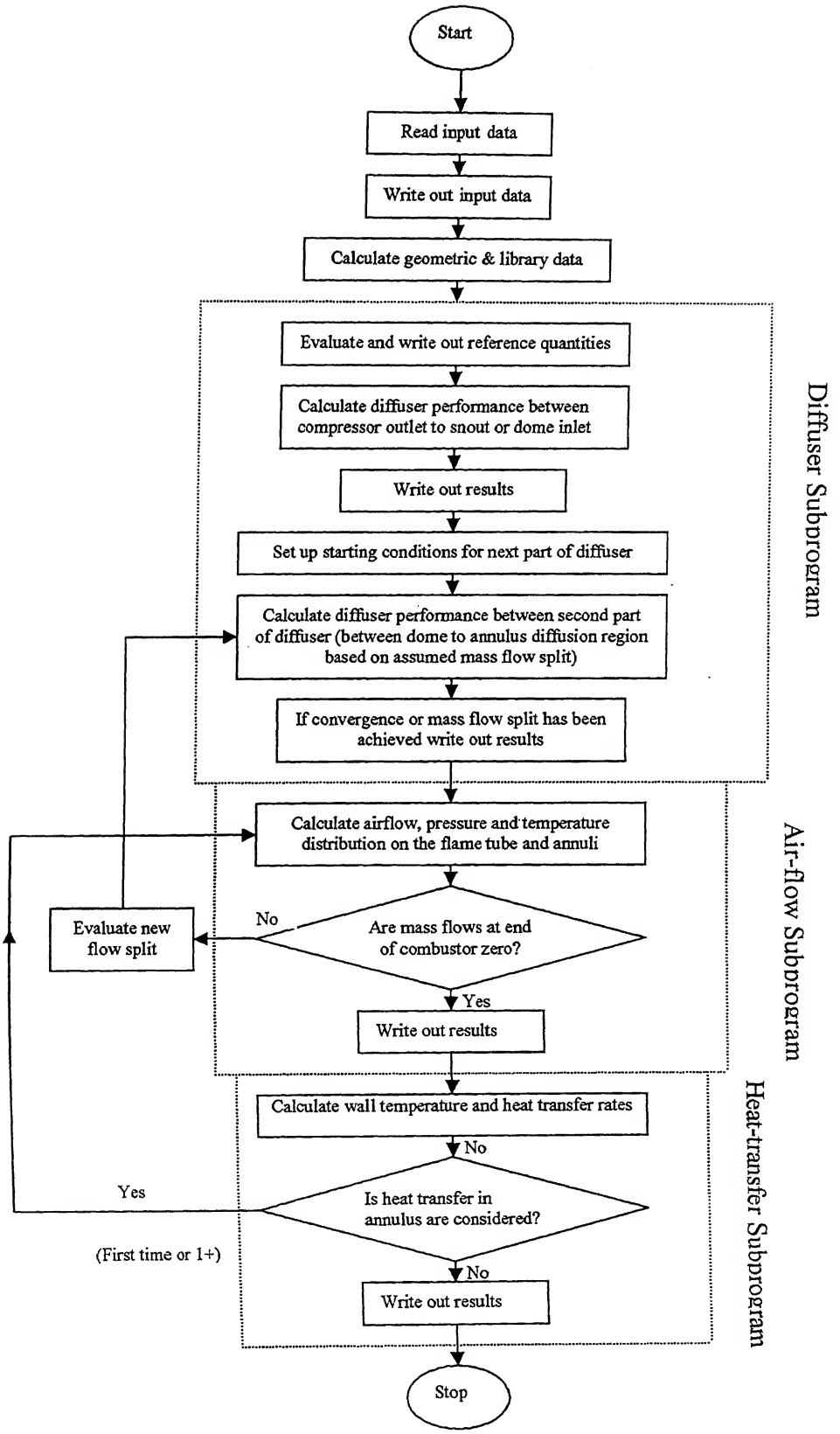

Figure A2 Overall Flowchart for Entire Program

A2 DIFFUSER SUBPROGRAM

The diffuser subprogram calculates the flow properties in the diffuser from the compressor outlet to the first calculation point in each annulus. The subroutines and Flowcharts are in the following subsections.

A2.1 Diffuser Subprogram Subroutines

Various subroutines pertaining to this subprogram are as follows:

Subroutine DIFLOW: This subroutine has three main functions-

1. To organize the calculation procedure used in the diffuser subprogram.
2. To calculate the flow properties in the two annuli between the cowl and outer casing if the mixing equation is being used.
3. To calculate the flow properties beyond the outlet of pre-diffuser (a fudge factor has been used for the results obtained in this region as to compensate for the eddy and turbulence losses to make available more realistic input values for the next calculation stations).

This subroutine has three entry points splitting the program into three separate parts. The three parts performs the following function:

(i) The first part organizes the calculation position between the pre-diffuser inlet to the cowl inlet. A correction for the passage curvature is also calculated.

(ii) The second part, following DIFLW, the calculation procedure between the dome and annulus diffusing passage is organized and flow properties are calculated at the outlet.

(iii) The third part, following Entry DIFLW2, calculates the flow in the diffuser with a given mass flow split using the stream tube method throughout.

Subroutine TUBCTS: This subroutine is called by DIFLOW. The subroutine does the following:

1. Calculates the inlet static pressure and the inlet stream tube properties.
2. Calculates the reference velocity, Mach number, and dynamic head.
3. Sets up an iteration loop to calculate the flow properties and the boundary layer characteristics.
4. Calculates the outlet velocity profile and the diffuser performance.

Subroutine TUBSTA: It is called by DIFLOW. This subroutine is called before the iteration on mass flow commences, and its function is to set up geometric data in a form that can be used by subroutine TUBSA1.

Subroutine TUBSA1: This subroutine is called by DIFLOW to perform a stream tube calculation in the diffuser part beyond pre-diffuser outlet to:

1. Calculate the stream tube properties.
2. Calculate the boundary layer characteristics.
3. Calculates the diffuser performance.

Subroutine TUBFW1: It is called by subroutine DIFLOW during the iteration on the mass flow split. This calculates:

1. The geometric positions of the flow split
2. The area mean velocity and weighted mean velocity for the flow streams into each annuls and the cowl or snout.

Subroutine TUNEIN: This is called by TUBCTS and TUBSA1 to calculate the input quantities for the stream tube calculation. In this the following calculations are performed-

1. If the static pressure is not given (i.e., if TUBEIN is called by TUBCTS), calculate the static pressure.
2. Split the flow into a number of stream tubes and calculates the total pressure for each stream tube.
3. Calculates the flow area for each stream tube when the flow is accelerated isentropically to Mach. Number 1.

Subroutine TUBANL: This is called by TUBCTS and TUBAS1 to calculate-

1. The pressure at each calculation point in the diffuser, Mach number.
2. The velocity and density at each calculation point.
3. Outlet velocity profile

Subroutine NEWRAD: This is called by TUBCTS and TUBSA1 to perform-

1. Position of flow separation (depending upon critical shape factor supplied from outside to the program).
2. Checks the solution for convergence.
3. Calculates a new guess for the boundary layer displacement thickness.

A2.2 Flowchart for Diffuser Subprogram

The overall flow chart for the diffuser subprogram is given in the Figure A3.

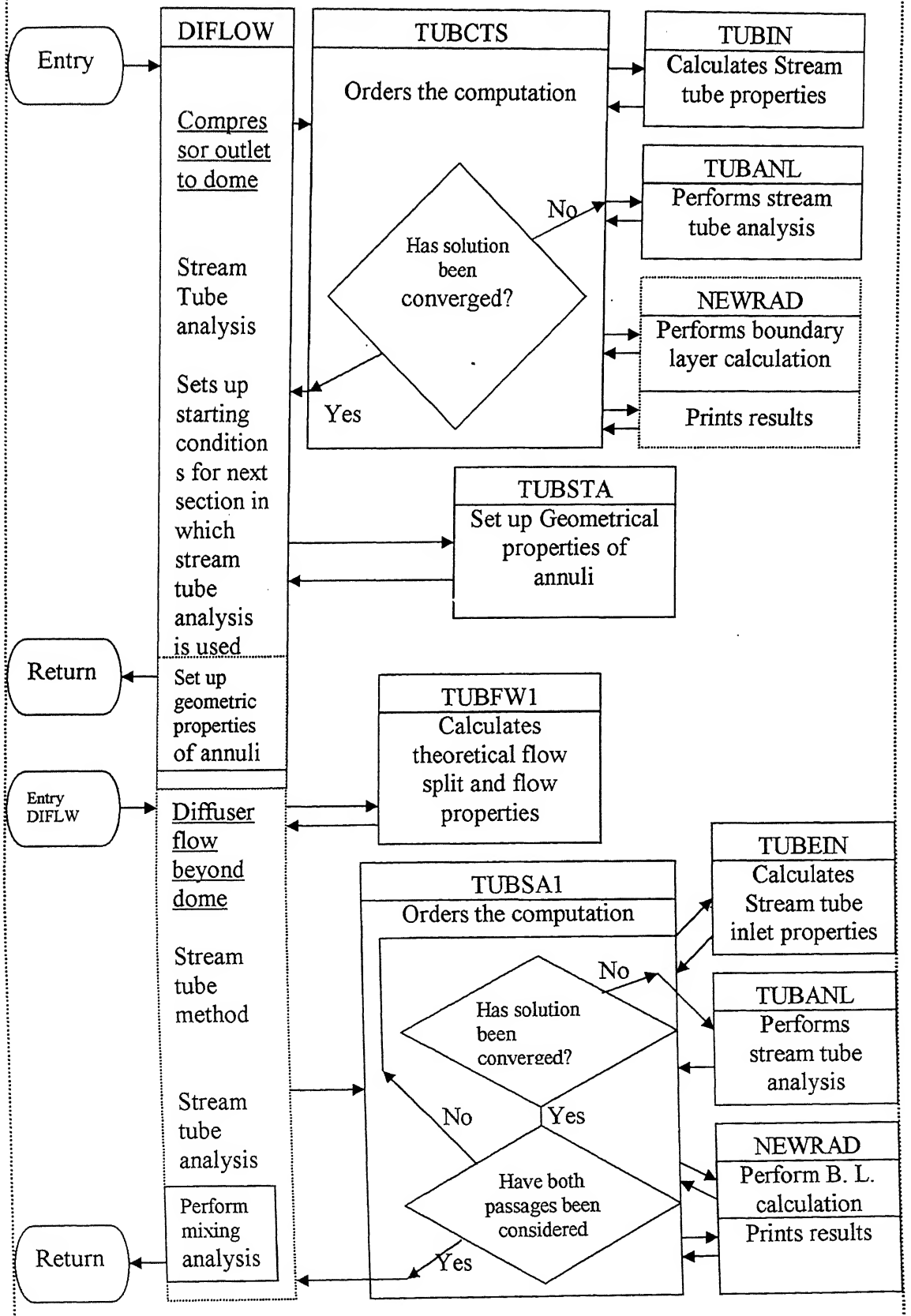

Figure A3 Overall Flowchart for Diffuser Subprogram

A3 AIR-FLOW SUBPROGRAM

The air-flow subprogram calculates the flow properties in the flame tube and annuli from the first calculation point, which corresponds the first hole row on the wall as distinct from the dome, to the end of the combustor. It also organizes the mass flow split iteration.

A3.1 Air-Flow Subprogram Subroutines: Subroutines of this subprogram are

Subroutine AIRFLO: This subroutine controls the air-flow calculations. It functions are-

1. An initial mass flow split is calculated based on the total hole area in the dome on each annulus.
2. Calculates the initial conditions on the dome at the start of each annulus.
3. Calculates the primary zone pressure and temperature also initial conditions for the flame tube calculations.

Subroutine DISJET: This subroutine determines jet discharge parameters which are:

1. Initial jet-air mass flow rate, discharge jet angle, and discharge coefficient. This jet information is used by subroutine JETMIX.
2. Initial jet-air mass flow rate, jet momentum, and axial jet momentum and jet enthalpy. This jet information is used by subroutine EQUAN and EQUFT.

Subroutine PRTEMP: This subroutine does the following functions:

1. Calculates conditions within the primary zone by solution of a simplified form of the flame tube equations, assuming the primary zone acts as a stirred reactor. Flame tube conditions are thus set up for the secondary-hole calculation point, so that from then on the flame tube equations can be solved in the normal way.
2. This also calculates the fraction of air entering the primary holes which recirculates upstream.

Subroutine EQUAN: This subroutine solves the equations for flow in the annuli. The main equation is a quadratic in annulus velocity at the point of calculation. The rest of subroutine is concerned with evaluating the constants in this equation.

Subroutine EQUFT: This subroutine solves the equations for flow in the flame tube down stream of the primary zone. The solution follows an iterative procedure. Calculations are performed for a control volume bounded by two adjacent calculation stations (say 1 and 2).

Subroutine HEATAD: This subroutine provides EQUFT with the heat release terms in the energy equation.

Subroutine JETMIX: This subroutine provides with the characteristics of the residual jets. Wall jets and penetration jets are calculated separately using the same model but different values of the mixing constants.

A3.2 Flowchart for Air0flow Subprogram: The overall flowchart for diffuser subprogram is given in Figure A4.

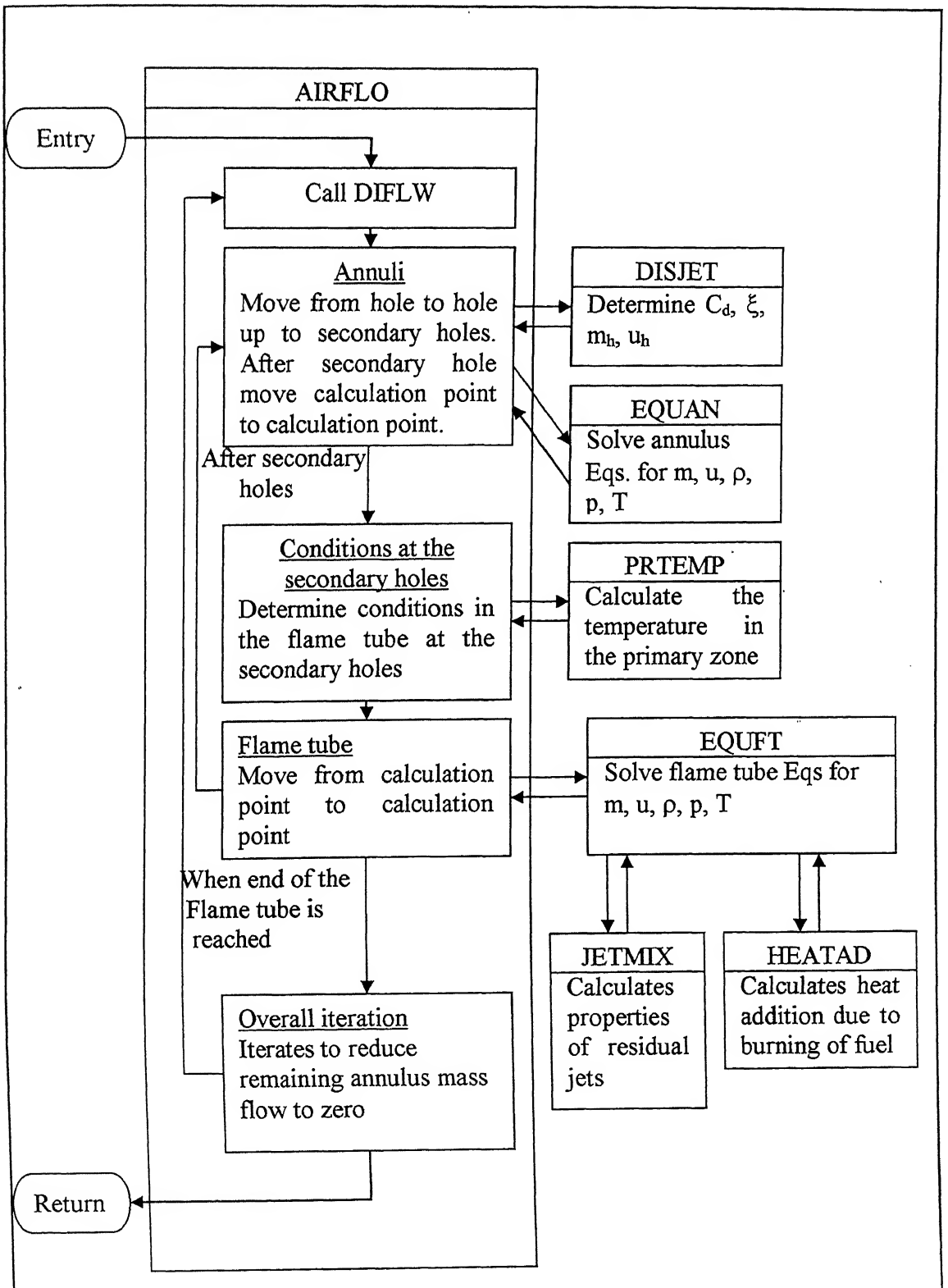

Figure A4 Overall Flowchart for Air-Flow Subprogram

A4 HEAT TRANSFER SUBPROGRAM

The heat transfer subprogram calculates the temperature distribution in the liner wall, film effectiveness and the rate of heat transfer among various components of the main combustor. Main subroutines and flowchart of the program is given in the following sections.

A4.1 Heat Transfer Subprogram Subroutines: The main subroutines of the subprogram are as follows.

Subroutine HEAT1: This subroutine carries out the following-

1. This subroutine performs non-iterative heat transfer calculation.
2. The coefficients in the heat-balance equation are evaluated, using subroutines EEFT, COOL, and PROP.

Subroutine HEAT2: This subroutine does the following functions-

1. This subroutine carries out an iterative heat-transfer calculation.
2. The subroutine also writes out the results for the heat transfer subprogram in the readable form.

Subroutine TWALL: This subroutine uses Newton's approximation to solve the heat balance equation, which is in the following form:

$$D_1T_w^4 + D_2T_w^{2.5} + D_3T_w = D_4$$

Subroutine EEFT: This subroutine calculates the emissivity of the flame.

Subroutine PROP: This subroutine obtains average values for the specific heat, thermal conductivity, and the dynamic viscosity of the gas mixture.

Subroutine COOL: This subroutine calculates wall cooling parameters according to the film cooling technique.

A4.2 Flowchart for Heat-Transfer Subprogram:

The overall flow chart for the heat transfer subprogram is given in the Figure A5.

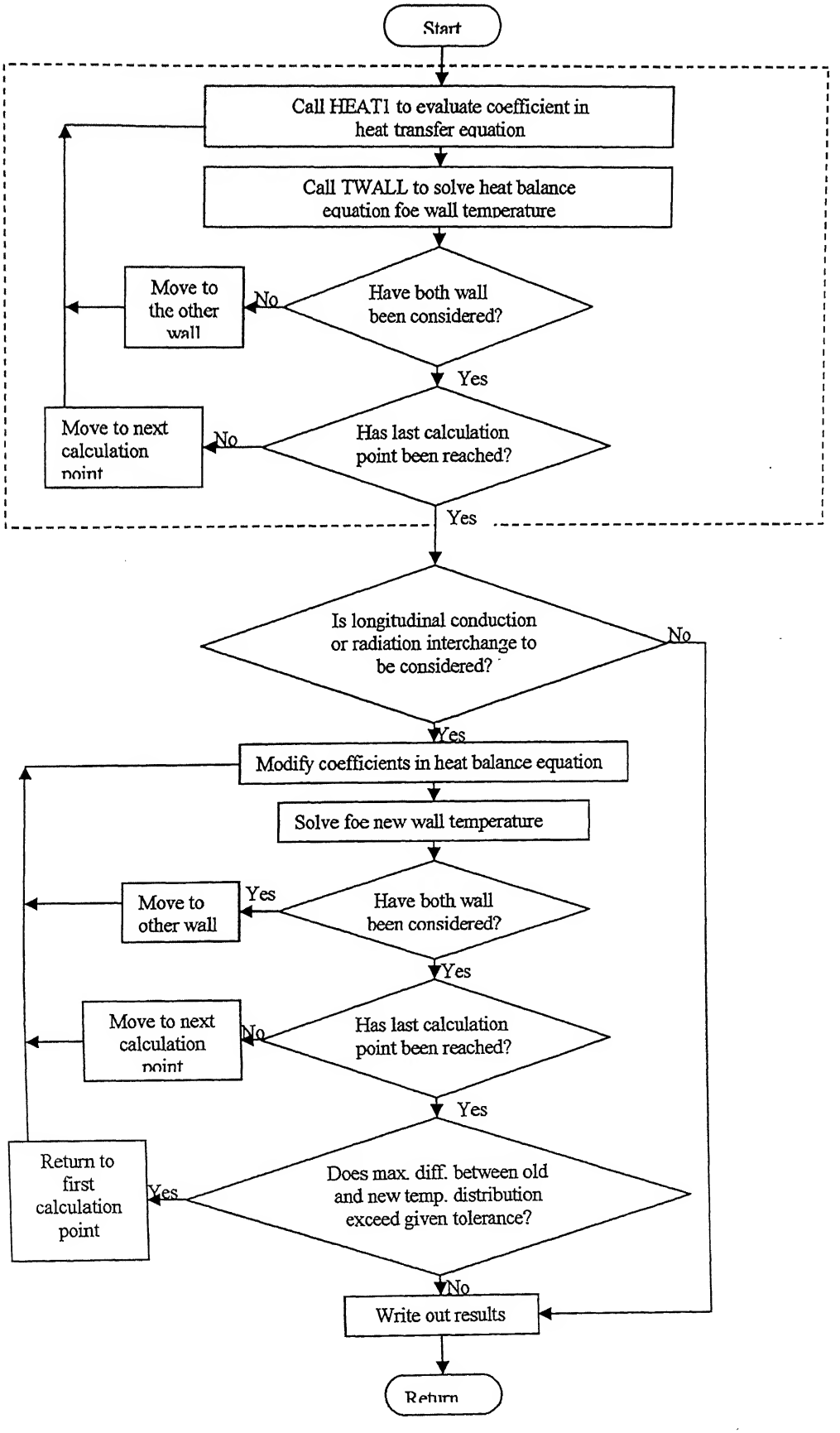

Figure A5 Overall Flowchart for Heat-Transfer Subprogram